

Comparative analysis of *in vitro* phenotypes of twelve
actual swine influenza A virus isolates

von Meike Janna Mands

Inaugural-Dissertation zur Erlangung der Doktorwürde
der Tierärztlichen Fakultät der Ludwig-Maximilians-Universität
München

Comparative analysis of *in vitro* phenotypes of twelve
actual swine influenza A virus isolates

von Meike Janna Mands
aus Gießen

München 2016

Aus dem Zentrum für Klinische Tiermedizin der Tierärztlichen Fakultät der
Ludwig-Maximilians-Universität München

Lehrstuhl für Krankheiten des Schweines

Arbeit angefertigt unter der Leitung von:
Univ.-Prof. Dr. Mathias Ritzmann

Angefertigt am Bayerischen Landesamt für Gesundheit und Lebensmittelsicherheit,
Oberschleißheim
Mentor: PD Dr. Antonie Neubauer-Juric

Gedruckt mit Genehmigung der Tierärztlichen Fakultät
der Ludwig-Maximilians-Universität München

Dekan: Univ.-Prof. Dr. Joachim Braun

Berichterstatter: Univ.-Prof. Dr. Mathias Ritzmann
Korreferent: Univ.-Prof. Dr. Gerd Sutter

Tag der Promotion: 16. Juli 2016

Abbreviations

AntiAnti	Antibiotic-Antimycotic 100x, Gibco®
Ca⁺⁺	Calcium
CD	Cluster of Differentiation; Surface Molecule
cDNA	Complementary Deoxyribonucleic Acid
CEF	Chick Embryo Fibroblasts
CHO	Chinese Hamster Ovary (cells)
CO₂	Carbon dioxide
cpe	Cytopathic Effect
cRNA	complementary Ribonucleic Acid
CSFV	Classical Swine Fever Virus
C_q	Cycle quantification
DAPI	4',6-diamidino-2-phenylindole (fluorescent stain)
DEPC	Diethylpyrocarbonate
DMEM	Dulbecco's Modified Eagle Medium
DMSO	Dimethyl Sulfoxide
DNA	Deoxyribonucleic Acid
EDTA	Ethylendiamin Tetra acetate
FACS	Fluorescence Activated Cell Sorting
FBS	Fetal Bovine Serum
Fig	Figure
FLI	Friedrich-Loeffler-Institut
h	Hours
H₂O	Water
HA	Hemagglutinin
g	Gravity
IAV	Influenza A Virus/es
IA	Influenza A
IF	Immunofluorescence
IFN	Interferon
IgG	Immunoglobulin G

IL	Interleukin
KHCO₃	Potassium hydrogen carbonate
log	Logarithm
M1	Matrix 1 protein
MDCK	Madin Darby Canine Kidney (cells)
MEM	Minimum Essential Medium
Mg⁺⁺	Magnesium
MHC(class)II	Major Histocompatibility Complex class II molecules
min	Minute(s)
ml	Milliliter
MOI	Multiplicity of Infection
mRNA	messenger Ribonucleic Acid
NA	Neuraminidase
NaHCO₃	Bicarbonate
NH₄Cl	Ammonium chloride
NP	Nucleoprotein
NPTr	Newborn Pig Trachea (cells)
NLS	Nuclear Localization Signal
NS1	Nonstructural protein 1
NS2	Nonstructural protein 2
NSK	Newborn Swine Kidney (cells)
PA	Polymerase Acid nonstructural Protein
PB1	Polymerase Basic nonstructural Protein 1
PB2	Polymerase Basic nonstructural Protein 2
PBMC	Peripheral Blood mononuclear Cells
PBS	Phosphate Buffered Saline
PEL	Porcine Embryonic Lung (cells)
PFA	Paraformaldehyde
p.i.	post infection
RNA	Ribonucleic Acid
RNP	Ribonucleoprotein

RPMI 1640	Roswell Park Memorial Institute 1640
RT	Reverse Transkriptase
RT-PCR	Reverse Transcription-Polymerase Chain Reaction
SE	Standard Error of the Mean
Sec	Section
SIV	Swine Influenza Virus
SJPL	St. Jude Porcine Lung (cells)
SLA	Swine Leukocyte Antigen (also see (MHC-II))
SWC3	Swine Workshop Cluster
t	Time
Tab	Table
Taq	Taq-Polymerase, derived from from bacteria <i>Thermus aquaticus</i>
TCID	Tissue Culture Infectious Dose
TE	Buffer with components of Tris(buffer) and EDTA
qPCR	quantitative Polymerase Chain Reaction
vRNA	viral Ribonucleic Acid

Contents

1	Introduction	1
2	Review of literature	3
2.1	Influenza A virus	3
2.1.1	Taxonomy	3
2.1.2	Morphology of Influenza A virus	3
2.1.3	Epidemiology of swine Influenza A virus (SIV) infections	4
2.1.3.1	The role of molecular methods in SIV epidemiology	6
2.1.4	Pathogenesis of SIV	6
2.2	Replication of influenza A viruses	7
2.2.1	Overview	7
2.2.1.1	Expression of viral proteins at different stages during the virus replication cycle	8
2.2.1.2	Role of the Influenza A virus nucleoprotein (NP)	9
2.2.1.3	Role of the Influenza A virus matrix 1 protein (M1)	10
2.2.2	Influenza virus replication in cell culture	11
2.2.2.1	IAV replication dynamics in different cell cultures	11
2.2.2.2	Replication of IAV in MDCK cells	12
2.2.2.3	Replication of IAV in A549 cells	13
2.2.2.4	Replication IAV in bovine derived cells	13
2.2.3	Myeloid cells and their role in immune response	13
2.2.3.1	Peripheral blood mononuclear cells (PBMC)	13
2.2.3.2	Virus infection of porcine fibrocytes	14
3	Materials	15
3.1	Viruses	15
3.1.1	Virus isolates	15
3.2	Cells	16
3.2.1	Cell lines	16
3.2.2	Primary cells	16
3.3	Cell culture medium	16
3.4	Kits for nucleic acid extraction	16
3.5	Kits for RT-PCR reactions	16
3.6	Information about real time RT-PCR primers, probes and reaction volumes . . .	17

3.6.1	Primers, probes and concentration mix for specific amplification of pdmH1 sequences	17
3.6.1.1	Reaction volume and concentration of MasterMix components for specific amplification of pdmH1 sequences	18
3.6.2	Primers and probes for specific M1-sequence amplifications used in singleplex-M real time RT-PCR protocols	18
3.6.2.1	Reaction volume and concentration of MasterMix components for M-Single-real time RT-PCR	18
3.6.3	Primers and probes for the Triplex-(H1/N1/M)-real time RT-PCR and Duplex-(H3/N2)-real time RT-PCR	19
3.6.3.1	Reaction volume and concentration of MasterMix components for Triplex-(H1/N1/M)-real time RT-PCR and Duplex-(H3/N2)-real time RT-PCR	20
3.7	Information about ‘conventional’ RT-PCR, primers and probes used for sequence analysis	21
3.7.1	Primers used for specific amplification of porcine H1, H3, N1, N2 gene sequences	21
3.7.1.1	Mastermix for ‘conventional’ RT-PCR used for specific amplification of porcine H1, H3, N1, N2 gene sequences	21
3.8	Antibodies	22
3.8.1	Antibodies used for indirect immunofluorescence analyses	22
3.8.2	Antibodies used for FACS analyses	22
3.9	Chemicals	23
3.10	Laboratory utilities	24
3.11	Consumables	25
3.12	Software	25
4	Methods	27
4.1	Molecular biological methods	27
4.1.1	Extraction of RNA	27
4.1.2	Reverse transcription polymerase chain reaction	27
4.1.2.1	Real time RT-PCR to detect and distinguish between sequences specific for H1, H3, N1, and N2 from current, in Southern Germany circulating porcine IAV	27
4.1.2.2	Real time RT-PCR for comparison of viral genome loads in infected cell cultures	28
4.1.2.3	Sequence analyses	28
4.2	Virological methods	30
4.2.1	Isolation of porcine fibrocytes	30
4.2.2	Cultivation of porcine embryonic lung cells, MDCK, KLU-2-R and A 549 cells	30
4.2.3	Virus propagation in cell culture	31
4.2.3.1	Preparation of tissue samples	31
4.2.3.2	Virus isolation and propagation	31
4.2.3.3	Virus quantification by endpoint dilution	31
4.2.4	Virus replication assays	32
4.2.5	Immunofluorescence assays	32
4.2.6	Scanning laser confocal microscopy and immunofluorescence microscopy	33

5	Results	35
5.1	Morphology of infected cells	36
5.2	Replication kinetics of respective SIV isolates after infection of MDCK, A549, KLU-2-R, PEL cells, and porcine fibrocytes	42
5.2.1	Dynamics of SIV replication in MDCK cells	42
5.2.2	Dynamics of SIV replication in A549 cells	42
5.2.3	Dynamics of SIV replication in KLU-2-R cells	43
5.2.4	Dynamics of SIV replication in porcine fibrocytes	43
5.2.5	Dynamics of infectious virus multiplication in porcine embryonic lung cells after SIV infection	44
5.3	Dynamics of viral RNA loads after infection of MDCK, A549, KLU-2-R cells, and porcine fibrocytes with current isolates of porcine IAV	56
5.3.1	Dynamics of viral RNA loads in SIV infected MDCK cells	56
5.3.2	Dynamics of viral RNA loads in SIV infected A549 cells	56
5.3.3	Dynamics of viral RNA loads in SIV infected KLU-2-R cells	57
5.3.4	Dynamics of viral RNA loads in SIV infected porcine fibrocytes	57
5.3.5	RNA load dynamics in correlation with the detection of infectious titers	57
5.4	Distribution of the SIV nucleoprotein (NP) and the matrix 1 protein (M1) in <i>in vitro</i> infected cells	67
5.4.1	Viral NP and M1 protein detection in <i>in vitro</i> infected cells at 0h p.i.	68
5.4.2	Viral NP and M1 protein detection in <i>in vitro</i> infected cells at 24h p.i.	70
5.4.2.1	Distribution of SIV proteins NP and M1 in <i>in vitro</i> infected MDCK cells	70
5.4.2.2	Distribution of SIV proteins NP and M1 in <i>in vitro</i> infected A549 cells	73
5.4.2.3	Distribution of SIV proteins NP and M1 in <i>in vitro</i> infected KLU-2-R cells	74
5.4.2.4	Distribution of SIV proteins NP and M1 in <i>in vitro</i> infected porcine fibrocytes	75
5.4.2.5	Distribution of SIV proteins NP and M1 in <i>in vitro</i> infected PEL cells	76
6	Discussion and Conclusion	81
6.1	SIV replication in MDCK and A549 cells is isolate independent and productive	82
6.2	SIV is not replication-competent in KLU-2-R cells	85
6.3	Infection and replication of SIV in porcine fibrocytes is isolate specific	87
6.4	Protein expression in PEL cells is comparable for all individual SIV isolates	88
6.5	Specific features of individual SIV isolates correspond in all cell systems tested	89
6.6	Conclusion	90
7	Summary	93
8	Summary (German)	95
9	Bibliography	97
	Danksagung	107

Introduction

Influenza is an acute respiratory disease of pigs, occurring frequently and worldwide, and thus posing a substantial economic concern for swine industry. From a public health perspective, infections with swine influenza A viruses (SIV) are of substantial importance not only to the health of swine populations but furthermore to the epidemiology of human influenza. The zoonotic potential of influenza A viruses (IAV) is well documented and human infections with swine derived IAV have been recorded over decades. Various studies suggest that viruses, currently circulating in wild birds, represent a large genetic pool of IAV presumably capable of infecting mammals [9][108]. Pigs are susceptible to infection with IAV of both avian and mammalian origin, because their tracheal epithelium contains both receptors preferred by either avian or human IAV. In this context, pigs have been implied as intermediate hosts for adaptation of avian IAV to mammals. They can function as a ‘mixing vessel’ in which reassortments between distinct viruses may result in new viruses with new specific pathogenic or even pandemic potential. In early 2009 such a pandemic H1N1 virus, obviously emerged from complex reassortment events, reached Europe and was then introduced into European swine populations. Before this incursion, three subtypes of IAV strains were circulating in the German swine population: avH1N1, huH1N2 and human-like swine H3N2. The ongoing co-circulation of pdmH1N1 viruses with endemic swine IAV gives rise to more reassortants carrying unknown biological properties and in consequence unpredictable zoonotic risks. Virulence and adaptation to a specific species are complex multi-factorial interactions between virus and host, which are likely driven by independent selective pressure [98]. Hence, the pathogenicity of IAV is dependent on multiple viral and host factors. Concerning viral factors, the basic pathogenicity relates mainly to properties of the hemagglutinin glycoprotein (HA). However, the HA is only one of the critical factors that affect the pathogenicity. Evidently, the general genetic constellation in a virus influences its characteristics. The lack of knowledge concerning phenotypic properties and pathogenic differences between porcine IAV subtypes, is one decisive drawback in this matter. In previously published studies, various strains of avian, porcine and human IAV have been investigated by different groups [1][59][64]. These strains contained sequence variation in their viral proteins, yet it was often assumed that their properties are typical of all IAV. However, single strains may not reflect comprehensive characteristics of an entire and diverse virus population, such as porcine IAV. The key issue assessed in this study was whether different porcine IAV vary in *in vitro* phenotypic properties, such as infectivity and virus replication. The experiments were designed to determine eventual differences between subtypes actually present in swine in the region of southern Germany. The investigated parameters included their replication kinetics of viral titers and RNA loads and the ability to induce viral protein expression. Five cell systems (MDCK, A549, KLU-2-R, PEL, and porcine fibrocytes) were selected as representatives for different host-cell systems.

Review of literature

2.1 Influenza A virus

2.1.1 Taxonomy

The family of *Orthomyxoviridae* includes six genera: *Influenzavirus A*, *B*, and *C*, *Thogotovirus*, *Quarantavirus* and *Isavirus* [71]. The respective virus species influenza A virus, influenza B virus, and influenza C virus cause influenza in diverse vertebrates, including birds, humans and other mammals [106].

Members of the genera *Influenzavirus A* and *B* contain eight single-stranded gene segments, while *Influenzavirus C* contains 7, thus being divergent in structure to the others. Influenza C viruses are less common and cause mostly mild diseases. Influenza B viruses are almost exclusively pathogenic to humans, despite having also been found in seals [76]. Influenza A viruses (IAV) can infect birds and diverse mammals and therefore pose a significant risk for multi-species infections. In addition, mutation and also reassortments occur frequently, resulting in new viruses causing annual epidemics and occasional pandemics in humans [98]. IAV carries two important surface glycoproteins - the hemagglutinin (HA) and the neuraminidase (NA) - which determine the type of IAV. Until now 16 hemagglutinin (H1-H16) and 9 neuraminidase (N1-N9) subtypes of IAV have been isolated. All 16 HA and 9 NA subtypes were found in wild waterfowl, while, due to specific species barriers, mammalian species are susceptible to just a few of the subtypes. Recently new influenza-virus-like genomes have been described in bats [100][101], which have not been isolated yet.

The nomenclature of the subtypes of Influenza A viruses bases on the surface antigens, hemagglutinin (H number) and neuraminidase (N number), represented in the scheme HxNx [70]. According to the World Health Organization guideline [73] every influenza virus strain is designated by its genus (Influenza A;B;C), followed by the host (if other than human), place of isolation, laboratory number of the isolate and the year of isolation. For IAV the HA and NA subtypes are enclosed in parenthesis; e.g.: A/swine/Garrel/IDT14891/2012 (H1N2).

2.1.2 Morphology of Influenza A virus

Influenza A viruses are spherical to pleomorphic, enveloped RNA viruses with a segmented negative- stranded RNA genome [70]. Together with the envelope membrane, the virions measure a diameter of 80-120nm [55]. The lipid envelope is studded with glycoprotein spikes of HA and NA and also contains smaller amounts of integral matrix (M2) proteins that function as an ion channel. The envelope and its three integral membrane proteins HA, NA, and M2 overlay a matrix of M1-proteins, which encloses the virion core. The central core contains the viral genome,

packaged with associated proteins, referred to as ribonucleoprotein (RNP) complex. The RNP consists of the viral RNA and four viral proteins: the predominant nucleoprotein (NP) and the RNA-polymerase proteins (polymerase acid protein (PA), polymerase basic protein 1 (PB1), polymerase basic protein 2 (PB2)) [55]. The eight viral genome segments of single-stranded RNA encode for the structural and also for nonstructural proteins 1 and 2 (NS1, NS2) of the virion [9].

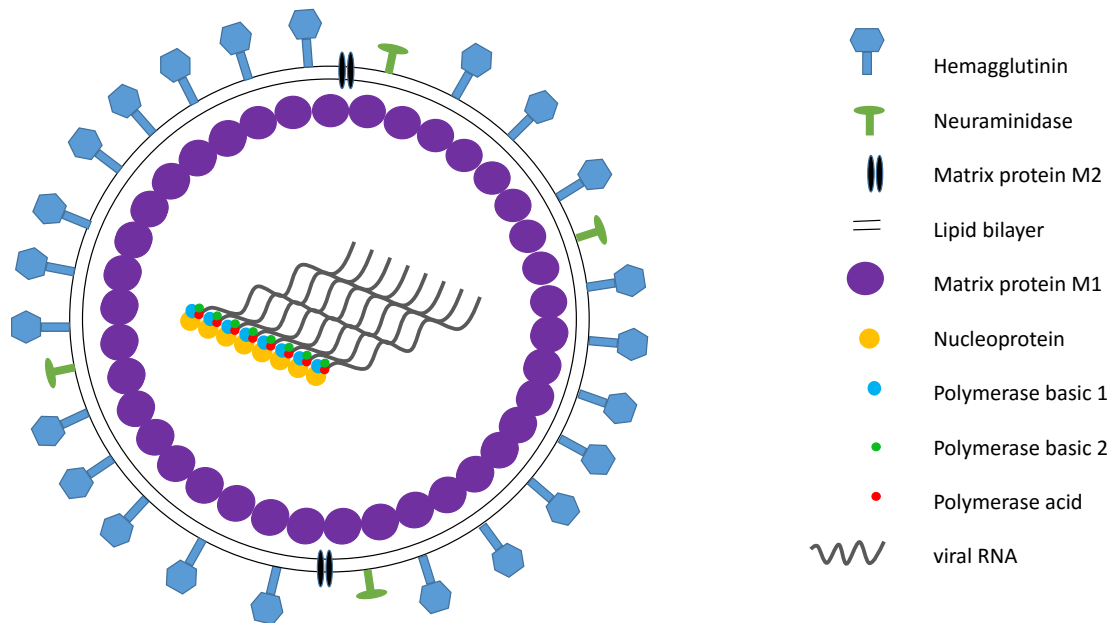


Figure 2.1: Schematic illustration of the morphology of an Influenza A virus particle.

2.1.3 Epidemiology of swine Influenza A virus (SIV) infections

Aquatic wild birds are reported as natural reservoir for influenza A viruses. All known subtypes circulate ubiquitously in wild waterfowl such as ducks and wild geese [108]. In these species, infections are generally localized to the intestinal tract, without causing disease. H1, H2, and H3 subtype viruses were isolated and identified to cause the yearly flu epidemic in humans, and only a limited number of subtypes was isolated from other mammalian species, e.g. pigs [94]. This implies that IAV is generally restricted in host range [37]. Viral segment reassortment can occur in cells which are infected in parallel with different IAV. The gene pool of IAV, circulating in avian species, provides a great genetic diversity for those ‘antigenic shifts’. The emerging reassortants, originating from the avian cycle, may encode completely novel antigenic proteins which could make them capable of adapting to humans and a wide variety of other mammalian species [37][108].

Among other factors the HA seems to be of importance for the determination of the host range. HA is responsible for the attachment of the virus to sialic acid molecules on the host’s cell surface [56]. Sialic acids are commonly found on the termini of many glycoconjugates, thus being ubiquitous in various tissues. The configuration of the sialic acid terminal is dependent on the linkage to the glycoconjugate. They can form either α -2,3 or α -2,6-linkages [9][45]. While avian IAV preferentially binds to α -2,3, human IAV preferentially bind to α -2,6-linked sialic acids, which correlates with the predominant sialic acids found in specific hosts. α -2,3-linkages dominate the epithelium cells of the aquatic bird’s intestinal tract, where they multiply [111]. In human tracheal epithelial cells of the upper respiratory tract, α -2,6-linked sialic acids predominate. Sialic

acids with terminal α -2, 3-linkages are also present in human respiratory epithelium, though, in less quantity and more distal than those with α -2, 6-linkages [66]. Consequently, humans can be infected by avian IAV, although with less efficiency than by human strains [9]. Regardless of the host species, the presence of both sialic acid linkage-types in an epithelium, increases the risk of reassortments between different IAV. In the tracheal epithelium of pigs both linkage-types of sialic acids are present [45]. Pigs are therefore susceptible to swine, avian and human influenza A viruses. Hence swine can function as an intermediate host for new emerging viruses, with pandemic and/or zoonotic potential [88][108]. Reassortments and mutations are known to have emerged in pigs, domestic poultry, humans, and horses [98].

The European SIV lineages differ from those found in North America and Asia. Three different subtypes became prevalent in pig population and represented the majority of SIV circulating in Europe for a long time [53]. An avian-to-swine transmission led to the ‘avian-like’ swine H1N1 (avH1N1) viruses isolated in 1979 [77]. The reported outbreak of swine influenza in Belgium provided evidence of avian IAV being capable of crossing species barriers outside laboratory conditions. Until then, no transmission of IAV across a species barrier from birds to mammals, resulting in clinical disease, had been demonstrated.

In the 1970s a human H3N2 influenza A virus was transmitted to pigs in Italy, Belgium and France. In the early 1980s this human H3N2 virus reassorted with the avH1N1 [13][19][51] and led to ‘human-like’ swine H3N2 virus, now posing the dominant H3N2 lineage in European pig population [91].

A decade later, in 1994, the ‘human-like’ swine H1N2 (huH1N2) emerged, also carrying internal genes from the avH1N1 lineage and genes of ‘human-like’ swine H3N2 origin [10][116]. This swine huH1N2 is now the predominant virus within this subtype in European pigs. All three subtypes successively replaced ‘classical swine H1N1’ viruses circulating by then. ‘Classical swine H1N1’ still circulates predominantly in North America [102].

In early 2009 a new pandemic H1N1 virus emerged in Mexico and reached Europe in the same year [27][70]. Phylogenetically this pandemic H1N1 2009 is a reassortant of Eurasian avH1N1 and a North American triple reassortant H1N2, that originated from classical swine H1N1, a North American human H3N2 and a North American avian H1N1 virus [27][58]. The pandemic in 2009 was primarily observed in humans, but soon it was reported to have entered domestic swine populations [57]. Already in 2010, upon surveillance for influenza A viruses in pigs in the United Kingdom, a reassortant influenza A virus was detected, which had genes from the pandemic (pdmH1N1) 2009 virus and HA and NA genes from swine H1N2 viruses [41]. Further new reassortant influenza A viruses consisting of seven genome segments from the pdmH1N1 virus and a neuraminidase segment from Eurasian porcine H1N1 IAV were soon detected in Germany [92]. Serosurveys conducted by Lange and Starick between the years 2009-2012 in Germany, demonstrated that 9% of IAV infected pig herds [58] had been infected with reassortants from pandemic H1N1 2009 [57][58][92][93]. The essential characteristics which enable an individual novel virus to form a stable lineage within a pig population are still unknown [56], but indications point to the ability of pdmH1N2 (N2 derived from swine ‘human-like H3N2’) reassortants to establish stable lineages, at least in German swine populations [32]. Recently published surveillance data on an European level by Watson et al. (2015) and Simon et al. (2014) corresponded with these findings. They concluded that infections with pdmH1N1 viruses are established in European pig population, being the third most-frequent genotype found in swine across Europe.

The proportion of circulating SIV subtypes varies among European regions. In Southern Germany avH1N1 is still the most common subtype with more than 60% out of 93 IAV infected holdings of pig as reported by Pippig et al. (2016). Furthermore, in their study reassortants of the pdmH1N1 virus were detected in more than 4%, whereas H1N2 was detected in 15% and H3N2 found in 9.7% of in total 198 specimens taken from 93 individual holdings.

Crossing species barriers was responsible for the pandemics in 1957 ('Asian' influenza) and 1968 ('Hong Kong' influenza) in which swine originated influenza A viruses infected humans [70]. Each pandemic causing virus emerged in a different way, thus making long-term predictions of new pandemics difficult [98]. The ongoing co-circulation of pdmH1N1 viruses with endemic swine IAV gives rise to more reassortants with unknown biological properties and uncertain zoonotic risk. Obviously an increasing number of circulating lineages will increase the likelihood of the emergence of a genotype with human-pandemic potential.

2.1.3.1 The role of molecular methods in SIV epidemiology

In veterinary diagnostics various methods are used to detect IAV infection in pigs. For a very long time virus diagnostics were based on classical methods, such as virus isolation in embryonated chicken eggs or MDCK cells. SIV subtype differentiation was routinely carried out by virus isolation in cell culture with subsequent subtype determination by hemagglutination inhibition assays, using specific antisera to each subtype [16]. Although these methods are quite sensitive and widely used, several days are required to come to a result. Since rapid and accurate detection of infecting viruses is a critical factor in the control of a potential infection in human and animal populations, new approaches to detect IAV became more relevant over the years [38]. Bressoud et al. (1990) and Yamada et al. (1991) applied a combination of reverse transcription with the polymerase chain reaction (RT-PCR) for rapid detection of IAV in human nasal swabs. This method offered several advantages over standard isolation techniques. A few years later RT-PCR assays were reported for the detection of SIV in nasal swab specimens of pigs as well [89]. As outlined before (Section 2.1.3), information about prevalent strains in a population or region of a country is essential for surveillance, outbreak, and treatment management. Consequently, establishing RT-PCR assays to detect and determine the subtype of SIV became relevant for diagnostics. Nowadays several multiplex RT-PCR assays that can identify the HA and NA of porcine IAV directly from clinical specimens have been established [16][22][24][38][39][68][98]. Nevertheless, the genetic heterogeneities of IAV may result in some difficulties of subtype determination by using current PCR protocols for analysis. Therefore, RT-PCR assays need to be regularly adjusted [24], thus posing a challenging task in diagnostics.

2.1.4 Pathogenesis of SIV

The infection of pigs with influenza A virus is of substantial importance to the swine industry. Being highly contagious the virus is transmitted via respiratory secretions, either directly or by air. Morbidity rates of up to 100% have been reported [51][108]. Therefore, Influenza A virus infection can cause a significant economic loss in an affected herd, even if many infections pass unnoticed.

SIV is one of the rare primary respiratory pathogens of swine, which means that the virus can induce respiratory disease on its own [104]. It can infect pigs of all ages. So far, no differences in the disease's outcome after infection with either of the known SIV subtypes (H1N1, H1N2 and H3N2) have been reported [104]. Pathogenesis and clinical presentation seem to be similar: The virus extensively replicates in lung epithelial cells, especially in cells of the bronchi, bronchioli and alveoli in the lower respiratory tract, causing the symptoms that are typical for swine flu [102]. The infection causes neutrophil infiltration and lung epithelial necrosis, possibly leading to severe lung lesions [21][104]. Van Reeth et al. (1998,2002) demonstrated temporal correlation between pro-inflammatory cytokines in lung lavage fluids of SIV infected pigs, lung virus titers, neutrophil infiltration and clinical signs. All parameters peaked between 18 and 24 h after inoculation [103][104]. Usually the virus is eliminated after one week [104]. The infected animals display a short period of fever, nasal discharge, coughing and difficulty in breathing. The infection is mostly accompanied with lethargy and anorexia [115]. There exist reports associating

SIV with reproductive disorders in sows [56].

Pathogenicity of influenza A virus is dependent on multiple viral and host factors. Concerning viral factors, the basic pathogenicity relates first of all to properties of the hemagglutinin glycoprotein (HA) [108]. The proteolytic cleavage site within the HA is an important factor of the pathogenicity in IAV [8]. During natural infection the HA precursor protein is cleaved into HA1 and HA2 by extracellular trypsin-like protease. This modification is necessary for the correct structure and function of the HA and in consequence for the infectivity of IAV. The distribution of activating proteases in the host is one of the determining factors of cell tropism and thus the pathogenicity of an influenza A virus. The cleavage of mammalian and low pathogenic avian IAV takes place extracellularly. This fact limits their infectivity in hosts to tissues where the appropriate proteases are encountered. Other IAV subtypes carry a proteolytic cleavage site in their HA that is cleaved intracellularly by ubiquitously occurring proteases. These viruses, such as specific avian H5 and H7 subtypes, are highly pathogenic and capable of infecting various cell types [94]. The correlation between HA-cleavage and infectivity of the virus has been shown in several studies [8][48]. Accordingly, Klenk et al. (1975) demonstrated that a trypsin treatment in *in vitro* cell systems induced a higher cleavage rate of the HA, leading to an increase of infectivity.

However, the HA is only one of the critical factors that affect the pathogenicity. Evidently, the general gene constellation in a virus influences the pathogenic characteristics [104].

Furthermore, HA and NA are important for the induction of an antibody response in the host. The fact, that influenza A viruses are genetically relatively unstable, poses a challenge for effective and specific vaccine production. Especially small point mutations ('antigenic drift') in IAV genomes can result in an evasion of the adaptive immune responses. Hence, vaccines, which induce an accurate immune response to such a wide variety of influenza A viruses, are a challenge for scientists. The ability to stimulate circulating antibodies to the HA of influenza A viruses is the main protective effect of most vaccines in use [104]. For the prevention and control of SIV infections in pigs, commercial swine influenza vaccines are available. Currently by the Paul-Ehrlich Institute authorized vaccines in Germany contain strains of inactivated Influenza A/swine Bakum/IDT1769/2003(H3N2), A/swine Bakum/1832/2000(H1N2), and A/Haselünne/IDT2617/2003(H1N1) [72]. Combining the three different subtypes, which circulated predominantly in swine in Germany, increases the probability of a sufficient protection. Since, a novel pandemic lineage has been introduced in pig populations, the stable co-circulation of respective three subtypes is disrupted. Therefore, the regular re-evaluation of swine influenza vaccines is necessary. Faster adjustments and replacements of vaccines against viruses with more contemporary strains is required.

2.2 Replication of influenza A viruses

2.2.1 Overview

In a first step, the receptor binding domain of the HA on the surface of IAV particles specifically binds to either α -2, 3- or α -2, 6-linked N-acetylneuraminic (sialic) acid containing molecules on the cell surface [9]. These sialic acids are found at the termini of many glycoconjugates in various epithelium cells of mammal and avian species [109]. During virus replication, the HA precursor protein is cleaved by proteases into HA1 and HA2. This modification is necessary for virus infectivity. The HA2 portion mediates the fusion of the virus envelope with the cell membrane, while the HA1 portion contains the receptor binding and antigenic sites [9].

Once attached to the cell the virus is internalized by receptor mediated endocytosis. The viral envelope of endocytosed viruses has to fuse with the endosomal membrane to release viral components into the cytoplasm. The increasing acidity in late endosomes initiates a low-pH

dependent conformational change of the HA structure that triggers membrane fusion to release viral RNPs into the cytosol [90]. Since influenza A virus replicates inside the nucleus of a host cell, the RNPs are transported to the nucleus mediated by the viral proteins' nuclear localization signals (NLSs) [107]. In the nucleus the viral RNA-polymerase, a component of the RNP-complex, starts transcribing the viral RNAs (vRNAs) into positive-sense messenger RNAs (mRNAs) [36]. These components of the RNP are essential for catalyzing the mRNAs synthesis, which explains why naked RNA is not infectious [54]. PB1 and PB2 mediate the polyadenylation of the viral mRNAs by a specific poly(A)polymerase of the host cell. Once polyadenylated and capped, mRNAs of viral origin can be transported to membrane-bound ribosomes at the endoplasmic reticulum and translated, just like host mRNA [9][55]. The newly synthesized structural and nonstructural viral proteins are either secreted through the Golgi-complex to the cell membrane, such as the envelope proteins HA, NA, and M2, or transported back to the nucleus [109].

The alternative type of transcription of the vRNAs results in the template or complementary RNA (cRNA), that is required for the production of full-length copies of the individual vRNAs. This is the first step in replication of influenza vRNAs. The second step is the copying of the cRNAs into new vRNAs. The switch from transcribing viral mRNAs to cRNAs synthesis requires newly synthesized viral proteins. Beaton et al. (1986) established an *in vitro* system that is able to catalyze transcription as well as replication of vRNAs. They determined roles of virus-specific proteins. Obviously newly synthesized NP, as well as the RNA polymerase subunits, are required for the synthesis of vRNAs from cRNAs [6][49]. However, this does not exclude the possibility of cellular factors being involved in the replication process. Furthermore, host proteins have been shown to be required for non-segmented RNA virus replication and transcription (e.g. cellular actin) [20][44].

During the late phase of infection, newly synthesized RNPs leave the nucleus for incorporation into new virions. The packaging and budding takes place at the cell surface membrane, where RNPs contact with the envelope proteins bound to the membrane [2]. After budding the virion still adheres to the cell membrane through HA and detaches once its NA has cleaved the cellular sialic acid residues [9].

Selective packaging signals ensure that the majority of virus particles contain a full genome of exactly eight segments in the virion. If not, the newly synthesized Influenza virus particle is probably not fully infectious. There are a number of other reasons for the production of not fully infectious virions, including false or inefficient replication of individual viral proteins or incorrect assembly of these proteins. The frequent mutations caused by errors in RNA translation and replication due to the use of the viral RNA dependent RNA polymerase [6] is another factor.

2.2.1.1 Expression of viral proteins at different stages during the virus replication cycle

Unlike most other RNA viruses, members of the genera *Influenzavirus A, B, C* replicate inside the nucleus of host cells. Therefore, the IAV replication cycle involves a complex series of nuclear import and export events [112]. This nuclear trafficking includes import of incoming viral RNPs and export of viral RNPs at different stages of the replication cycle. Newly synthesized RNPs travel to the plasma membrane, where the virus assembly and budding takes place. Furthermore, some of the newly synthesized viral proteins are transported from the endoplasmic reticulum to the nucleus. The polypeptides important for virus replication, such as the proteins of the polymerase complex (PB1, PB2 and PA), the NP and the nonstructural protein NS1 are the first viral proteins to be translated and synthesized. Subsequently, all these proteins are transported back into the nucleus. Since these proteins are required to switch cRNA transcription to vRNA synthesis (Section 2.2.1), it seems logical, that these steps occur early in replication.

Previous studies suggest that the timing of these initial steps in virus replication are to some

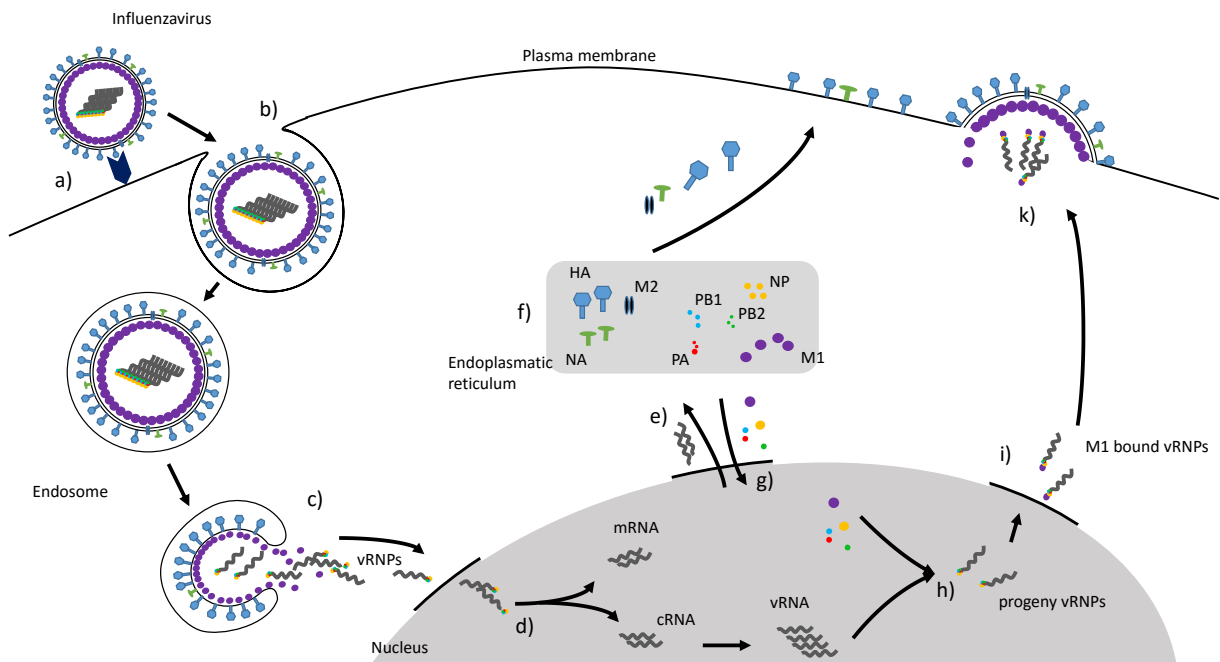


Figure 2.2: Schematic illustration of the major steps in influenza A virus replication. a) Binding to a sialic acid containing receptor of a target cell; b) Internalization by receptor mediated endocytosis; c) pH dependent fusion of the viral and endosomal membranes and releasing of viral RNPs (vRNPs) into the cytosol; d) Replication in the cell nucleus; e) Export of viral mRNA; f) Protein synthesis; g) Import of newly synthesized proteins; h) Assembly and formation of progeny vRNPs; i) Export of M1 bound vRNPs; k) Packaging and budding of progeny virions.

extend cell type dependent [50][62][67]. On the one hand, experiments with HeLa and L292-cells revealed NP synthesis to begin within the first two hours post infection (p.i.) [109]. On the other hand, after an initial lag period of approximately 15 to 20 min, uncoating of influenza A virus proceeded linearly until 90min after infection in experiments using MDCK cells [50]. This correlates with findings of others in experiments using MDCK cells, in which NP expression is first detected four hours after infection [1]. Finally, release from endosomes occurred about 25min after internalization and therefore expression of NP was somewhat faster in Chinese hamster ovary (CHO) cells [62].

Irrespective of the time differences reported concerning the onset of NP synthesis, all studies suggested M1 synthesis to start two to four hours later. Furthermore, HA, NA, and M2-proteins and the nonstructural protein NS2 are synthesized late in infection [69]. It has been shown, that NS2 diffuses into the nucleus and mediates the nuclear export of viral ribonucleoproteins [75]. The three integral membrane proteins HA, NA and M2 are transported to the plasma membrane, where they associate for the virus assembly. The newly synthesized M1 protein is shuttled to the nucleus as well as to the cytosol [110]. All of these bidirectional transport events are highly regulated and occur at specific phases in the IAV replication. As shown in previous studies, M1 is essential for import [109] and export of RNPs [12], thus being an ultimate requirement for efficient infectivity of influenza A virions. The fact that viral proteins are expressed at different times after infection and localize to distinct cellular compartments can be used to judge different stages of virus replication, when analyzing viral protein expression.

2.2.1.2 Role of the Influenza A virus nucleoprotein (NP)

The major structural component of the RNPs is the NP. It binds viral RNA with high affinity, thus maintaining the RNA template in a conformation suitable for transcription and also pack-

aging into progeny virions [20]. Therefore, NP shuttles between the nucleus and the cytoplasm, while transporting RNPs in both directions [109]. Consequently, various steps in virus replication are reflected by the respective distribution of NP within an infected cell. Whittaker et al. (1996) demonstrated that once synthesized and imported into the infected nucleus, NP remains nuclear until M1 mediates the export. Further experiments in which M1 synthesis was inhibited, confirmed that in this case re-imported NP remained in the nucleus, even late in infection. Therefore, the trafficking regulation of RNPs is reflected in the intracellular distribution pattern of their major structural component, the NP.

Multiple evidence imply that NP is also essential in the process of switching RNA synthesis from transcription mode to replication mode (Section 2.2.1) [6][49]. Biswas et al. (1998) showed that NP interacts directly with PB1 and PB2, the proteins binding the RNA-polymerase. The precise steps required during genome replication remain unknown, but newly synthesized cRNA seems to depend on a supply of non-RNP associated NP to produce a copy of the viral RNA template [6]. At early times in the infection cycle, NP is found predominantly in the nucleus bound in RNPs where it is probably needed for genome replication. Furthermore, newly synthesized NP is rapidly imported in the nucleus. At an advanced state in infection, the export of RNPs to the cell periphery becomes dominant and substantial amounts accumulate in the cytoplasm [20]. Studies indicate a direct association between M1 and NP, considering that M1 molecules are unable to bind directly to RNA [80], while the RNP's export depends on M1 [63]. Furthermore, NP interacts with F-actin and micro filaments of the host's cytoskeleton [3][44]. NPs of influenza A strains are phosphorylated, but the 'phosphopeptide fingerprints' vary considerably, depending on the virus strain [46][47]. The phosphorylation is supposed to be one reason why viral NP can cooperate with other proteins. Kistner et al. (1985) showed that the host-specific phosphokinases plays an important modifying role in the process of NP-phosphorylation. Correlations between phosphorylation patterns and virus - yielded in MDCK, HeLa, L-cells, and primary chick embryo fibroblasts (CEF) - implied that modifications of the NP might change in different host cells. The modification of NP in one cell type could be less efficient than in other cell types, being one of several reasons why IAV strains replicate in different host cells with variable efficiency [47].

2.2.1.3 Role of the Influenza A virus matrix 1 protein (M1)

The M1 protein is a major structural component of Influenza A virus particles. It associates with the viral envelope and with the nucleocapsid of the virus particle [112], thus connecting these components. After endocytosis into cells, the low pH in the endosome triggers the RNPs to dissociate from the viral M1 [12]. RNPs and M1 are transported independently after uncoating from the endosome. The cleaved RNPs expose a nuclear localization signal (NLS) to be actively transported to the nuclear pores [107]. There is evidence that M1 also possesses a NLS domain [113], but the protein is distributed predominantly into the cytoplasm at this state of replication. While all of the penetrating NP associated RNPs move rapidly to the nucleus, the entry of M1 is slower and not essential for infection [62]. The synthesis of new M1 proteins occurs late in the infection cycle. However, newly synthesized M1 proteins have a strong affinity for RNPs, therefore migrating into the nucleus [85]. The presence of M1 in the nucleus is necessary for the RNPs export. Binding of M1 to the RNP-complex mediates their export from the nucleus and into the cytoplasm [112].

Results of Whittaker et al. (1996) indicate, that M1 also plays a role in preventing the nuclear re-import of premature RNPs. The difference between import-competent vRNPs, which have entered via endocytosis and the newly synthesized premature vRNPs seems to be the absence and presence of M1, respectively. Finally, it was shown that the M1 protein also plays an important role in virus budding, being an essential component for virus-like particle formation [30].

2.2.2 Influenza virus replication in cell culture

2.2.2.1 IAV replication dynamics in different cell cultures

For replication of influenza A viruses, embryonated chicken eggs are the biological system of choice [78]. However, the observation that HA variations after virus cultivation in embryonated eggs [87], together with the risk of shortage of appropriate eggs in the event of an epidemic or pandemic, resulted in a significant demand for a tissue culture based laboratory system. Therefore, establishing and evaluation of different host cell systems is a relevant subject to scientific research to this day.

IAV is known to have a high capability of replication in epithelial lung cells of the entire respiratory tract, especially in cells of the bronchi, bronchioli and alveoli in the lower respiratory tract. Therefore, a lot of cell systems with features of respiratory epithelium were investigated over the years, such as the permanent cell lines A549, Hep-2, and MRC-5 [59][82]. Resulting infectious virus titers did not significantly differ between low pathogenic avian, porcine, and human IAVs tested in respective studies [59][82]. With regard to the susceptibility of ‘mixing-vessel’ swine to either avian, human or porcine IAV, pig derived cells were also of particular interest. Seo et al. (2001) showed that St. Jude porcine lung cells (SJPL) support high replication titers for IAV. Their aim was to establish a mammalian cell system which supports the growth of all IAV subtypes in order to produce human influenza vaccines. The SJPL cell line was established from a lung of a 4-week-old female Yorkshire pig and was positive for the epithelial cell marker cytokeratin. Seo et al. (2001) compared the replication efficiencies of human influenza A and B viruses, avian IAV strains of different subtypes, including the highly pathogenic H5N1 IAV, as well as equine and swine IAV in SJPL cells with their replication in MDCK cells. Infectious virus titers, cytopathic effects (cpe), and the replication kinetics of the tested influenza viruses were comparable in both cell lines. Other cells from the respiratory tract of pigs also seem to be highly susceptible to IAV [23][64]. Primary pig cells like newborn pig trachea (NPTr) or newborn swine kidney (NSK) cells were tested to be susceptible to various pig viruses which cause respiratory diseases [23]. Ferrari et al. (2003) demonstrated, that all different types and subtypes of influenza virus - isolated from human (human H1N1, H3N2 and B), fowl (fowl H6N2, H9N2, H5N2, H7N1), and swine (swine H1N1, H3N2) species - replicated in both cell culture systems. Demonstrated infectious virus titers were similar to those detected in chicken embryos ($10^{7.5}$ - $10^{8.5}$). In previously published studies the *in vitro* replication aspects of various different strains of avian, porcine and human IAV were investigated by different groups [23][42][48][59][64][78]. However, experiments did not focus on differences between the individual subtypes infecting one species, but rather on differences between cell types or IAV derived from different hosts in general. Although IAV strains clearly contained sequence variation in their viral proteins, it was often assumed that their observed properties are representative for all porcine, human, or avian IAV. Massin et al. (2010) approached a comparison of porcine and avian originated IAV strains in two cell types by detecting RNA replication and infectious virus titers. Again, only one individual strains per SIV subtype, A/swine/Finistere/2899/82 (H1N1), A/swine/Scotland/410440/94 (H1N2), and A/swine/Gent/1/84 (H3N2), was used. Clearly, assessing the phenotypic properties of one strain per subtype does not necessarily allow for conclusions about comprehensive characteristics of a porcine IAV subtype in general.

Taken together, it has been shown that influenza viruses show similar kinetics of replication in various cell culture systems, if growth is supported at all. In several studies a step-plateau-like increase of infectivity for influenza A viruses was demonstrated in the first 4h-12h after infection in various cell types [64][7][26][34][81]. This rapid replication within 24h is a common feature for avian and mammalian strains. In most studies an exogenous protease treatment was performed in the cell culture systems to mediate membrane fusion activity of the HA of the viruses. As outlined in Section 2.1.4 and 2.2.1. HA0 is cleaved on the cell surface during natural infection

by extracellular trypsin-like protease. Many cell systems do not express these proteases. Klenk et al. (1975) demonstrated the correlation of trypsin treatment in *in vitro* cell systems to the induction of more efficient cleavage of the HA and thereby increasing the infectivity of the virus. However, adding trypsin to the system might mask strain specific properties in individual cell culture systems.

2.2.2.2 Replication of IAV in MDCK cells

There are only few cell lines capable of efficiently supporting replication of IAV. Many cell types are known to be susceptible to some strains of IAV, but not to all of them. Most cell lines used are limited to the propagation of one or two strains of influenza A virus [29]. Finding a suitable plaque assay system for influenza A virus has been considered desirable for adequate quantitative studies and of great value for genetic studies since the early 20th century. Therefore, Gaush and Smith characterized MDCK cells with respect to cell growth and immunologic properties as well as their susceptibility to several viruses [28]. The MDCK cell line was derived from a kidney of a female cocker spaniel and was reported to be susceptible to virus infection [31]. In further studies Gaush et al. (1968) established the MDCK cell line for plaque assays of several influenza A and B virus strains. The cell line was susceptible to several virus strains of influenza A and B, including one porcine IAV. Their findings have been confirmed and extended by others, showing that a wide variety of influenza A and B virus strains grow productively in MDCK cells [25][47][99]. A comparative study in 1996 demonstrated MDCK to displayed 100% sensitivity (in a sample size of 63) in human influenza A virus isolation, when compared to a green monkey continuous cell line (Vero) and human lung embryonated cells (MRC-5) [82].

To this day the MDCK cell line is used as a reference cell system for *in vitro* IAV propagation to which other cell systems are compared. In the past decades production of influenza A vaccines in animal cell cultures has been assessed as an important alternative to the traditional method using embryonated chicken eggs. This includes the MDCK suspension cell line MDCK-SUS2 [78]. Still chicken eggs continue to be the system of choice for the production of influenza A viruses in large quantities, since human IAV titers obtained in MDCK cells tend to be lower than in embryonated chicken eggs. Unfortunately, some arguments point to a selective growth of human influenza A viruses in embryonated chicken eggs. They demonstrated to be selective for subpopulations of the virus bearing HAs that differ in one or more amino acids from the predominant sequence of the respective viruses detected replicating in humans [84][87]. Propagating influenza A viruses in MDCK cells, does not cause these mutations, in general. Human influenza A virus H5N1 - related to a highly pathogenic avian influenza A virus in Hongkong - was shown to remain highly pathogenic, even after passaging once in mammalian MDCK cells. The pathogenicity was determined by inoculating the MDCK propagated virus intranasally or intravenously into chicken, resulting in fatality within 48h [17][97].

In MDCK cells one cycle of IAV progeny production requires 8h-10h [29], and rapid replication of virions results within the first 24h p.i. [1][114]. Abdoli et al. (2012) and Rimmelzwaan et al. (1998) established that the total amount of IAV propagated in MDCK cells is relatively independent to the input MOI (1-0.0001). After infecting with a MOI of 1-0.1 maximum virus load - expressed in tissue culture infectious dose 50% (TCID₅₀) - is reached within the first 24h and then remains stable for next 48h. While a MOI of 0.01-0.0001 results also in an increase within the first 24h but maximum titers are reached mostly 24h later, namely at 48h p.i. The optimum time for harvesting IAV has been shown to be 72h p.i. due to the fact that virus has reached the maximum production of progeny daughter virus at this time and pH may start to change [1]. Hence, 72h after infection was considered a good point of time for harvesting, because irrespective of the amount of input virus the maximum output is collectible.

Taken together, currently MDCK lines represent one of the most efficient and broadly used cell system for influenza A virus replication available.

2.2.2.3 Replication of IAV in A549 cells

The A549 cell line was derived from a 58-year-old Caucasian male in 1972. The cell line was established from lung adenocarcinoma tissue and possesses an epithelial morphology. Human influenza A virus can be detected in both, nasal and throat swabs, and replicates in epithelial cells throughout the human respiratory tract. Several arguments imply a greater susceptibility of the lower than the upper respiratory tract [102]. Nevertheless, this cell line is commonly used as a relevant model to study influenza A virus replication *in vitro*, even if many aspects such as signal transduction differ from normal *in vivo* airway epithelial [33][42][59][105]. Studies showed a weak chemokine expression only in A549 cells induced by influenza A viruses, which is likely to be advantageous for propagation of influenza A viruses [65][105]. Li et al. (2009) tested human lung cells for replication of seasonal H1N1 (A/HK/403946/09(H1N1)), swine-originated H1N1 (A/HK/415742/09(H1N1)) and avian (A/Vietnam/1194/04 Clade 1) IAV by comparing viral loads, cpe and immunofluorescence expression of viral NP. The A549 and embryonic lung fibroblasts used in their study propagated viral loads of $> 10^6$ copies/ml for the human influenza A strains, while the avian H5N1 strain - as in most studies - reached even higher loads. Furthermore, all viruses tested caused cpe in A549 cells and NP expression in the respiratory tract cells.

2.2.2.4 Replication IAV in bovine derived cells

In contrast to porcines bovines are not known to be susceptible to IAV infection. One reason is the fact, that they possess a specific antiviral state against influenza viruses, which originates in their ability of inducing Interferon (IFN- α) [40], but further studies are definitely needed to elucidate the complete picture. The KLU-2-R cells used in this study, were prepared and characterized at the Friedrich-Loeffler-Institut (FLI) and derived from a lung of a male bovine fetus. KLU-2-R is a finite cell line which presents a strung-out morphology and which was used in this study as the bovine equivalent to porcine PEL cells. To this day there is no data available on the susceptibility of KLU-2-R cells for IAV.

2.2.3 Myeloid cells and their role in immune response

2.2.3.1 Peripheral blood mononuclear cells (PBMC)

Monocytes originate from specific progenitor cells in the bone marrow from whence they are released into the blood circulation [74]. Monocytes comprise several subpopulations of cells, which differ in size, granularity and functionality [96]. They can migrate into various tissues and subsequently differentiate into different immune cells, e.g. macrophages, dendritic cells or fibrocytes [74]. The expression of specific surface markers is widely used to identify different maturation stages within a cell lineage or to evaluate relationships among different cell types [86]. In swine several peripheral blood monocyte subpopulations have been described, differentiating them by their expression of cell surface molecules (CD) [14][74][86]. Chamorro et al. (2005) defined their subsets on the basis of expression of Swine Workshop Cluster (SWC3), CD14, CD163, and swine leukocyte antigen (SLA) DR markers (also named MHC class II). The SWC molecule is highly expressed in the myeloid differentiation pathway and hence it is a distinct indicator for peripheral blood monocytes [86]. Ondrackova et al. (2013) based his subsets on the CD14, CD163, and MHC class II expression after identifying swine monocytes by their CD172a expression. An alternative way of characterizing porcine monocytes is based on the expression of CD163 [86]. The minor population which is positive for the CD163 marker, shares many characteristics with primary fibrocytes, expressing high levels of CD16 and MHC class II [4].

2.2.3.2 Virus infection of porcine fibrocytes

Fibrocytes belong to the myeloid cells, which enter sites of tissue injuries and mediate wound healing through the production of extracellular matrix proteins [15]. Furthermore, fibrocytes possess antigen presenting functions, by inducing proliferation of CD4+ and CD8+ T-cells [5][15]. Bucala et al. (1994) first described the fibroblast-like cells and their emergence from the blood and termed them ‘fibrocytes’. Fibrocytes, have been described in humans, mouse, macaques and pigs [5][11][15][117]. Porcine fibrocytes are clearly distinguishable from macrophages and monocytes by their typical spindle-shaped morphology [15][11][117] and the expression of CD14, CD16, CD172a, MHC class II, CD80/86, and collagen I [4]. Balmelli et al. (2008) revealed that fibrocytes respond to a variety of Toll-like-receptors ligands, which shows that fibrocytes perceive a large variety of different pathogens and participate in the initiation of immune responses. Fibrocytes share features with dendritic cells [11][15] and Influenza A viruses can infect dendritic cells and macrophages [18][95]. To determine the susceptibility of fibrocytes to virus infections, Balmelli et al. (2005) used a classical swine fever virus (CSFV). The viral detection method did not show virus entry but only *de novo* synthesized proteins. The results showed newly synthesized proteins, demonstrating fibrocytes to be susceptible to productive infection by CSFV. Infection of porcine fibrocytes with an influenza A virus produced for vaccination (FLUAV/Sw/Belzig/2/2001), two avian and three porcine influenza viruses was studied in a recent thesis [60]. Immunoperoxidase assays and viral RNA detection by RT-PCR showed viral antigen in porcine fibrocytes inoculated with porcine and avian IAV isolates. For none of the tested IAV strains productively replication in porcine fibrocytes was shown, as viral titers were determined on MDCK after inoculation. The obtained results could not prove an infectious virus particle in fibrocytes, only the intra cellular presence of viral antigens and viral RNA, without further multiplication within 72h of inoculation.

Materials

3.1 Viruses

3.1.1 Virus isolates

In total twelve virus isolates were used in this study. All viruses were isolated from tissue samples, as indicated in Table 3.1, taken from pigs with respiratory disease provided by pathologists of the Bavarian Health and Food Safety Authority for diagnosis of Influenza A virus infection. Partial genomes of virus isolates A/swine/Bavaria/101001/2013(H3N2), A/swine/Bavaria/18002/2013(H3N2), A/swine/Bavaria/114003/2010(H1N2), A/swine/Bavaria/225002/2011(H1N2), A/swine/Bavaria/338011/2012(H3N2) and A/swine/Bavaria/57002/2013(pdmH1N1) have been described previously in Pippig et al. (2016). Partial genomes of virus isolates A/swine/Bavaria/199002/2014(H1N1), A/swine/Bavaria/400001/2013(H1N1), A/swine/Bavaria/53002/2014(H1N1), A/swine/Bavaria/174002/2014(H1N2), A/swine/Bavaria/42001/2014(pdmH1N2), and A/swine/Bavaria/242001/2013(pdmH1N2) were determined in this study (Section 4.1.2.3)

Table 3.1: List of virus isolates used in this study.

Virus	Internal abbreviation	Organ material
A/swine/Bavaria/199002/2014(H1N1)	i199	lung
A/swine/Bavaria/400001/2013(H1N1)	i400	lung
A/swine/Bavaria/53002/2014(H1N1)	i53	lung
A/swine/Bavaria/174002/2014(H1N2)	i174	trachea
A/swine/Bavaria/114003/2010(H1N2)	i114	lung
A/swine/Bavaria/225002/2011(H1N2)	i225	lung
A/swine/Bavaria/101001/2013(H3N2)	i101	lung
A/swine/Bavaria/18002/2013(H3N2)	i18	lung
A/swine/Bavaria/338011/2012(H3N2)	i338	lung
A/swine/Bavaria/42001/2014(pdmH1N2)	i42	lung
A/swine/Bavaria/242001/2013(pdmH1N2)	i242	lung
A/swine/Bavaria/57002/2013(pdmH1N1)	i57	lung

3.2 Cells

3.2.1 Cell lines

- Madin Darby Canine Kidney (MDCK), ATCC®Nr.CCL-34™
- A549, humane lung carcinoma cells, ATCC®Nr.CCL-185™

3.2.2 Primary cells

- KLU-2-R, embryonic bovine lung cells, Nr.CCLV-RIE 091, Friedrich-Loeffler-Institut, Greifswald, Germany
- Porcine embryonic lung cells, Bavarian Health and Food Safety Authority, Oberschleißheim, Germany
- Porcine fibrocytes, isolated as described in Section 4.2.1

3.3 Cell culture medium

- Minimal Essential Medium (MEM) with Earl's Salts & L-Gluthamine, Gibco®, Life Technologies, Germany
- Roswell Park Memorial Institute (RPMI) 1640, Gibco®, Life Technologies, Germany
- Dulbecco's modified Eagle medium (DMEM+GlutaMAX™), high glucose, pyruvate, Gibco®, Life Technologies, Germany
- TPCK-Trypsin, 50mg powder, derived from bovine pancreas, Thermo Scientific, Germany
- NaHCO₃ (84.0 g/l = 1 mol), SERVA, Heidelberg, Germany
- Fetale bovine Serum (FBS), Biochrom, Berlin

3.4 Kits for nucleic acid extraction

- QIAamp® Viral RNA Mini Kit (250), QIAGEN, Germany
- RNeasy Mini Kit (250), QIAGEN, Germany
- Biosprint 96-One-for-all-Vet Kit (384), QIAGEN, Germany
- QIAquick gel extraction kit, QIAGEN, Germany

3.5 Kits for RT-PCR reactions

- AGPath-ID™ One Step RT PCR KIT, Life Technologies, Germany
- SuperScript®III One-Step RT-PCR System with PlatinumTaq®, Life Technologies, Germany

3.6 Information about real time RT-PCR primers, probes and reaction volumes

3.6.1 Primers, probes and concentration mix for specific amplification of pdmH1 sequences

pdmH1-Mix 1:

Primer	IVA-H1-USA-833F	5'- CTAGTGGTACCGAGATATGCA-3'
	IVA-H1-USA-920R	5'-TATTGCAATCGTGGACTGGTGT-3'
Probe	IVA-H1-USA-856FAM	5'-FAM-CGCAATGGAAAGAAATGCTGGATCTGG-BHQ1-3'

Table 3.2: IVA-H1-Mix-1: Primer and probe sequences and final concentration as described by Hofmann et al. (2010).

Material	Volume(μ l)	Concentration(pmol/ μ l)
Primer H1-USA-833F	20	100
Primer H1-USA-920R	20	100
Probe H1-USA-856FAM	2.5	100
0.1 x TE (pH 8)	157.5	
Total volume	200	

pdmH1-Mix 2:

Primer	A/CAL/H1N1-FW-2	5'- ACACAGAATGCCATTGACGA-3'
	A/CAL/H1N1-RV-2	5'-CTTTCCAGGTGGTTGAACTCT-3'
Probe	A/CAL/H1N1-Probe-2	5'-FAM-TGAAAAGATGAATACACAGTTCACAGCA-BHQ1-3'

Table 3.3: IVA-H1-Mix-2: Primer and probe sequences and final concentration as described by Hofmann et al. (2010).

Material	Volume(μ l)	Concentration(pmol/ μ l)
Primer H1-FW-2	20	100
Primer H1-RV-2	20	100
Probe H1 Probe-2	2.5	100
0.1 x TE (pH 8)	157.5	
Total volume	200	

3.6.1.1 Reaction volume and concentration of MasterMix components for specific amplification of pdmH1 sequences

performed with AgPath-ID™ One-Step RT PCR-Kit (#4387391 Applied Biosystems) according to manufacturer's instructions

Table 3.4: Mastermix for specific H1pandemic2009 IAV PCR

Material	Volume(μl)	Concentration(pmol/μl)
H ₂ O (DEPC)	4.5	
2x Reaction Mix	12.5	
Reverse Transkriptase (RT)	1	
IVA-H1N1-1/2-Mix	2	(Tables 3.3 / 3.2)
Total volume	20	
RNA template	5	

3.6.2 Primers and probes for specific M1-sequence amplifications used in singleplex-M real time RT-PCR protocols

M-Gene:

Primer	M for	5'-AGATGAGTCTTCTAACCGAGGTCG-3'
	M rev	5'-TGCAAAGACACTTTCCAGTCTCTG-3'
Probe		5'-ROX-TCAGGCCCCCTCAAAGCCGA-BHQ2-3'

M primers and probe as described by Hofmann et al. (2010)

3.6.2.1 Reaction volume and concentration of MasterMix components for M-Single-real time RT-PCR

performed with SuperScript®III One-Step RT-PCR System with Platinum®Taq according to manufacturer's instructions

Table 3.5: Mastermix M-PCR, final concentrations as described by Pippig et al. (2016).

Material	Volume(μl)	Concentration(pmol/μl)
2x Reaction Mix	12.5	
Platinum®Taq Mix	0.25	
Primer M-F	0.5	10
Primer M-R	0.5	10
Probe M	0.15	10
H ₂ O(DEPC)	6.1	
Total volume	20	
RNA template	5	

3.6.3 Primers and probes for the Triplex-(H1/N1/M)-real time RT-PCR and Duplex-(H3/N2)-real time RT-PCR

M-Gene:

Primer M for 5'-AGATGAGTCTTCTAACCGAGGTCG-3'
 M rev 5'-TGCAAAGACACTTTCCAGTCTCTG-3'
 Probe 5'-ROX-TCAGGCCCCCTCAAAGCCGA-BHQ2-3'

M primers and probe as described by Hofmann et al. (2010)

H1:

Primer H1 for 5'-TTCATTGAAGGRGGATGGAC-3'
 H1 rev 5'-GCWGCRTARCCAGAMCC-3'
 Probe 5'-YAK-CCATACCATCCATCTATCATTCC-BBQ-3'

H1 primers and probe as described by Pippig et al. (2016)

H3:

Primer H3 for 5'-CRACAGGRATGMGGAAT-3'
 H3 rev 5'-CTGAAACCRATACCARCCGT-3'
 Probe 5'-6FAM-CCARCCATTYTCTATGAAHCCTGCTATTGC-BBQ-3'

H3 primers and probe as described by Pippig et al. (2016)

N2:

Primer N2 for 5'-RCARGGRACCACRCTRGGAC-3'
 N2 rev 5'-ATGCAGCCATGCTTTTCCA-3'
 Probe 5'-Cy5-CYAAATGAAATGGAACACCCAAYTCATTC-BBQ-3'

N2 primers as described by Pippig et al. (2016), N2 probe as described by Nagarajan et al. (2010)

N1:

Primer N1 for 5'-AGRCCTTGYYTCTGGGTTGA-3'
 N1 rev 5'-ACCGTCTGGCCAAGACCA-3'
 Probe 5'-FAM-ATYTGACGYAGYGGGAGCAGCAT-BHQ1-3'

Table 3.6: N1-concentration mix: Primers, probe and final concentration as described by Fereidouni et al. (2012).

Material	Volume(μ l)	Concentration(pmol/ μ l)
Primer N1-F	50	100
Primer N1-R	50	100
Probe N1	6	100
0.1 x TE (pH 8)	344	
Total volume	450	

3.6.3.1 Reaction volume and concentration of MasterMix components for Triplex-(H1/N1/M)-real time RT-PCR and Duplex-(H3/N2)-real time RT-PCR

performed with SuperScript[®]III One-Step RT-PCR System with Platinum[®]Taq according to manufacturer's instructions

Table 3.7: Reaction volume and concentration of MasterMix components as described by Pippig et al. (2016).

Material	Volume(μ l)	Concentration(pmol/ μ l)
2x Reaction Mix	12.5	
Platinum [®] Taq Mix	1	
Primer H1-F	1.25	10
Primer H1-R	1.25	10
Probe H1	0.4	10
Primer M-F	0.5	10
Primer M-R	0.5	10
Probe M	0.15	10
N1-Mix	2	(Table 3.6)
H ₂ O(DEPC)	0.45	
Total volume	20	
RNA template	5	

Table 3.8: Reaction volume and concentration of MasterMix components as described by Pippig et al. (2016).

Material	Volume(μ l)	Concentration(pmol/ μ l)
2x Reaction Mix	12.5	
Platinum [®] Taq Mix	1	
Primer H3-F	1.5	10
Primer H3-R	1.5	10
Probe H3	0.4	10
Primer N2-F	1.5	10
Primer N2-R	1.5	10
Probe N2	0.4	10
Total volume	20	
RNA template	5	

3.7 Information about ‘conventional’ RT-PCR, primers and probes used for sequence analysis

3.7.1 Primers used for specific amplification of porcine H1, H3, N1, N2 gene sequences

H1 Primer:	H1-F	5'-ATGCTAACAAYTCCACMGACACTGT-3'
	H1-R	5'-TCCTGTCCATCCYCCTTCWATGAATCC-3'
H3 Primer:	H3-F	5'-ATGCRGTGCCAAACGGAACGC-3'
	H3-R	5'-CTGAAACCR TACCARCCGT-3'
N1 Primer:	N1-F	5'-GYAATGGTGT TGGATAGGRAG-3'
	N1-R	5'-ACCGTCTGGCCAAGACCA-3'
N2 Primer:	N2-F	5'-AGAGAACCYTATGTRTCATGYG-3'
	N2-R	5'-ATAAKTGGAADCAATGCTATAATC-3'

Primer sequences as described by Pippig et al. (2016).

3.7.1.1 Mastermix for ‘conventional’ RT-PCR used for specific amplification of porcine H1, H3, N1, N2 gene sequences

performed with SuperScript[®]III One-Step RT-PCR System with Platinum[®]Taq according to manufacturer’s instructions

Table 3.9: Information about the Mastermix for conventional RT-PCR used to generate amplicons of H1-specific sequences

Material	Volume(μl)	Concentration(μM)
2x Reaction Mix	12.5	
Platinum [®] Taq Mix	1	
Primer H1-F	0.5	0.2
Primer H1-R	0.5	0.2
H ₂ O(DEPC)	5.5	
Total volume	25	
RNA template	5	

Table 3.10: Information about the Mastermix for conventional RT-PCR used to generate amplicons of H3-specific sequences

Material	Volume(μl)	Concentration(μM)
2x Reaction Mix	12.5	
Platinum [®] Taq Mix	1	
Primer H3-F	1	0.4
Primer H3-R	1	0.4
H ₂ O(DEPC)	4.5	
Total volume	25	
RNA template	5	

Table 3.11: Information about the Mastermix for conventional RT-PCR used to generate amplicons of N1-specific sequences

Material	Volume(μ l)	Concentration(μ M)
2x Reaction Mix	12.5	
Platinum [®] Taq Mix	1	
Primer N1-F	1.5	0.6
Primer N1-R	1.5	0.6
H ₂ O(DEPC)	3.5	
Total volume	25	
RNA template	5	

Table 3.12: Information about the Mastermix for conventional RT-PCR used to generate amplicons of N2-specific sequences

Material	Volume(μ l)	Concentration(μ M)
2x Reaction Mix	12.5	
Platinum [®] Taq Mix	1	
Primer N2-F	1.5	0.6
Primer N2-R	1.5	0.6
H ₂ O(DEPC)	3.5	
Total volume	25	
RNA template	5	

Tables 3.9-3.12: Final concentrations of Mastermix for specific amplification of porcine H1, H3, N1, and N2 gene sequences as described by Pippig et al. (2016).

3.8 Antibodies

3.8.1 Antibodies used for indirect immunofluorescence analyses

- OBT0939 Purified matrix protein(M), Goat, ImmunologicalsDirect, GB (used in dilution 1:500)
- BZL06905 Mouse Influenza A Nucleoprotein, Mouse, Biozol, Germany (used in dilution 1:500)
- Alexa Fluor[®] 488 donkey anti-mouse IgG (H+L), Life Technologies, Germany (used in dilution 1:1000)
- Alexa Fluor[®] 546 rabbit anti-goat IgG Antibody, Molecular Probes, Invitrogen, USA (used in dilution 1:1000)

3.8.2 Antibodies used for FACS analyses

- Anti-MHC class I (SLA-1), 74-11-10 Mouse anti-pig IgG2b kindly provided by Prof. Dr. Armin Saalmüller (University Vienna)

- Anti-MHC class II (SLA-DR) MSA3 Mouse anti-pig IgG2a kindly provided by Prof. Dr. Armin Saalmüller (University Vienna)
- Anti-SWC-3 74-22-15A Mouse anti-pig IgG2b (used in dilution 1:10) kindly provided by Prof. Dr. Armin Saalmüller (University Vienna)
- Anti-CD 14, MIL2 Mouse anti-pig, IgG2b, Biozol, Eching, Germany (used in dilution 1:10)
- Anti-CD 163, Biozol, Eching, Germany (used in dilution 1:10)
- Anti-CD 6, Biozol, Eching, Germany (used in dilution 1:100)
- Anti-CD 172a, Biozol, Eching, Germany (used in dilution 1:100)

3.9 Chemicals

- Agarose, SERVA, Germany
- Antibiotic-Antimycotic 100x, Gibco[®], Life Technologies, Germany
- Aqua demin, Bavarian Health and Food Safety Authority, Germany
- Dimethylsulfoxid (DMSO), Sigma, Germany
- EDTA (Ethylenediamin tetraacetate, 0.3723g/l), AppliChem GmbH, Germany
- Ethidium bromide (C₂₁H₂₀BrN₃), Carl Roth[®], Karlsruhe (used in dilution 10mg/ml water)
- Ficoll (separation medium, density $\rho=1,077$) PAA, Pasching, Austria
- Glycerin, Carl Roth, Germany
- KHCO₃ (Potassium hydrogen carbonate, 1g/l), AppliChem GmbH, Germany
- Mounting Medium (1 : 2 Glycerin and PBS)
- NH₄Cl (Ammonium chloride)(8.29g/l), AppliChem GmbH, Germany
- OH(CH₂O)_nH (Paraformaldehyde), Sigma, Germany
- PBS without Ca⁺⁺/Mg⁺⁺, MP Biomedicals, Germany
- ProLong[®]Diamond Antifade Mountant with DAPI, Invitrogen GmbH, Germany
- A151.1 Roti[®]-Block, 10x concentrate, Carl Roth, Germany
- 10x TBE-Buffer, Biorad, Bio Rad, Germany (used in dilution 1x with aqua demin)
- Trypanblue 0.5%, SERVA, Germany
- 0.5% Trypsin EDTA (10x), Gibco[®], Life Technologies, Germany
- Triton X-100, SERVA, Germany

3.10 Laboratory utilities

- HeraSafe, Biological Safety Cabinet, Kendro Laboratory Products, Germany
- CO₂ incubator CB 150, Binder, Germany
- Hermle Z 233 MK-2, Centrifuge with cooling system, Unitec GmbH, Germany
- Hereaus Megafuge 1.0 Centrifuge, Thermo Scientific, Germany
- Eppendorf centrifuge 5810R, Germany
- Cryofuge 5500i, Hereaus, Germany
- Micro centrifuge, Carl Roth[®], Germany
- Biorad CFX96 Real Time System, C1000Touch Thermal Cycler, Life Science, Germany
- Stratagene Mx30002P, Thermo cycler, Biozym scientific GmbH, Germany
- Biometra T3000 Thermo cycler, Biozym scientific GmbH, Germany
- Biosprint96, Thermo cycler Thermo Fisher, Germany
- Nanodrop 1000 Spectrophometer, Biotechnologie GmbH, Germany
- ShiroGEL horizontal 96 System, Minigele electrophoresis, PEQLAB, Germany
- Standard Power Pack P25T, Electrophoresis, Biometra GmbH, Germany
- Zeiss Observer Z1 AX10, Carl Zeiss MiroImaging GmbH, Germany
- Axioscope 2plus, upright immunfluorescence microscope, Zeiss, United States
- Leitz Wetzlar, inverted microscope, Leitz, Germany
- BZ-X700 (All-in-One Fluorescence Microscope), KEYENCE, Germany
- Olympus CK X41, Microscope, Japan
- Olympus E620, Digital JCR Camera, Japan
- BD FACSCanto II cytometer, Becton Dickinson, Germany
- ChemiDoc[™]XRS+ System with Image Lab[™]Software #1708265, Biorad
- Lab dancer, IKA[®], Germany
- Ultra turrax[®] T25, IKA[®], Germany
- Eppendorf multipette[®] plus, pipetting aid, Eppendorf AG, Germany
- Eppendorf, Easypet, pipetting aid, Eppendorf AG, Germany

3.11 Consumables

- Cellstar[®] 6-Well Cellculture Multiwell Plate, Greiner Bio One, Germany
- Cellstar[®] 24-Well Cellculture Multiwell Plate, Greiner Bio One, Germany
- Cellstar[®] 96-Well Polystyrol Microplate, Greiner Bio One, Germany
- Cellstar[®] Filter Top Cell Culture Flask, 75cm², Greiner Bio One, Germany
- Nunc[™]Cell Culture treated Flask with vent caps, 175cm², Thermo Scientific, Germany
- Hard Shell[®]PCR Plates, 96-Well, Bio Rad Laboratories, USA
- epT.I.P.S.[®] Motion, Eppendorf Quality[™], Germany
- Combitips advanced[®], 10ml, 5ml, 1ml, Eppendorf Biopur[®], Germany
- Eppendorfer Safe lock tubes, Germany
- Individual PCR Tubes, 8-tube strip, white, Bio Rad, Germany
- PCR single cap 8-softstrips, Biozym scientific GmbH, Germany
- Polystyrene Tubes conical bottom, 15ml, Greiner Bio One, Germany
- Polystyrene Tubes conical bottom, 50ml, Greiner Bio One, Germany
- BD 2ml Syringe Luer Lok[™]Tip, Springfield, USA
- Microseal[®] seals, United Kingdom
- Pall[®] Acrodisc[®] 32mm Syringe Filter with 0.45µm Supor Membrane, Pall Corporation, USA
- Microscope slide, Thermo Scientific, Germany
- Glas disks 24-well, Gibco[®], Germany
- Nitril[®]Next Gen[®], gloves, Medidrate, Germany

3.12 Software

- Bio-Rad CFX Manager 3.0, Bio Rad, Life science, United States
- Nanodrop ND-1000 V3.8.1 Biorad, Bio Rad, Germany
- FlowJo 7.6.3., FlowJo,LLC, Oregon, USA
- BLAST (<http://www.ncbi.nlm.nih.gov/BLAST>)
- ClustalOmega (<http://www.ebi.ac.uk/Tools/msa/clustalo/>)
- OriginPro 9.0
- Zen Blue Edition,(confocal imaging), Zeiss, Germany

Methods

4.1 Molecular biological methods

4.1.1 Extraction of RNA

RNA was extracted from animal tissue using the Qiagen RNeasy Mini Kit and cell cultures inoculated with organ material were processed using the QIAamp Viral RNA Mini Kit, both according to the manufacturer's instructions. Total RNA from infected cell samples and their associated supernatants, that were harvested as described in Section 4.2.4, was extracted using the Qiampr Biosprint96 One-for-All-Vet Kit according to the manufacturer's protocol.

4.1.2 Reverse transcription polymerase chain reaction

The polymerase chain reaction (PCR) is a laboratory technology in molecular biology used to amplify targeted DNA segments to detectable levels *in vitro*. The reverse transcription-polymerase chain reaction (RT-PCR nomenclature Bustin et al. (2009)) combines the general principle of PCR with preceding conversion of the RNA template into a complementary DNA (cDNA) using a reverse transcriptase. Compared to a 'conventional' end-point PCR, where the reaction product is detected at the end of the process, a real time PCR allows detection of fluorescence signals in 'real time' while progressing. Therefore, a TaqMan-PCR approach was used, in which hybridization with a sequence specific fluorescent probe and thereby detection of the amplified product is performed simultaneously during PCR cycling.

In order to identify currently circulating porcine IAV subtypes in Bavaria, RNA extracted from tissue samples from the respiratory tract of pigs was subjected to multiple real time RT-PCR assays as described in the following Section 4.1.2.1.

4.1.2.1 Real time RT-PCR to detect and distinguish between sequences specific for H1, H3, N1, and N2 from current, in Southern Germany circulating porcine IAV

In a first step IAV RNA was detected using a one-step real time RT-PCR targeting the matrix protein gene based on the publication by Spackman et al. (2002) but using modified reverse primers as given in Pippig et al. (2016) (Section 3.6.1). To rapidly distinguish between different IAV subtypes, RT-PCR protocols specifically detecting viral RNA sequences which encode for the H1, H3, N1, and N2, were performed as described by Pippig et al. (2016). The following modifications were done: Primers, specific for sequences encoding for the matrix protein, for N1, and for H1 were combined into one triplex assay. Furthermore, one duplex assay combining detection of H3 and N2 encoding sequences was established (Section 3.6.1).

One-step real time RT-PCR assays for detection of pdmH1 sequences were used as described by Hoffmann et al. (2010). Information about primer sequences and real time RT-PCR protocols are given in Section 3.7. Amplification parameters are given in Tables 4.1-4.3.

4.1.2.2 Real time RT-PCR for comparison of viral genome loads in infected cell cultures

To assess replication kinetics of viral RNA a one-step real time RT-PCR protocol was used. Because all SIV had to be detected in one real time RT-PCR assay, probes targeting subtype specific HA and NA genes proved inadequate. The RT-PCR had to target the matrix protein, shared by all IAV subtypes (Table 3.5). Therefore, RNA extracted from samples as described in Section 4.1.1, was amplified using a real time RT-PCR specific for matrix protein sequences. Every assay included negative controls to determine a cutoff value. In addition, a standardized control sample of SIV RNA was used to allow for comparison of quantification cycle (c_q) between independent assays. Amplifications were carried out in 96-well plates using the Biorad C1000Touch Thermal Cycler and analyzed with help of the Bio-Rad CFX Manager 3.0 software. The c_q values were compared by using identical analysis settings. As no absolute quantification was done (e.g. by using a standard curve) c_q values were directly compared and not put into relation to genome copy numbers.

4.1.2.3 Sequence analyses

Isolates representative for actually circulating SIV subtypes in Bavaria were selected for further analyses. In a first step partial nucleotide sequences of HA and NA were determined to confirm the respective subtypes. To this aim RNA was extracted from SIV infected cells as described in Section 4.1.1. By one-step RT-PCR (Tables 3.9-3.12) amplification of H1-, N1-, H3-, N2-specific sequences was done using protocols previously established by Pippig et al. (2016) and given in Section 3.7.1. Thermal PCR profiles are given in Tables 4.4 -4.7. PCR products were visualized after agarose gel electrophoresis, using the intercalating substance ethidiumbromide and purified of the agarose gel via the QIAquick Gel Extraction Kit according to the manufacturer's instructions. Quality and quantity of the purified DNA was assessed using the Nanodrop 1000 Spectrophotometer, (software Nanodrop ND-1000 V3.8.1 Biorad). Nucleotide sequences were determined using forward and revers primers independently (Eurofins MWG Operon, Ebersberg).

Table 4.1: Thermal profile of the real time RT-PCR for specific amplification of pdmH1 sequences.

Temperature	Duration	
45°C	10min	
95°C	10min	
95°C	15sec	
55°C	20sec	} 42 cycles
72°C	30sec	

Table 4.2: Thermal profile for the singleplex-M real time RT-PCR.

Temperature	Duration	
50°C	30min	
95°C	15min	
94°C	30sec	
56°C	30sec	} 42 cycles
72°C	20sec	

Table 4.3: Thermal profile of the Triplex-(H1/N1/M)-real time RT-PCR and Duplex-(H3/N2)-real time RT-PCR.

Temperature	Duration	
50°C	30min	
94°C	2min	
94°C	15sec	
50°C	30sec	} 45 cycles
68°C	60sec	

Table 4.4: Amplification parameters to generate amplicons of H1-specific sequences via 'conventional' RT-PCR.

Temperature	Duration	
50°C	30min	
95°C	2min	
95°C	60sec	
52°C	30sec	} 35 cycles
68°C	60sec	
68°C	5min	

Table 4.5: Amplification parameters to generate amplicons of H3-specific sequences via 'conventional' RT-PCR.

Temperature	Duration	
50°C	30min	
95°C	2min	
95°C	15sec	
53°C	30sec	} 45 cycles
68°C	60sec	
68°C	5min	

Table 4.6: Amplification parameters to generate amplicons of N1-specific sequences by 'conventional' RT-PCR

Temperature	Duration	
50°C	30min	
95°C	2min	
95°C	15sec	
45°C	30sec	} 45 cycles
68°C	60sec	
68°C	5min	

Table 4.7: Amplification parameters to generate amplicons of N2-specific sequences by 'conventional' RT-PCR.

Temperature	Duration	
50°C	30min	
95°C	2min	
95°C	15sec	
48°C	30sec	} 45 cycles
68°C	60sec	
68°C	5min	

Amplification protocols by Pippig et al. (2016).

4.2 Virological methods

4.2.1 Isolation of porcine fibrocytes

Porcine fibrocytes were derived from peripheral blood mononuclear cells (PBMC), which were isolated out of anti coagulated pig blood, using methods adapted after Balmelli et al. (2005). Briefly, PBMC were isolated from the blood of four individual pigs by density gradient centrifugation over Ficoll-paque according to the manufacturer's protocol. 2ml/well of the cell suspension (10^7 cells/ml) were seeded in six-well dishes or 100 μ l/well (with the cell suspension adjusted accordingly) in 96-well dishes and incubated at 37°C in Dulbecco's modified Eagle's medium (DMEM) containing 20% fetal bovine serum (FBS) under a 5% CO₂ atmosphere. The cells seeded in 96-well dishes were used for subsequent characterizing of the surface molecules. After 48h medium was removed and changed to DMEM containing 10% FBS. About twelve days later, elongated, spindle-shaped primary fibrocytes were obtained and split in a ratio of 1:2 or 1:3, relative to the present amount of cells. No further passaging was done and cells of this second passage were used in the assays of this study.

Additionally, surface molecule expressions on the secondary passage of cultured porcine fibrocytes were initially characterized. To this aim cells seeded in the 96-well dishes were incubated with (MHC I 50 μ l/well; MHC II and SWC-3 40 μ l/well; CD14, CD6, CD16 50 μ l/well; CD163 & CD172a 100 μ l/well) surface molecule specific antibodies for 10min at room temperature. After three subsequent washing steps with Phosphate Buffered Saline (PBS) without Ca⁺⁺ and Mg⁺⁺ the cells were incubated with the appropriate fluorochrome labeled anti-species IgG antibodies for another 20min at room temperature. CD163 and CD172a antibodies (100 μ l/well) were fluorescein isothiocyanate (FITC) labeled and incubated for 45min at room temperature in the dark. Subsequently the cells were washed and covered with PBS without Ca⁺⁺ and Mg⁺⁺. Finally the cells were detached with 0.5% trypsin EDTA from the respective cell culture dish and transferred into FACS tubes after the FACS manufacturer's instructions. For proper analysis a cell control which had not been incubated with any of the antibodies as well as a control for unspecific direct binding of every individual anti-species IgG antibody was used and processed in parallel.

4.2.2 Cultivation of porcine embryonic lung cells, MDCK, KLU-2-R and A549 cells

All cells were propagated at 37°C and 5% CO₂. When reaching a density of 95-100% cells were subcultured depending on the cell type. After washing once with PBS without Ca⁺⁺ and Mg⁺⁺, the cells were detached from the flask with 0.5% trypsin EDTA, transferred to Polystyrene tubes and centrifuged by 900Xg for five minutes. Subsequently the cell pellet was resuspended with the appropriate medium and given into a new flask, proportionally to the intended splitting rate.

Porcine embryonic lung cells (PEL) were obtained from the Bavarian Health and Food Safety Authority. The cells were originally prepared from lungs of pig embryos. PEL cells were cultivated in Roswell Park Memorial Institute 1640 (RPMI 1640) medium, 10 to 15% FBS and 2x AntiAnti. For MDCK cells Minimum Essential Medium (MEM) was supplemented with 4% FBS and 0.8% NaHCO₃. A549 were grown in RPMI 1640 medium supplemented with 10% FBS. KLU-2-R were maintained in DMEM containing 10% FBS. PEL cells were passaged up to eight times before phenotypical changes were observed. Consequently, PEL were split at a ratio of 1:2 or 1:3 depending on the cell number and used at passage 3 to 4. In the study passages 228-250 (MDCK), LGL passage 11-23 (A549), and 65-80 (KLU-2-R) were used.

4.2.3 Virus propagation in cell culture

4.2.3.1 Preparation of tissue samples

Lung or trachea material of pigs, selected by their indicative lung pathology, was analyzed by IAV-specific PCR (Section 3.6.3) for the presences of IAV genomes. If genome contents were judged to be high enough ($c_q < 30$) virus isolation was attempted. A sample of 1g was taken under sterile conditions and dispersed with an ultra turax (ultra turax T25). The dispersed material was suspended in MEM containing 10x AntiAnti for 1h at 8°. Subsequently the suspension was centrifuged at 4000Xg for 30min at 8°C. The resulting supernatant was filtered through a 0.45 μ m Supor Membrane.

4.2.3.2 Virus isolation and propagation

MDCK cells were seeded into six-well plates at a density of 3×10^5 cells/well in cell culture medium supplemented with 4% FBS and 0.8% NaHCO₃. 24h after seeding the monolayer of cells was washed once with MEM. Cells were inoculated with 1ml/well of the suspension, prepared as described in Section 4.2.3.1 and another 1ml of MEM supplemented with 1x AntiAnti was added. After incubating for 2h at 37°C, 5% CO₂ the inoculum was removed, cells were washed once with medium and then incubated at 35°C, 5% CO₂ with 2ml of MEM supplemented with 1x AntiAnti, and 2 μ g/ml TPCK-Trypsin to allow for an enhanced cleavage of HA precursor protein. Infected cells were harvested when cpe was prominent but not later than 72h after infection. In a first step the plates containing infected cells were stored at -80°C, then thawed and frozen two more times to disrupt the cells and by this to release adhering mature viral particles. To remove cell detritus the virus suspensions were centrifuged at 1000Xg for 5min. For further amplification of the isolated viruses, MDCK cells grown in 175cm² flasks were infected using 1-2ml of the material resulted from the virus isolation procedure described above (defined as passage one). After incubating for 2h at 37°C the inoculum was removed, cells were washed once with medium and then incubated at 35°C with MEM supplemented with 2 μ g/ml TPCK-Trypsin and 1x AntiAnti. Again infected cells were harvested when cpe was prominent but not later than 72h post infection (p.i.). Flasks containing infected cells were stored at -80°C, then thawed and frozen as described above. Subsequently, virus suspensions were centrifuged at 1000Xg for 5min to remove cell detritus. The supernatants were aliquoted and the cell pellet dismissed.

4.2.3.3 Virus quantification by endpoint dilution

Virus titers were determined on MDCK cells and expressed as tissue culture infectious dose 50% per 100 μ l (TCID₅₀/100 μ l). MDCK cells were seeded 24h before inoculation in 96-well plates in medium supplemented with 4% FBS. Serial log₁₀ dilutions of virus suspensions (10^1 to 10^8) were prepared in MEM. Cells were washed once with MEM and then each dilution (100 μ l) was added to the cells in ten replicates. Cells were then incubated for 2h at 37°C. The virus suspensions were removed, plates were washed once with MEM and then supplemented with 100 μ l/well of MEM containing 2 μ g/ml TPCK-Trypsin and 1x AntiAnti. The 96-well plates were stored in a CO₂(5%) incubator at 35°C. At 72h p.i. the cytopathic effects were evaluated using an inverted microscope and virus titers were calculated using the Spearman-Kärber method [43]. For the individual virus stocks that were used in the following experiments, the virus quantification was done at least twice. Virus stocks were only used if the determined titers did not differ by more than $1 \log_{10}$ between the two independent quantification assays. In all assays untreated cells and mock infected cells were analyzed in parallel.

4.2.4 Virus replication assays

In all sets of experiments cells in six-well plates were infected simultaneously with all viruses assessed. 0h, 24h and 72h p.i. virus titers and viral genome loads were determined. Therefore, MDCK, KLU-2-R, A549, and porcine fibrocytes were seeded in six-well plates for 24h before replication assays were started. Cells from one well were used to determine the number of cells at the time of infection and thus to calculate the respective input multiplicity of infection (MOI). The defined MOI was 0.5. To this aim, cells were detached using trypsin and then stained with 0.09 % trypan blue-PBS solution to distinguish living from dead cells. Living cells were counted using a Fuchs-Rosenthal-counting chamber.

Cells in six-well dishes were infected using the defined MOI of the individual viruses in 1ml of the respective cell culture medium per well. After incubating for 2h at 35°C, 5% CO₂ the inoculum was completely removed, cells were washed carefully, covered with 2ml medium containing 1x AntiAnti and again incubated at 35°C, 5% CO₂. KLU-2-R, PEL, and porcine fibrocytes were additionally supplied with 5% FBS.

In every set of experiments, one well of cells received the same treatment as described, but without viral infection. Furthermore an untreated cell control was conducted to judge possible problems with the cells themselves. Infectious virus and viral RNA was quantified in supernatants and cells independently at different time points p.i., namely directly after washing the viral suspension off the cells and adding fresh medium (0h), 24h, and 72h p.i. Therefore, supernatants were carefully removed and transferred into sterile aliquot tubes and then centrifuged at 100,000Xg for 3min to remove contaminating cellular material. The remaining cells in the six-well plates were covered with 2ml of respective cell culture medium and then frozen at -80°C. After thawing the cell lysates were centrifuged at 100,000Xg for 3 min. The cell pellet was dismissed and the resulting supernatant aliquoted and frozen at -80°C. Virus titers in supernatants and cells were determined as described in Section 4.2.3.3, with the difference that only 5 replicas per dilution were used and that quantification was done only once.

4.2.5 Immunofluorescence assays

To assess viral protein expression in the various cell types, indirect immunofluorescence assays were performed. For that purpose, cells were grown on cover slips in 24-well plates for 24h. The cells were then infected at a MOI of 0.5. After 2h at 35°C, wells were rinsed with PBS without Ca⁺⁺ and Mg⁺⁺ and covered with 1ml of the respective cell culture medium containing 1x AntiAnti. Medium for KLU-2-R, PEL, and porcine fibrocytes contained additional 5% FBS. The cells were incubated at 35°C for another 24h. At each of the indicated time steps, namely directly after removal of the inoculum defined as 0h p.i. and 24h p.i., cells were washed once with PBS without Ca⁺⁺ and Mg⁺⁺ and fixed with 2% paraformaldehyde in PBS without Ca⁺⁺ and Mg⁺⁺ (PFA) for 15min at room temperature. After removing the PFA and repeated washing with PBS without Ca⁺⁺ and Mg⁺⁺, the cell membranes were permeabilized using 0.1% Triton X-100 for 15min. Then unspecific antibody binding sites were reduced using blocking with 10% RotiBlock-PBS for 24h. Cover slips were stored at 8°C until use. Cells on the cover slips were incubated for 60min with a mixture of two antibodies to specifically detect the IAV proteins M1 and NP. Both primary antibodies were used in a dilution of 1:500 in PBS without Ca⁺⁺ and Mg⁺⁺. After incubation, cells were washed three times with PBS without Ca⁺⁺ and Mg⁺⁺, by immersing them into the washing solution for 15min. Afterwards, cells were incubated for 60min with anti-species IgG antibodies. Both these Alexa Fluor[®] conjugated antibodies were used in dilution of 1:1000. The utilized primary monoclonal antibodies were of different species IgG (derived from mouse and goat), allowing for the differentiation between antibodies bound to M1 and to NP. Again, cells were washed twice with PBS without Ca⁺⁺ and Mg⁺⁺ and then once with distilled water. Finally, the cover slips were air-dried and mounted with ProLong[®]Diamond

Antifade Mountant with DAPI onto microscope slides.

4.2.6 Scanning laser confocal microscopy and immunofluorescence microscopy

Firstly, the specimens were analyzed using a Keyence BZ-X700 (All-in-One Fluorescence Microscope). A 10x PlanApo λ NA 0.45 (WD 4.00) objective lens was used. It is incidental that the protein expression, hence the fluorescence intensity, differed from cell type to cell type. Improving individual pictures for every *in vitro* cell system, would go hand in hand with a lack of comparability between the different cell types. Therefore, picture settings were determined in initial experiments to ensure the necessary comparability. Picture settings were: channel blue: 1/10sec (shadow 150); green:1/2, 5sec (shadow 85); red: 1/2, 3sec (shadow 75).

Secondly, the samples were viewed on a Zeiss Observer.Z1 AX10 confocal laser scanning microscope, with a Zeiss LSM 710 laser-unit and EXFO X-Cite Q, Series 120PC fluorescence lamp. Picture settings were determined in initial experiments and then kept constant throughout the following analyses to allow for comparison. A 40x Zeiss EC plan NEOFLUAR APO objective was used and images digitally stored using the software Zeiss ZEN 2008. The triple channel mode was used for the triple-label immunofluorescence analyses. Z stacks through individual cells were collected in six optical sections with a thickness of approximately 0.4 μ m. Start and endpoint of these optical intervals were the top and the bottom of an individual cell. The confocal zoom setting was 2.5.

Results

The aim of the experiments outlined in the following Section, was to assess whether in Southern Germany currently circulating subtypes of porcine influenza A virus vary in their *in vitro* phenotypes. In order to compare specific characteristics, the replication kinetics in various cell culture systems were investigated. For a comparison at different points of time post infection (p.i.), the amount of infectious units, the extend and morphology of virus specific cytopathic effect (cpe), the viral protein expression, and viral genome loads were chosen as parameters.

All viruses used in this study were isolated between the year 2010 and 2014 from tissue samples taken from pigs with respiratory disease, provided by pathologists of the Bavarian Health and Food Safety Authority for diagnosis of Influenza A virus infection (Table 3.1). All isolates were derived from pig holdings throughout Bavaria. One decisive condition for selecting the individual isolates was the ability to propagate the virus in cell culture (Section 4.2.3.2). Isolates of the year 2014 were subtyped by RT-PCR and selected strains were confirmed by sequence analysis. On the one hand isolates described by Pippig et al. (2016) were used within this study. On the other hand, additional viruses were isolated in the frame of this study. The latter isolates (from the year 2014) were subtyped by RT-PCR and subsequently confirmed by analysis of partial sequences of the HA and the NA. All isolates were named after the WHO guideline. For the purpose of clarity we refer to those isolates with the following in-house abbreviations (also described in Table 3.1):

A/swine/Bavaria/199002/2014(H1N1) i199
 A/swine/Bavaria/400001/2013(H1N1) i400
 A/swine/Bavaria/53002/2014(H1N1) i53
 A/swine/Bavaria/174002/2014(H1N2) i174
 A/swine/Bavaria/114003/2010(H1N2) i114
 A/swine/Bavaria/225002/2011(H1N2) i225
 A/swine/Bavaria/101001/2013(H3N2) i101
 A/swine/Bavaria/18002/2013(H3N2) i18
 A/swine/Bavaria/338011/2012(H3N2) i338
 A/swine/Bavaria/42001/2014(pdmH1N2) i42
 A/swine/Bavaria/242001/2013(pdmH1N2) i242
 A/swine/Bavaria/57002/2013(pdmH1N1) i57

MDCK, A549, KLU-2-R, porcine embryonic lung cells, and porcine fibrocytes were selected as *in vitro* system. Currently, MDCK cells represent one of the most efficient and widely used cell system available for IAV replication and were therefore included as a reference system. A549 cells were chosen as a representative for human derived lung cells, representing this *in vivo* host. The bovine cell line KLU-2-R was selected, since it should prove less efficient for SIV replication.

Swine derived cells were important to represent pigs as hosts. Since fibrocytes play a role in the mediated immune system, it was of interest whether SIV strains could infect these cells or not. In all experiments described in this Chapter an input MOI of 0.5 was used. The infectivity of the used virus suspension was controlled after the infection by titration on MDCK cells (Section 4.2.3.3) to confirm the utilized MOI.

5.1 Morphology of infected cells

In a first step, the morphology of the infected cells and the extent of the cytopathic effect (cpe) were assessed at 0h, 24h, and 72h p.i. The experimental setup is described in Chapter 4.2. The 0h p.i. point of time was defined as the time step when the input virus containing supernatants were removed after a preceding two hour incubation period.

Cpe is a modification of cells after virus inoculation, observable via light-microscopy. The structural changes can, among others, be a result of cell lysis - induced by the interaction of influenza A virus with the cell - or of cell death because the cells become incapable of growing. In the experiments of this study, the investigated cpe showed clear correlations to the time-infectivity-kinetics. At 24h, cpe could be detected in cells, which reflects the time SIV needs for several rounds of replication and visible destruction of a cellular monolayer. To judge the observed virus specific cpe, a reference for every cell type was established without adding infectious virus to the cells. One more additional six-well in every infection assay was included without any further treatment, to judge generally alterations in the growth of cells. Hence, the detected modifications could be attributed to virus induced cpe. As observed in our experiments and shown in Figures 5.2 and 5.3, cpe included rounding of the infected cells and detachment from the plates. Therefore, the extend of cpe was quantified by judging the percentage of rounded and detached cells (Tables 5.1 and 5.2).

As expected, no effect could be observed at 0h p.i. First effects became visible at 24h p.i. on MDCK and A549 cells infected with H3N2 isolates, independent of the isolate (Table 5.1). However, at 72h p.i. all SIV isolates induced a distinct cpe in these well established cell lines. The extend of cpe in A549 cells was comparable to the one in MDCK. Nevertheless, the most distinctive cpe of all cell types analyzed was observed on MDCK cells. Notable less cpe was observed for MDCK cells infected with either of the H1N2 isolates, when compared to the other virus strains. The extend of cpe detected in A549 cells did not show significant differences between the individual subtypes (Tables 5.1 and 5.2).

Porcine fibrocytes, obtained after culturing PBMCs of individual donors (Section 4.2.1), appeared as elongated, spindle-shaped cells, as has been reported for mouse, human and pig fibrocytes. The secondary peripheral blood-derived fibrocytes from four individual donors, that were used in the following experiments, were characterized with respect to expression of myeloid markers and molecules related to antigen presentation. Irrespective of the individual donor, albeit with slight variations, high levels of MHC II, CD6, CD16 and CD163 were detectable. In addition, the porcine SWC3 marker was also expressed at a high level. Data are exemplary shown in Figure 5.1

In porcine fibrocytes only the three H3N2 isolates and two H1N2 isolates induced detectable cpe. The extend was notably less than the cpe induced in A549 and MDCK cells. The observations are summarized in Table 5.2. Finally, in KLU-2-R cells, no cpe at all was observed throughout the experiment. Infected cells were indiscernible from the control wells, which were not infected with SIV. Taken together, all H3N2 strains initiated cpe in three out of four cell systems examined and also the most prominent cpe of all strains. While in MDCK and A549 cells cpe was for the first time detectable after 24h, in porcine fibrocytes effects were observed 72h p.i. only. As displayed in Tables 5.1 and 5.2, there was a clear correlation of the extend of cpe and the isolates of a specific SIV subtype. On bovine KLU-2-R cells no cpe became obvious,

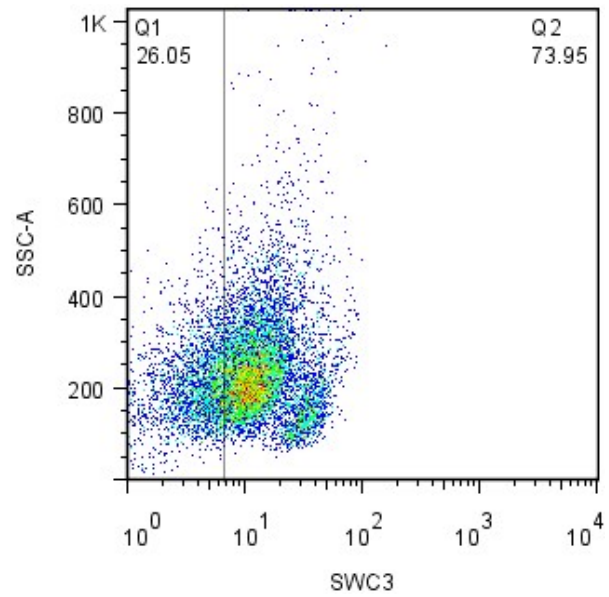
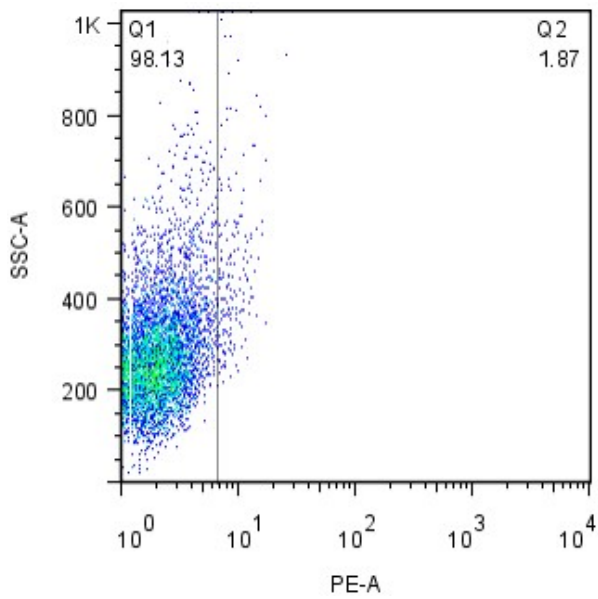
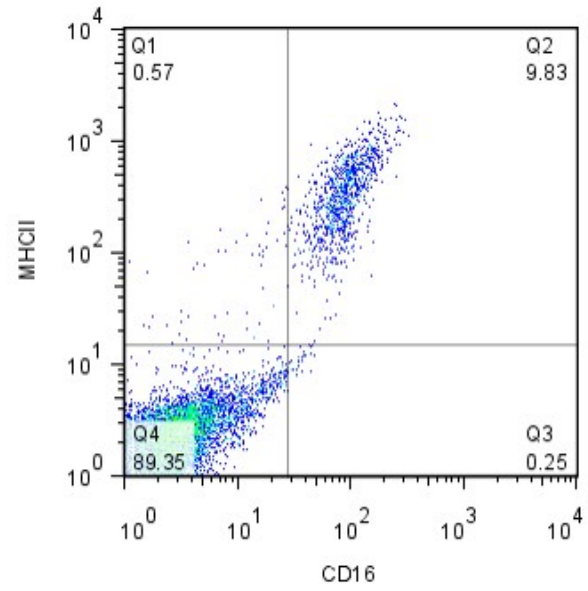
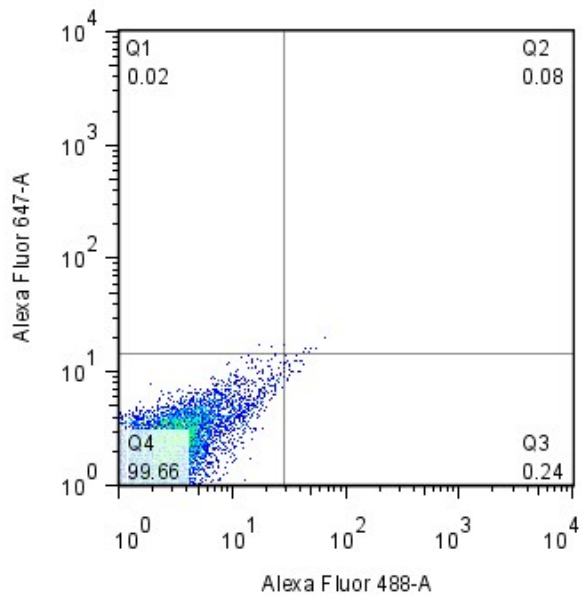
reflecting the low susceptibility of bovines to IAV.

Table 5.1: Extent of cytopathic effects at 24h post infection from 1-5; N=negative; 1=<10%; 2=10-25%; 3=25-50%; 4=50-75%; 5=>75%.

Cells	H1N1			H1N2			H3N2			pdmH1		
	i199	i400	i53	i174	i114	i225	i101	i18	i338	i57	i42	i242
MDCK	N	N	N	N	N	N	1	1	1	N	N	N
A549	N	1	N	N	N	N	1	1	1	N	N	N
KLU-2-R	N	N	N	N	N	N	N	N	N	N	N	N
Fibrocytes	N	N	N	N	N	N	N	N	-	N	N	-

Table 5.2: Extent of cytopathic effects at 72h post infection from 1-5; N=negative; 1=<10%; 2=10-25%; 3=25-50%; 4=50-75%; 5=>75%.

Cells	H1N1			H1N2			H3N2			pdmH1		
	i199	i400	i53	i174	i114	i225	i101	i18	i338	i57	i42	i242
MDCK	2	2	2	1	1	1	3	3	3	3	3	2
A549	2	2	2	2	2	2	3	3	3	2	2	1
KLU-2-R	N	N	N	N	N	N	N	N	N	N	N	N
Fibrocytes	N	N	N	N	1	1	2	2	-	N	N	-



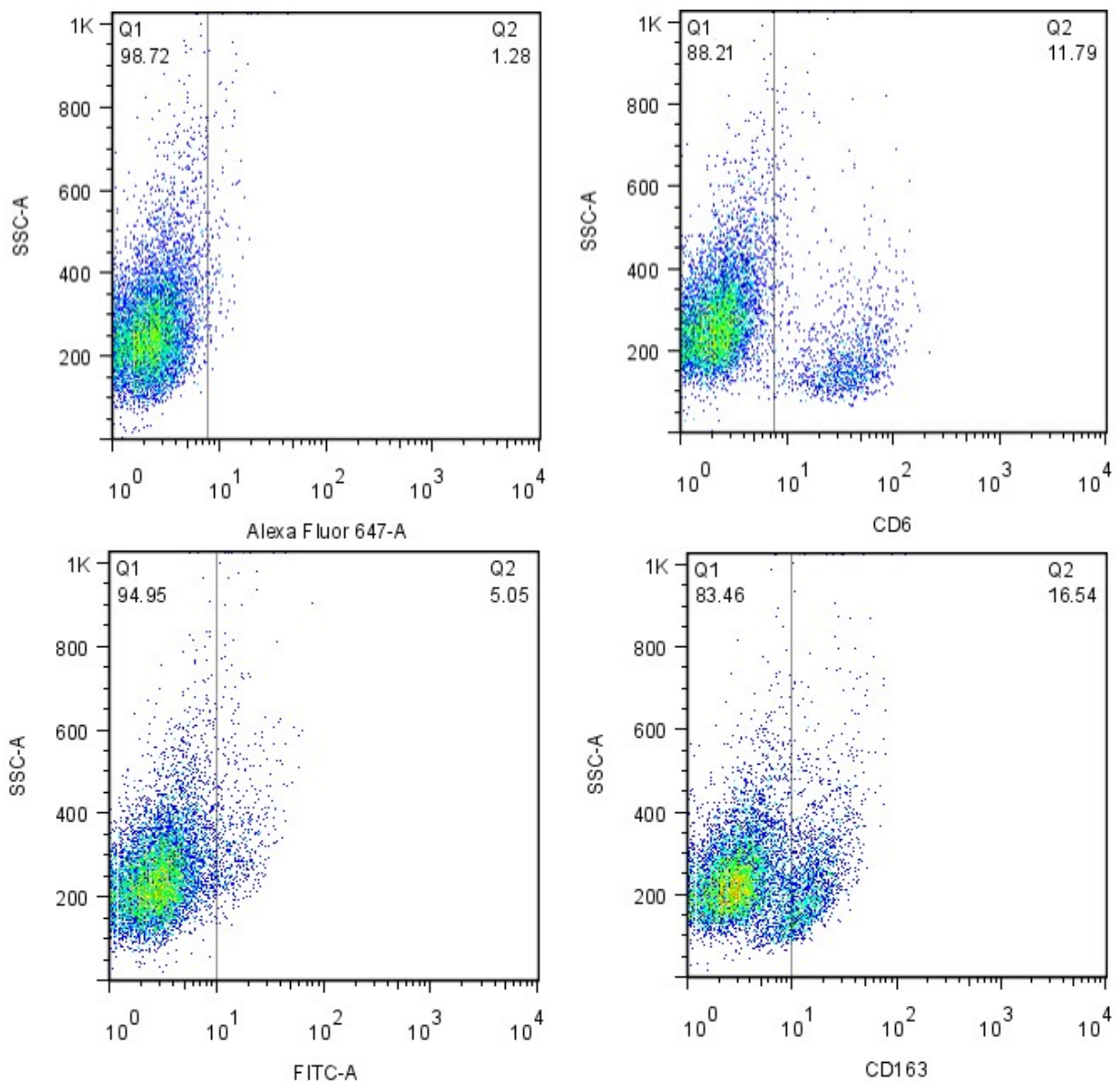
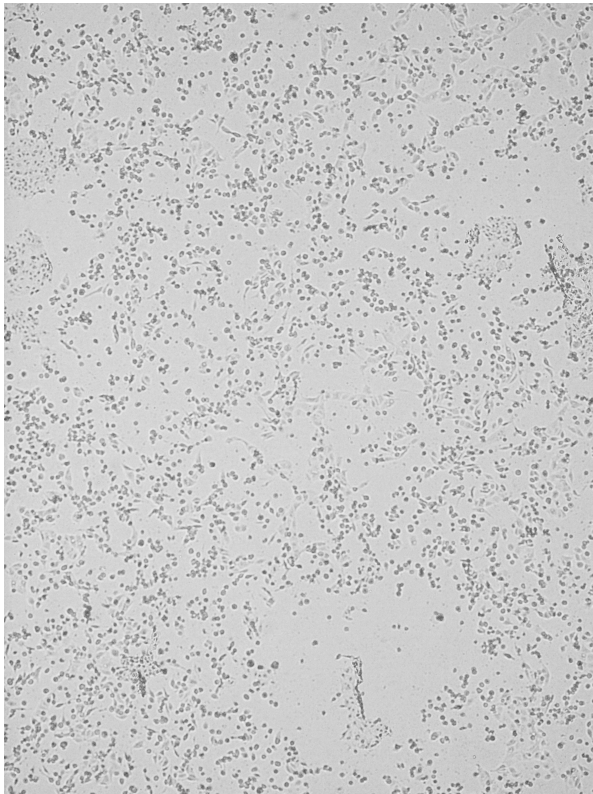
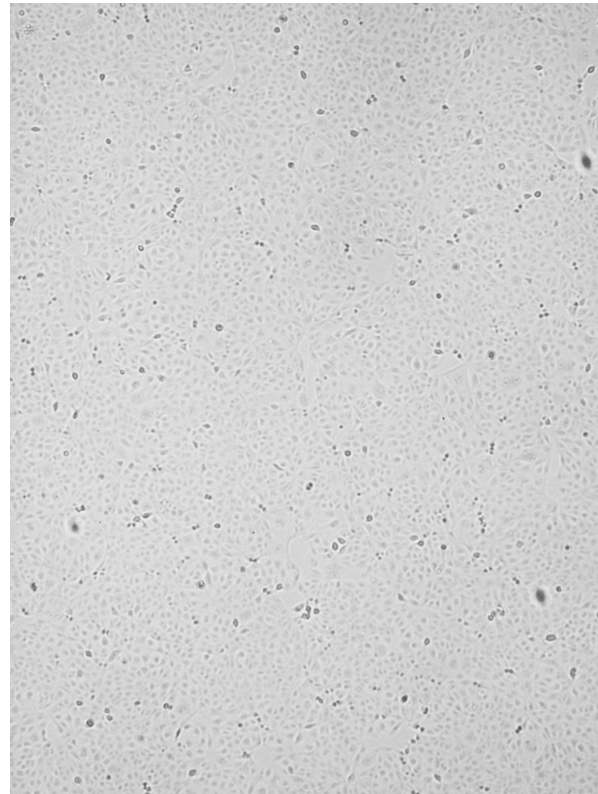


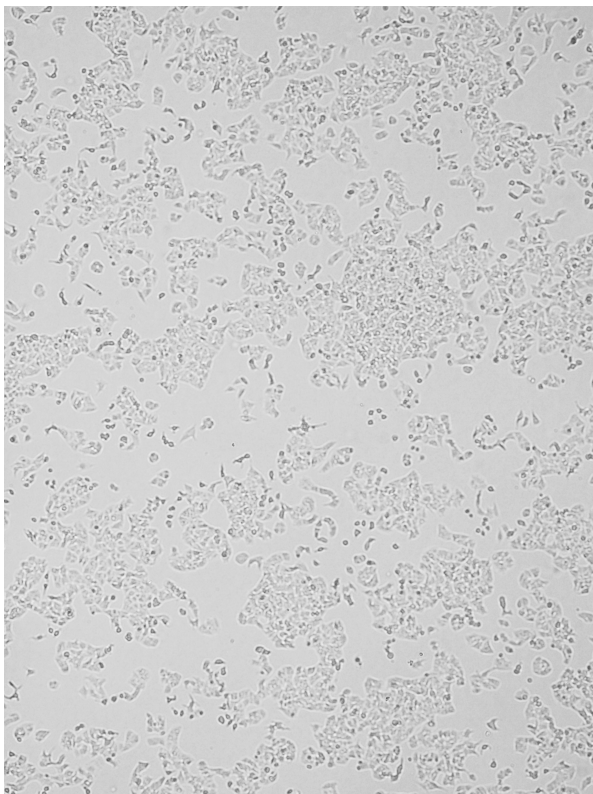
Figure 5.1: Quantitative analysis of porcine fibrocytes for expression of MHC II, CD6, CD16, and the porcine SWC3 marker. Data of one of the four individual sets of porcine fibrocytes used in the study is exemplarily shown. Cell surface staining was performed using antibodies specific for the respective markers, as described in Section 4.2.1. Antigens are given below the individual plots in the right panel. In the left panels data of comparative analyses employing anti-species IgG antibodies only are given. Analysis was done in a BD FACS Canto II cytometer using FlowJo software 7.6.3. Percentage of single and double positive cells is indicated in the upper right position of the quadrants. In a minor cell population CD16 was detected also in co-expression with MHC-II first row.



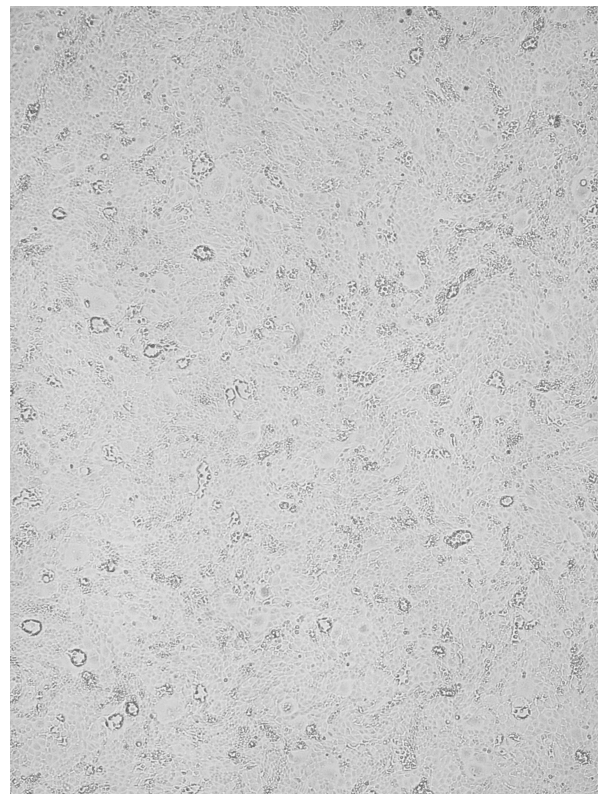
MDCK-i101



MDCK cells



A549-i101



A549 cells

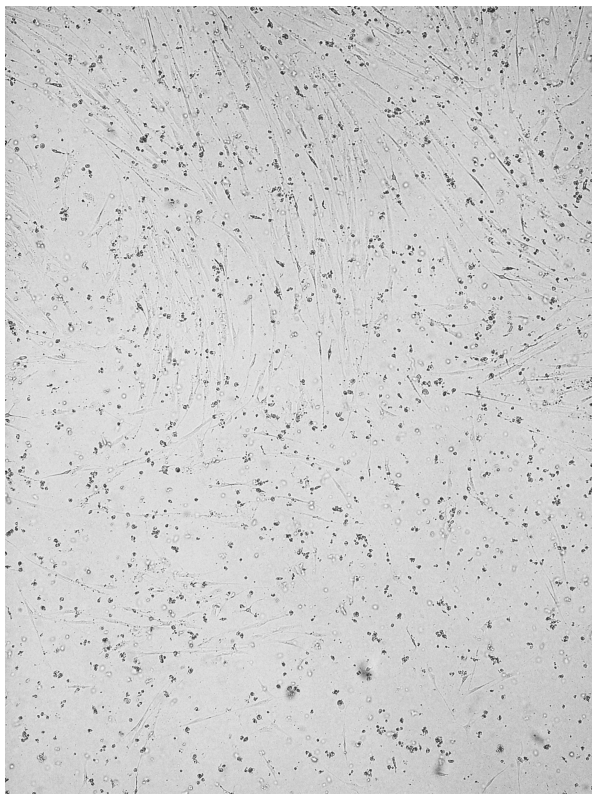
Figure 5.2: Cytopathic effects (cpe) in late (72h p.i.) SIV H3N2 isolate (i101) infected cells. MDCK, A549, KLU-2-R cells and porcine fibrocytes were infected at an MOI of 0.5 and after incubating for 72h the cpe was assessed. Pictures were digitally taken with a Olympus E620 Digital JCR Camera and representative examples for each cell system are given in the illustrations.



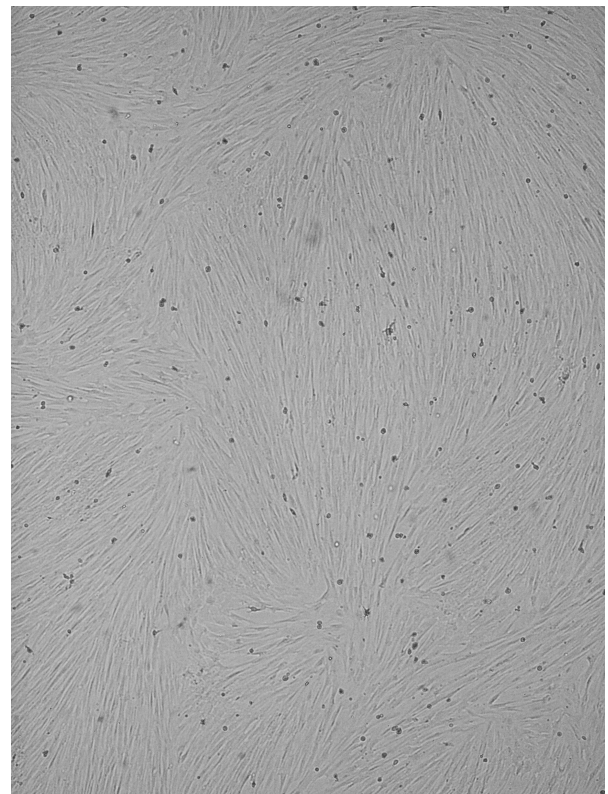
KLU-2-R-i101



KLU-2-R cells



porcine fibrocytes-i101



porcine fibrocytes

Figure 5.3: Cytopathic effects (cpe) in late (72h p.i.) SIV H3N2 isolate (i101) infected cells. MDCK, A549, KLU-2-R cells and porcine fibrocytes were infected at an MOI of 0.5 and after incubating for 72h the cpe was assessed. Pictures were digitally taken with a Olympus E620 Digital JCR Camera and representative examples for each cell system are given in the illustrations.

5.2 Replication kinetics of respective SIV isolates after infection of MDCK, A549, KLU-2-R, PEL cells, and porcine fibrocytes

Infectious virus titers are a crucial parameter for *in vitro* characterization of phenotypes of porcine influenza A viruses. In the present study, it was important to determine whether the SIV strains used were capable of replicating and producing infectious virus progeny in the different cells. For this purpose, the cells were infected with a specific MOI as outlined in Section 4.2.4. In addition to analyzing the morphology of infected cells (Section 5.1), infectious virus titers associated with the cells and the supernatants were determined at 0h, 24h, and 72h p.i. and expressed as TCID₅₀/100µl. The results were obtained in at least three individual and independent experiments and calculated to a mean viral titer with a \pm standard error of the mean (SEM) for every point of time assessed. The results of the replication assays are described in this Section and depicted in Figures 5.4-5.7.

5.2.1 Dynamics of SIV replication in MDCK cells

MDCK cells were infected at a MOI of 0.5. The input infectivity of the virus suspension used was reassessed after the infection was done to confirm the MOI. The input MOIs were calculated to vary between 0.1 and 0.7 for assays on MDCK cells.

Directly after removing the virus inoculum and the washing of the cells (at the point of time defined as 0h p.i, Section 4.2.4), residual infectious virus was still minimally present ($10^{0.2}$ - $10^{0.9}$ TCID₅₀/100µl) in most supernatants. An increase in virus titers in supernatants of infected cells of more than $2\log_{10}$ was observed at 24h p.i. for all virus isolates. Those titers, measured in supernatants, did not significantly alter 48h later in infection (t=72h p.i., variation of -1.32 to +0.76 of \log_{10}), as depicted in Figures 5.4 and 5.9.

In addition, virus infectivity was measured in association with the MDCK cells after carefully removing supernatants. All tested SIV strains had notable infectious titers at this time (t=0h p.i.) associated with cells. However, 24h p.i. the mean titers of all virus isolates varied between $10^{3.3}$ and $10^{4.7}$ TCID₅₀/100µl. All strains reached their detected maximal mean titers at this time. Two viruses (i18 (H3N2); i174 (H1N2)) had lower infectious virus titer maxima, namely only around $10^{2.0}$ to $10^{2.5}$ TCID₅₀/100µl, but the increase of the infectious load within 24h p.i. was obvious (Figure 5.4 d and h). In general, virus titers declined after a peak at 24h. The infectious virus titers determined in MDCK at 72h p.i. showed a mean viral load around $10^{3.0}$ TCID₅₀/100µl or lower for all virus strains, irrespective of the subtype. This observation could be the result of a faster replication, peaking before 72h p.i. in MDCK in comparison to the other cells (Table 5.2).

Summing up, all twelve virus isolates were expectedly capable of producing infectious virus progeny in MDCK cells. This cell line supported the highest infectious virus titers throughout the experiment and in fact the highest mean viral loads of all tested isolates (Figure 5.4 b). Neither obvious differences in multiplication kinetics, nor in the overall virus production could be observed between the different SIV subtypes in the MDCK cells.

5.2.2 Dynamics of SIV replication in A549 cells

A549 cells were infected at a MOI of 0.5, which was again reassessed after infection. For A549-experiments, input MOIs between 0.1 and 0.6 were confirmed. As has been described for MDCK cells (Section 5.2.1), immediately after washing the input virus off the cells (t=0h p.i.), infectious virus was detectable in the associated cells, except for one single isolate (i225 (H1N2)). Notably, these cell-associated virus titers increased during the first 24h p.i. Most viruses reached their

maximum at 24h after infection (mean titers $10^{1.4}$ - $10^{3.6}$ TCID₅₀/100 μ l), except for two H3N2 (i101, i338) and one H1N2 (i114) isolate. For those isolates higher titers were observed after 72h p.i. (Figure 5.5 e, g, and h). All other isolates showed no clear differences between their infective titers at 24h and 72h p.i.

Although the cells were carefully washed, residual infectious virus was observed in supernatants at 0h p.i., correlating with the findings in MDCK cells. Titers in supernatants increased markedly within the first 24h. Afterwards, titers in most supernatants did not vary much (Figure 5.9).

In conclusion, the observed kinetics of multiplication correlated well with those detected in MDCK cells, as depicted in Figures 5.8 and 5.9.

5.2.3 Dynamics of SIV replication in KLU-2-R cells

As reported for the other cell types, KLU-2-R cells were infected at a MOI of 0.5. Again, the used virus suspension was reassessed after the infection was carried out to confirm the input MOI. Variations were calculated to be between 0.1 and 0.6 for assays with KLU-2-R.

No virus multiplication could be detected in KLU-2-R cells, irrespective of the infecting virus. The highest levels of cell associated infectivity were observed directly after inoculating and washing of the cells at 0h p.i. The observed mean titers varied around 10^1 TCID₅₀/100 μ l, probably indicating a recovery of cell-bound input virus. The maximum titers that were reached in all assays, could be detected in cells infected by the pdmH1N1 strain (i57) ($10^{1.8}$ TCID₅₀/100 μ l). Over the following 72h, infectious virus in cells decreased to minimal loads around $10^{0.2}$ TCID₅₀/100 μ l. At 72h p.i., infectious virus was not detectable anymore in three independent experiments (Figure 5.6d, f and h).

The infectious virus titers in supernatants showed somewhat different kinetics. Accordingly, infectious virus was also present at 0h p.i., except for samples i242 (pdmH1N2) and i225 (H1N2). The viral titers detected in supernatants of H1N1 and H1N2 isolates remained constant at low levels within the next 72h (Figure 5.9). In contrast for H3N2 and pandemic subtypes an increase of viral loads in their supernatants was noted at 24h p.i. ($10^{0.5}$ to $10^{1.4}$ TCID₅₀/100 μ l). After that, no further increase could be detected for the respective isolates. As depicted in Figures 5.8 and 5.9, the kinetics of SIV multiplication in KLU-2-R cells were remarkably different to multiplication in A549 and MDCK.

5.2.4 Dynamics of SIV replication in porcine fibrocytes

The reassessed MOI for infections of porcine fibrocytes varied between 0.2 and 0.7, thereby confirming the intended input MOI of 0.5. Residual infectious virus was present in supernatants and associated with cells immediately after washing of the cells, correlating with the findings in MDCK, A549 and KLU-2-R cells. Interestingly enough, no IAV replication could be observed in porcine fibrocytes, except for one individual H3N2 strain. Titers of the respective isolate i101 (H3N2) increased for more than $1\log_{10}$ at 24h p.i. (Figure 5.7 g), posing an interesting exception among the tested virus strains. The other H3N2 isolate used in this assay and one H1N2 strain (i114) produced relatively constant low viral titers (around 10^1 TCID₅₀/100 μ l) throughout the 72h of incubation. For two respective isolates (i18 (H3N2), i114 (H1N2)) no significant decrease could be observed, in contrast to other virus isolates, where titers decreased over time. In this series of experiments both investigated pandemic strains induced titers around 10^1 - 10^2 at 0h and at 24h p.i. A decrease in titer was observed later than for the rest of the samples, namely at 72h p.i., while titers of H1N1 and H1N2 strains already showed a decrease at 24h p.i.

In contrast, titers in supernatants increased between 0h and 24h p.i., irrespective of the subtype. In conclusion, neither of the virus titers, except for the H3N2 viruses, increased at any point of time but rather decreased when infecting porcine fibrocytes. No production of infectious

virus progeny could be observed. The highest titers were detected in infections with the H3N2 subtypes with a mean titer of 10^3 TCID₅₀/100 μ l. In average for the other remaining isolates titers did not exceeded $10^{1.5}$ TCID₅₀/100 μ l. Hence, detected mean titers in porcine fibrocytes never reached levels comparable to those in MDCK or A549 cells.

5.2.5 Dynamics of infectious virus multiplication in porcine embryonic lung cells after SIV infection

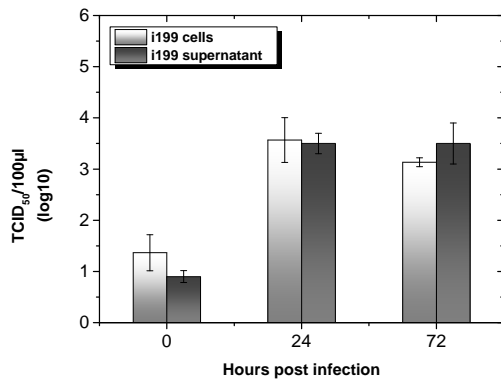
Whereas SIV replication in all other cell systems was assessed in at least three individual and independent experiments, PEL cells were used only once. Results of this single experiment only allow for the conclusion that all virus isolates were capable of replication in these cells, albeit at surprisingly low levels. As observed in assays on MDCK, A549 and KLU-2-R cells and porcine fibrocytes, residual infectious virus was present in supernatants and in cells, immediately after washing of the cells. As depicted in Table 5.4, a notable replication of all viruses, excluding isolate i199 (H1N1) could be observed in PEL within the 72h incubation period, as not only associated with cells but also in supernatants. Maximum titers varied from $10^{1.1}$ - $10^{2.9}$ TCID₅₀/100 μ l (Table 5.3). These results represent one independent experiment, which is the reason why these findings are without strong impact for further interpretation.

Table 5.3: Viral titers determined in supernatants of PEL cells infected with SIV isolates. PEL cells were infected as described in Section 4.2.4. At 0h, 24h, and 72h p.i. supernatants of infected cells were harvested and viral titers were determined. Viral titers are expressed as \log_{10} per 100 μ l. The results of one experiment are given. (N)= no sufficient result

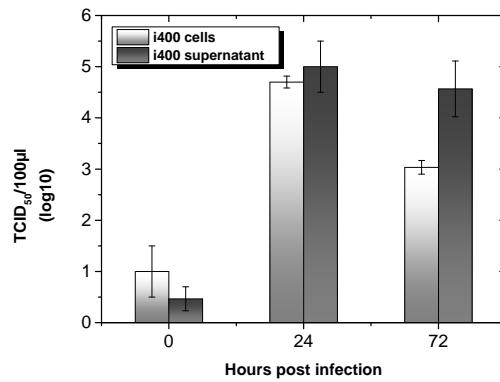
	H1N1			H1N2		
Hours	i199	i400	i53	i174	i114	i225
0	$10^{1.5}$	$10^{0.7}$	$10^{0.7}$	0	0	$10^{1.1}$
24	$10^{0.9}$	$10^{2.1}$	$10^{1.9}$	0	$10^{1.9}$	$10^{1.5}$
72	$10^{0.7}$	$10^{2.9}$	$10^{2.9}$	$10^{1.1}$	$10^{2.9}$	$10^{1.5}$
	H3N2			pdmH1		
Hours	i101	i18	i338	i57	i42	i242
0	$10^{0.7}$	$10^{1.5}$	$10^{1.1}$	0	0	$10^{0.7}$
24	$10^{1.9}$	$10^{1.5}$	$10^{1.5}$	$10^{1.9}$	0	$10^{1.1}$
72	$10^{2.9}$	$10^{1.1}$	N	$10^{0.9}$	0	$10^{1.7}$

Table 5.4: Virus titers determined in PEL cells infected with SIV isolates. PEL cells were infected as described in Section 4.2.4. At 0h, 24h, and 72h p.i. supernatants of infected cells were harvested and viral titers were determined. Viral titers are expressed as \log_{10} per 100 μ l. The results of one experiment are given. (N)= no sufficient result

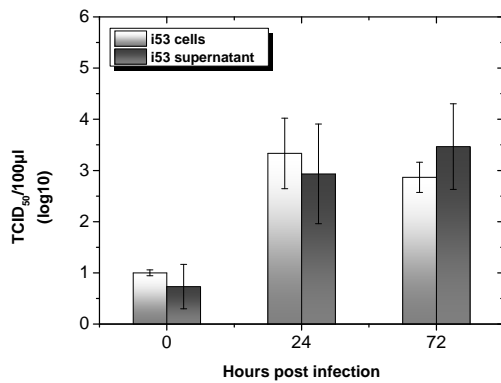
	H1N1			H1N2		
Hours	i199	i400	i53	i174	i114	i225
0	$10^{1.7}$	$10^{1.7}$	$10^{1.3}$	$10^{0.7}$	$10^{1.5}$	0
24	$10^{0.7}$	$10^{2.1}$	$10^{1.9}$	$10^{0.7}$	$10^{2.3}$	$10^{1.3}$
72	$10^{0.9}$	$10^{2.7}$	$10^{1.3}$	$10^{0.7}$	$10^{2.9}$	$10^{0.9}$
	H3N2			pdmH1		
Hours	i101	i18	i338	i57	i42	i242
0	$10^{1.1}$	$10^{1.5}$	0	$10^{1.7}$	$10^{1.1}$	$10^{0.9}$
24	$10^{2.3}$	$10^{2.1}$	$10^{2.3}$	$10^{1.7}$	$10^{1.3}$	$10^{1.1}$
72	$10^{2.7}$	$10^{0.9}$	N	$10^{1.5}$	$10^{1.7}$	0



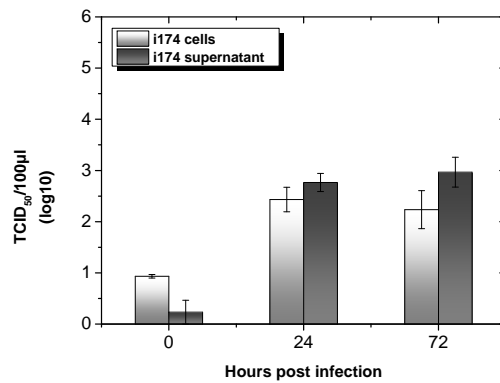
a



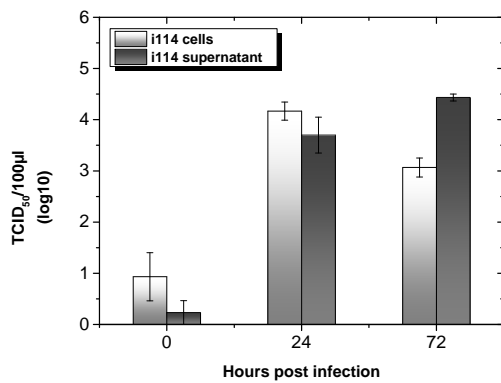
b



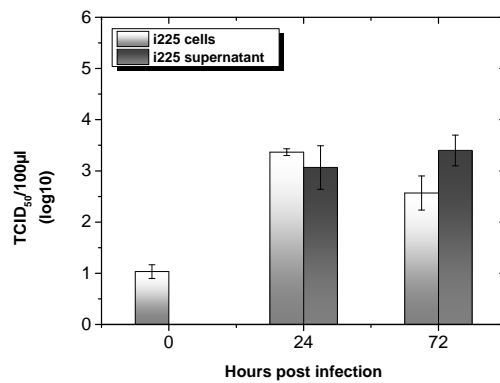
c



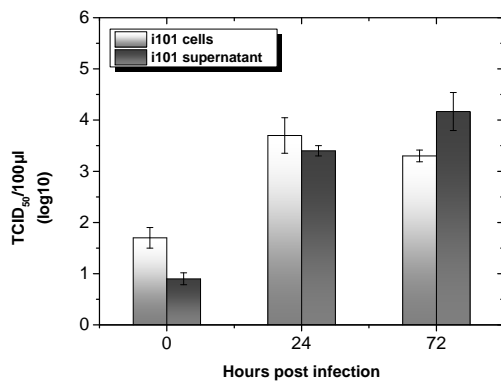
d



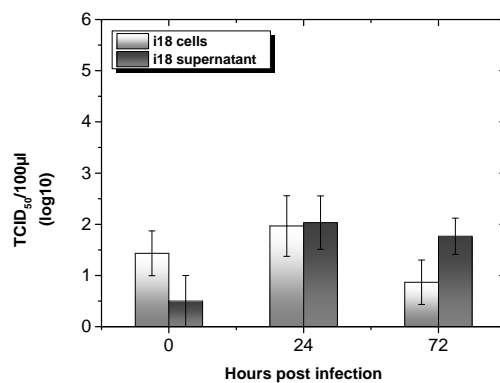
e



f



g



h

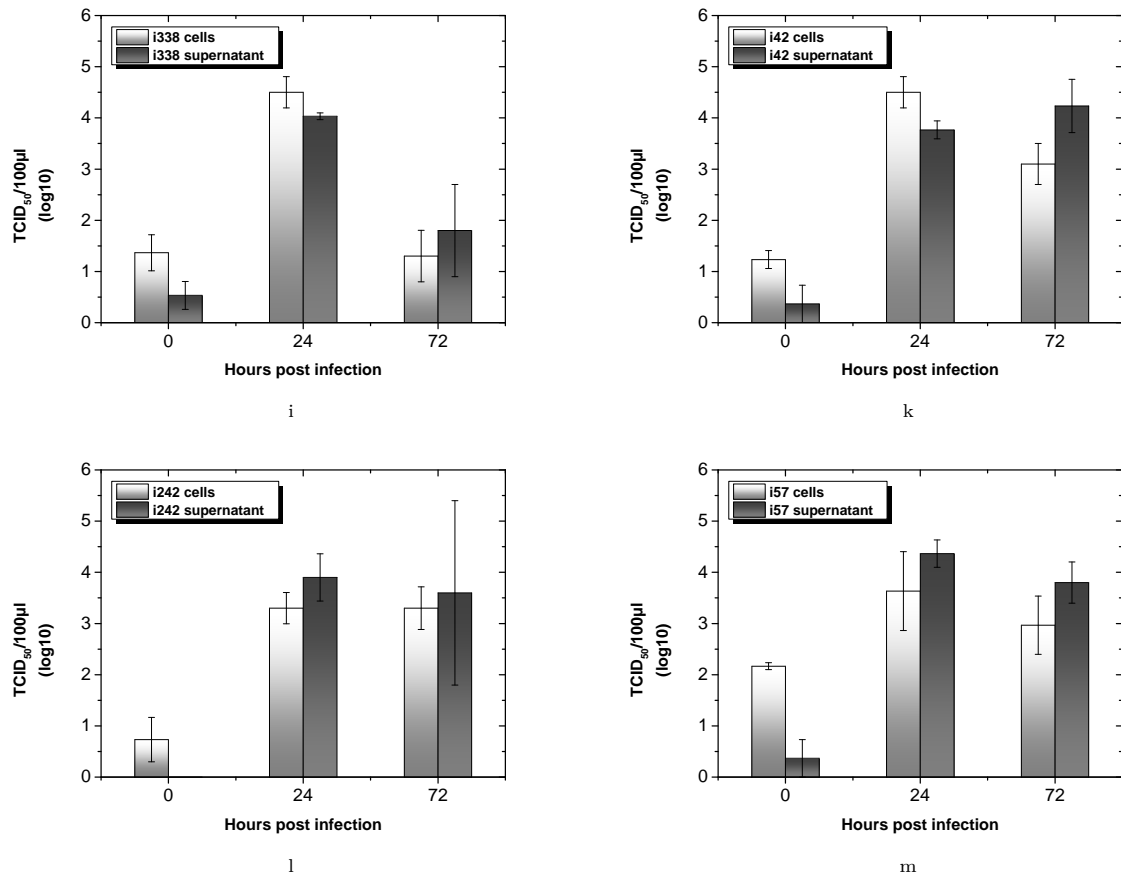
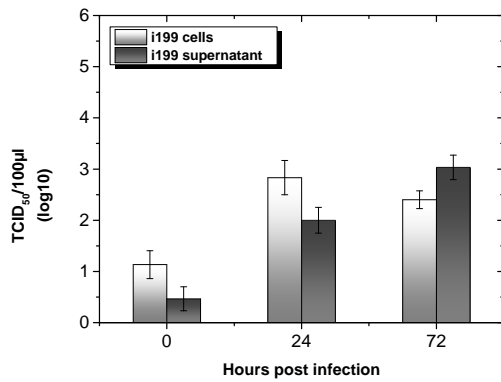
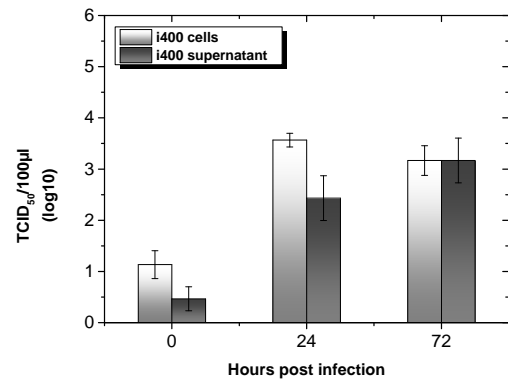


Figure 5.4: Virus titers determined for infections of MDCK cells with twelve different Influenza A virus isolates at 0h, 24h, and 72h p.i. As described in Section 4.2.4 cells were infected with respective SIV and supernatants and cells harvested separately, to determine viral titers (TCID₅₀/100μl). The following virus isolates were used:

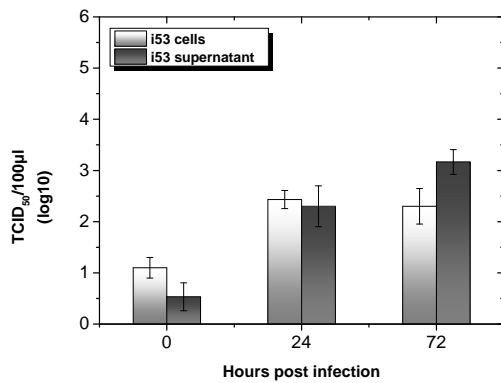
- (a) A/swine/Bavaria/199002/2014(H1N1), (b) A/swine/Bavaria/400001/2013(H1N1), (c) A/swine/Bavaria/53002/2014(H1N1), (d) A/swine/Bavaria/174002/2014(H1N2), (e) A/swine/Bavaria/114003/2010(H1N2), (f) A/swine/Bavaria/225002/2011(H1N2), (g) A/swine/Bavaria/101001/2013(H3N2), (h) A/swine/Bavaria/18002/2013(H3N2), (i) A/swine/Bavaria/338011/2012(H3N2), (k) A/swine/Bavaria/42001/2014(pdmH1N2), (l) A/swine/Bavaria/242001/2013(pdmH1N2), (m) A/swine/Bavaria/57002/2013(pdmH1N1).



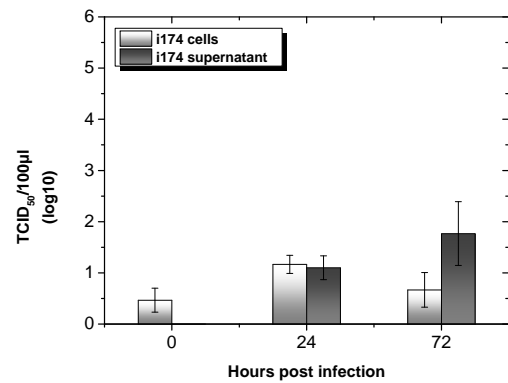
a



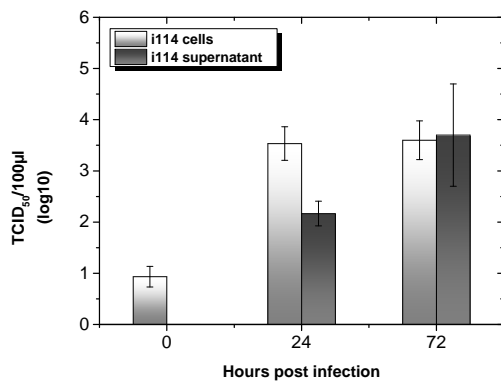
b



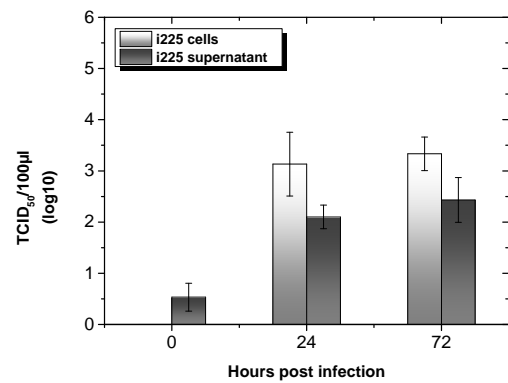
c



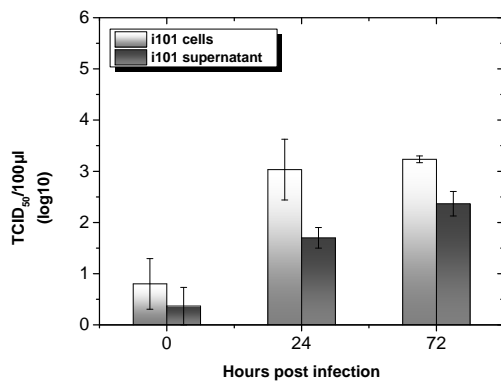
d



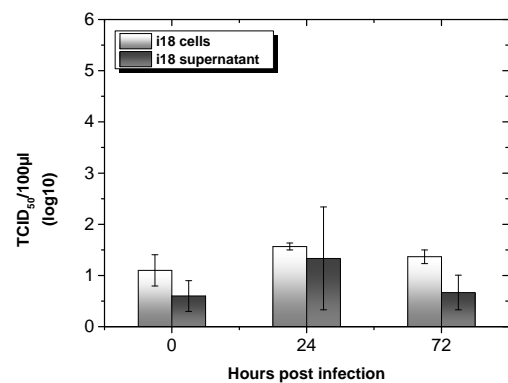
e



f



g



h

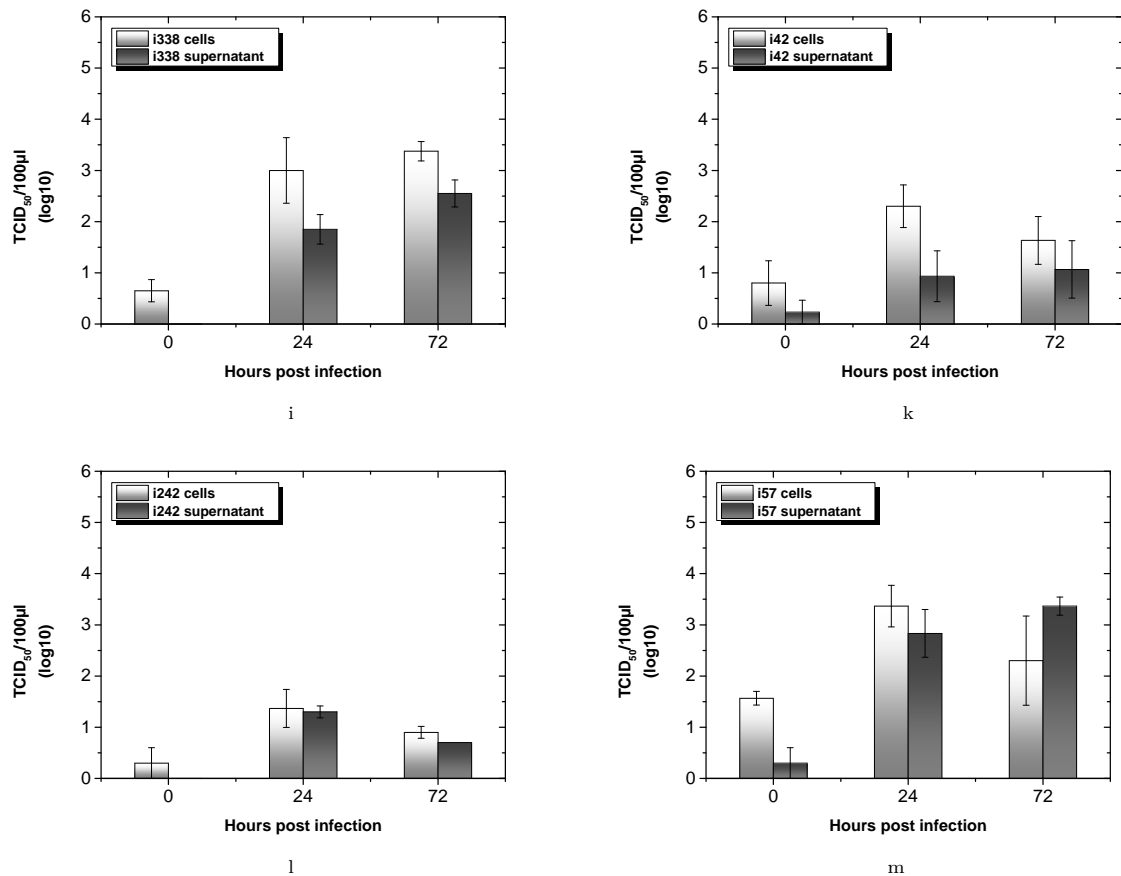
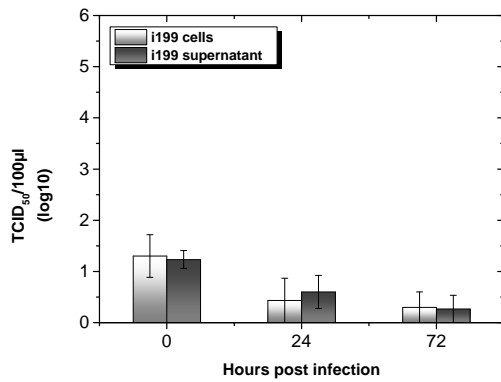
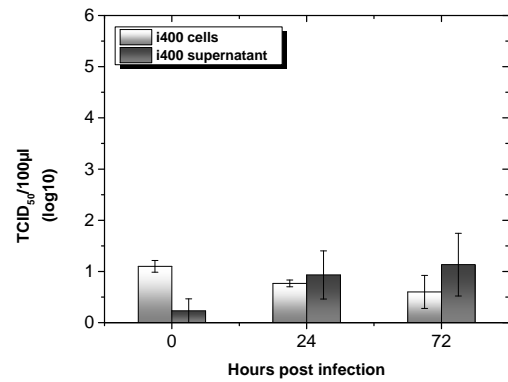


Figure 5.5: Virus titers determined for infections of A549 cells with twelve different Influenza A virus isolates at 0h, 24h, and 72h p.i. As described in Section 4.2.4 cells were infected with respective SIV and supernatants and cells harvested separately, to determine viral titers (TCID₅₀/100µl). The following virus isolates were used:

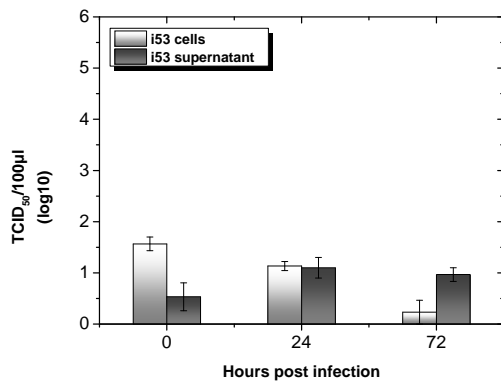
(a) A/swine/Bavaria/199002/2014(H1N1), (b) A/swine/Bavaria/400001/2013(H1N1), (c) A/swine/Bavaria/53002/2014(H1N1), (d) A/swine/Bavaria/174002/2014(H1N2), (e) A/swine/Bavaria/114003/2010(H1N2), (f) A/swine/Bavaria/225002/2011(H1N2), (g) A/swine/Bavaria/101001/2013(H3N2), (h) A/swine/Bavaria/18002/2013(H3N2), (i) A/swine/Bavaria/338011/2012(H3N2), (k) A/swine/Bavaria/42001/2014(pdmH1N2), (l) A/swine/Bavaria/242001/2013(pdmH1N2), (m) A/swine/Bavaria/57002/2013(pdmH1N1).



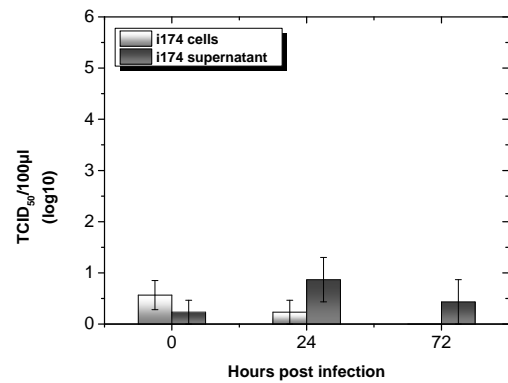
a



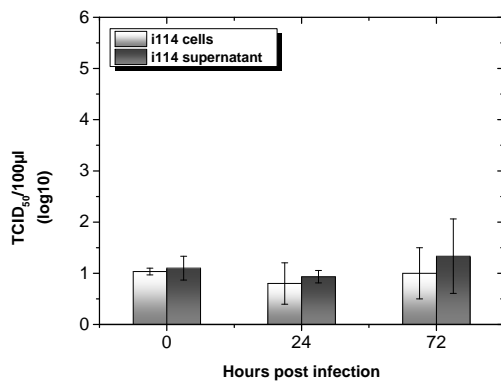
b



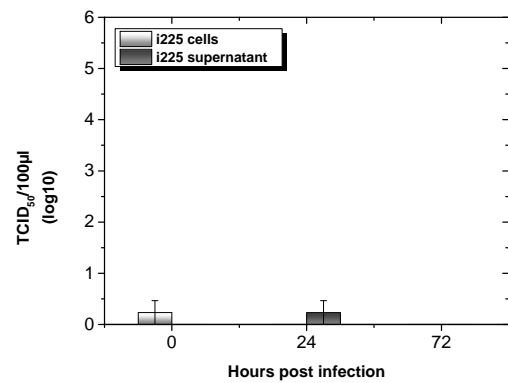
c



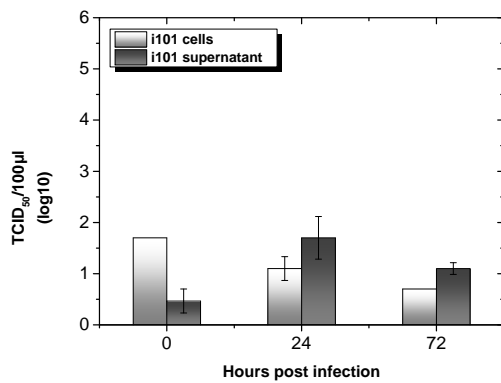
d



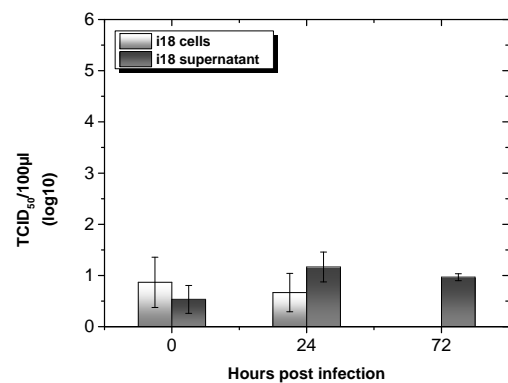
e



f



g



h

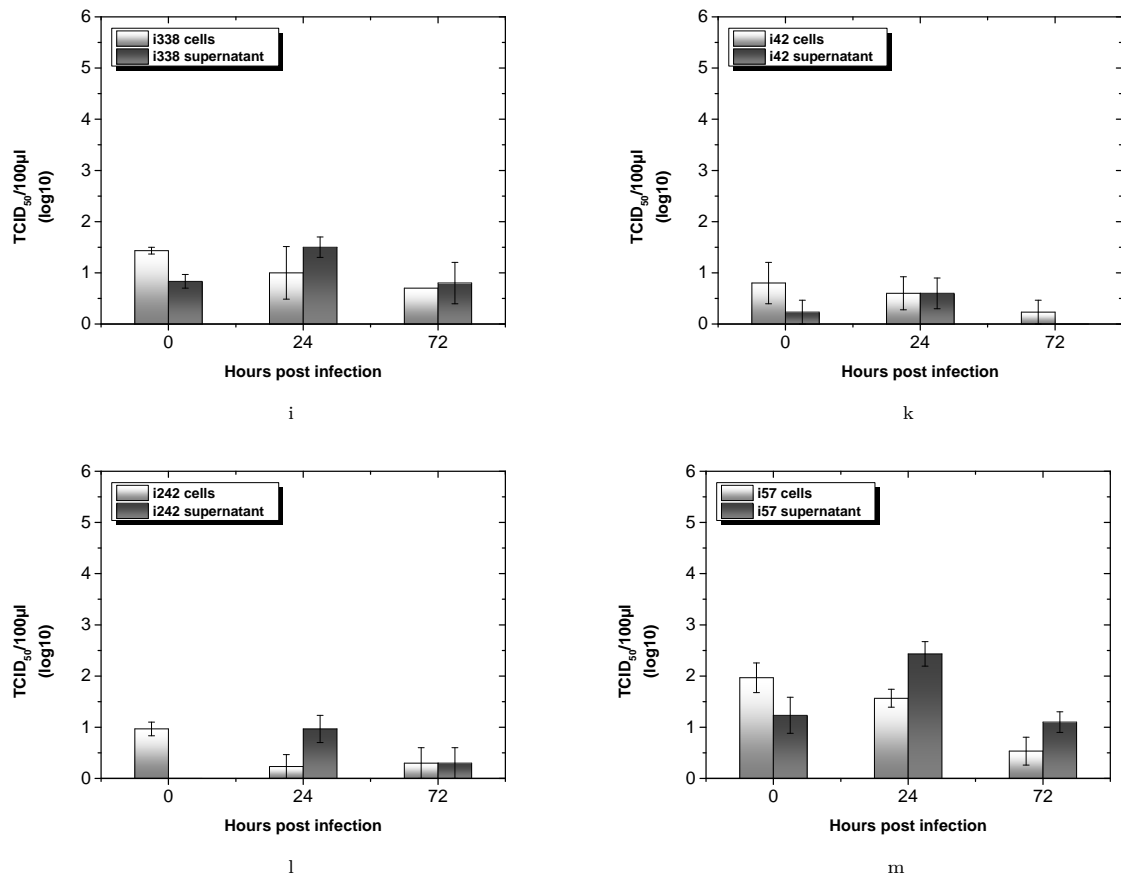
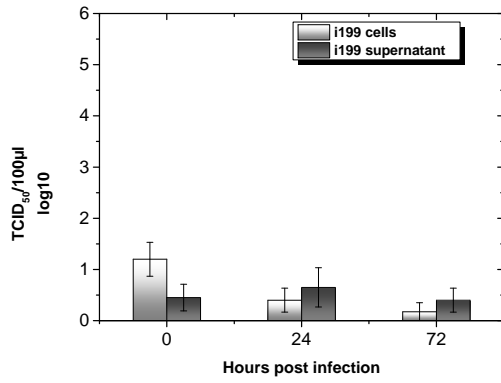
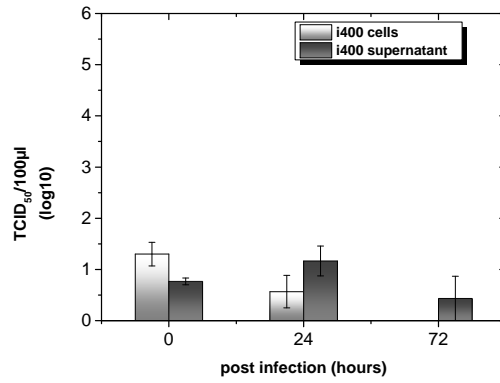


Figure 5.6: Virus titers determined for infections of KLU-2-R cells with twelve different Influenza A virus isolates at 0h, 24h, and 72h p.i. As described in Section 4.2.4 cells were infected with respective SIV and supernatants and cells harvested separately, to determine viral titers (TCID₅₀/100µl). The following virus isolates were used:

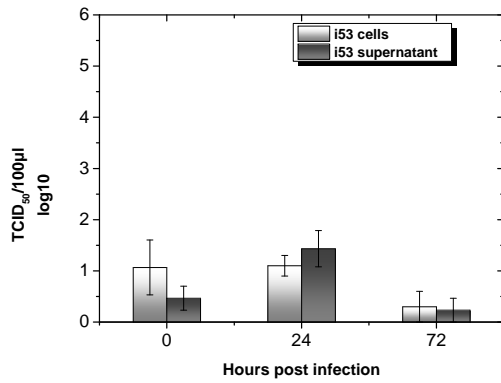
- (a) A/swine/Bavaria/199002/2014(H1N1), (b) A/swine/Bavaria/400001/2013(H1N1), (c) A/swine/Bavaria/53002/2014(H1N1), (d) A/swine/Bavaria/174002/2014(H1N2), (e) A/swine/Bavaria/114003/2010(H1N2), (f) A/swine/Bavaria/225002/2011(H1N2), (g) A/swine/Bavaria/101001/2013(H3N2), (h) A/swine/Bavaria/18002/2013(H3N2), (i) A/swine/Bavaria/338011/2012(H3N2), (k) A/swine/Bavaria/42001/2014(pdmH1N2), (l) A/swine/Bavaria/242001/2013(pdmH1N2), (m) A/swine/Bavaria/57002/2013(pdmH1N1).



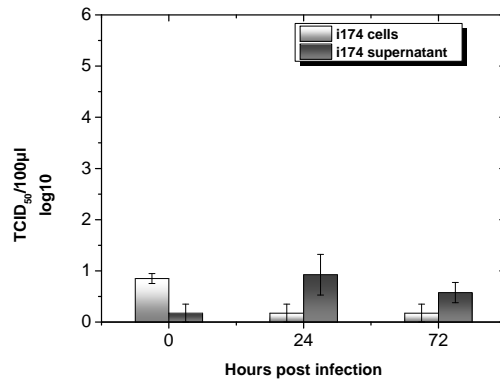
a



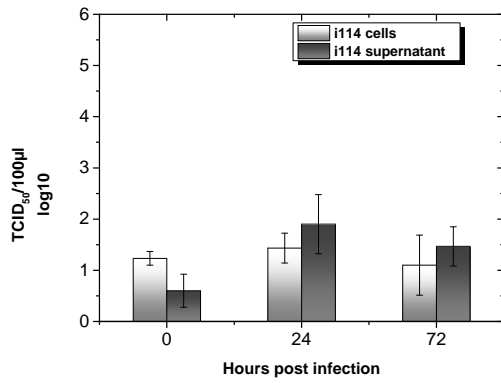
b



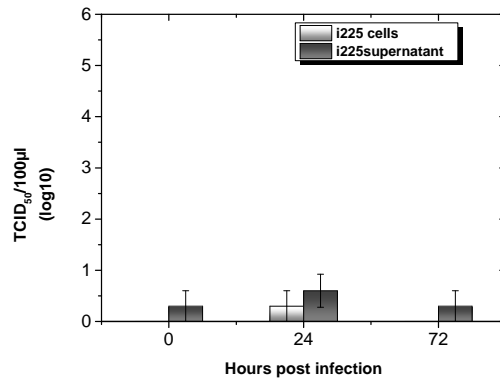
c



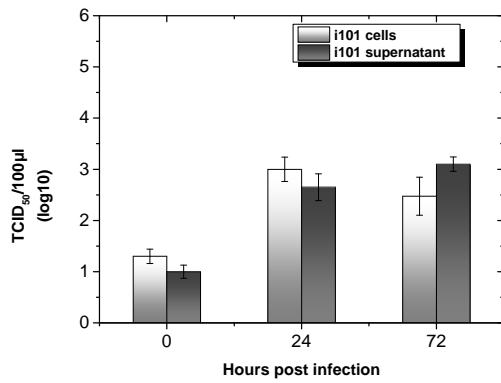
d



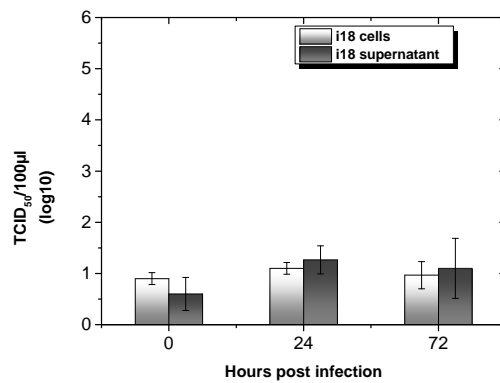
e



f



g



h

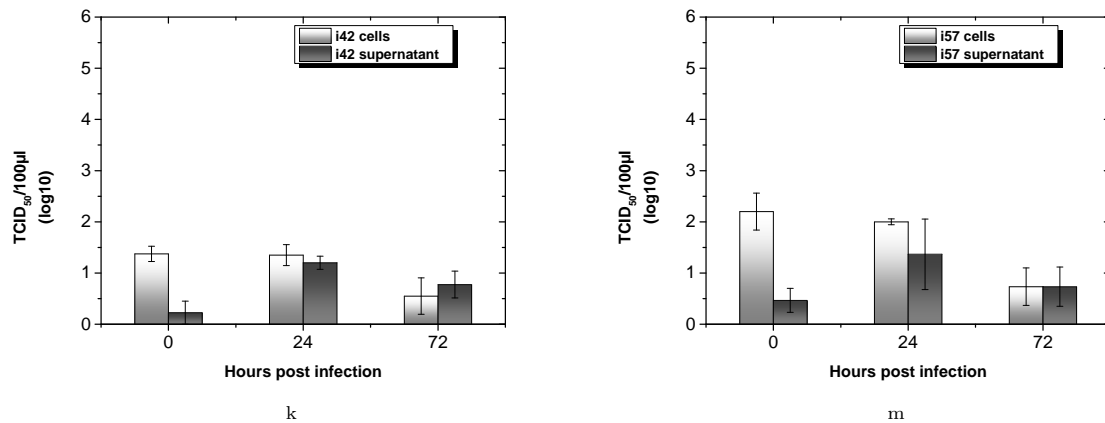


Figure 5.7: Virus titers determined for infections of porcine fibrocytes with twelve different Influenza A virus isolates at 0h, 24h, and 72h p.i. As described in Section 4.2.4 cells were infected with respective SIV and supernatants and cells harvested separately, to determine viral titers (TCID₅₀/100µl). The following virus isolates were used:

(a) A/swine/Bavaria/199002/2014(H1N1), (b) A/swine/Bavaria/400001/2013(H1N1), (c) A/swine/Bavaria/53002/2014(H1N1), (d) A/swine/Bavaria/174002/2014(H1N2), (e) A/swine/Bavaria/114003/2010(H1N2), (f) A/swine/Bavaria/225002/2011(H1N2), (g) A/swine/Bavaria/101001/2013(H3N2), (h) A/swine/Bavaria/18002/2013(H3N2), (k) A/swine/Bavaria/42001/2014(pdmH1N2), (m) A/swine/Bavaria/57002/2013(pdmH1N1).

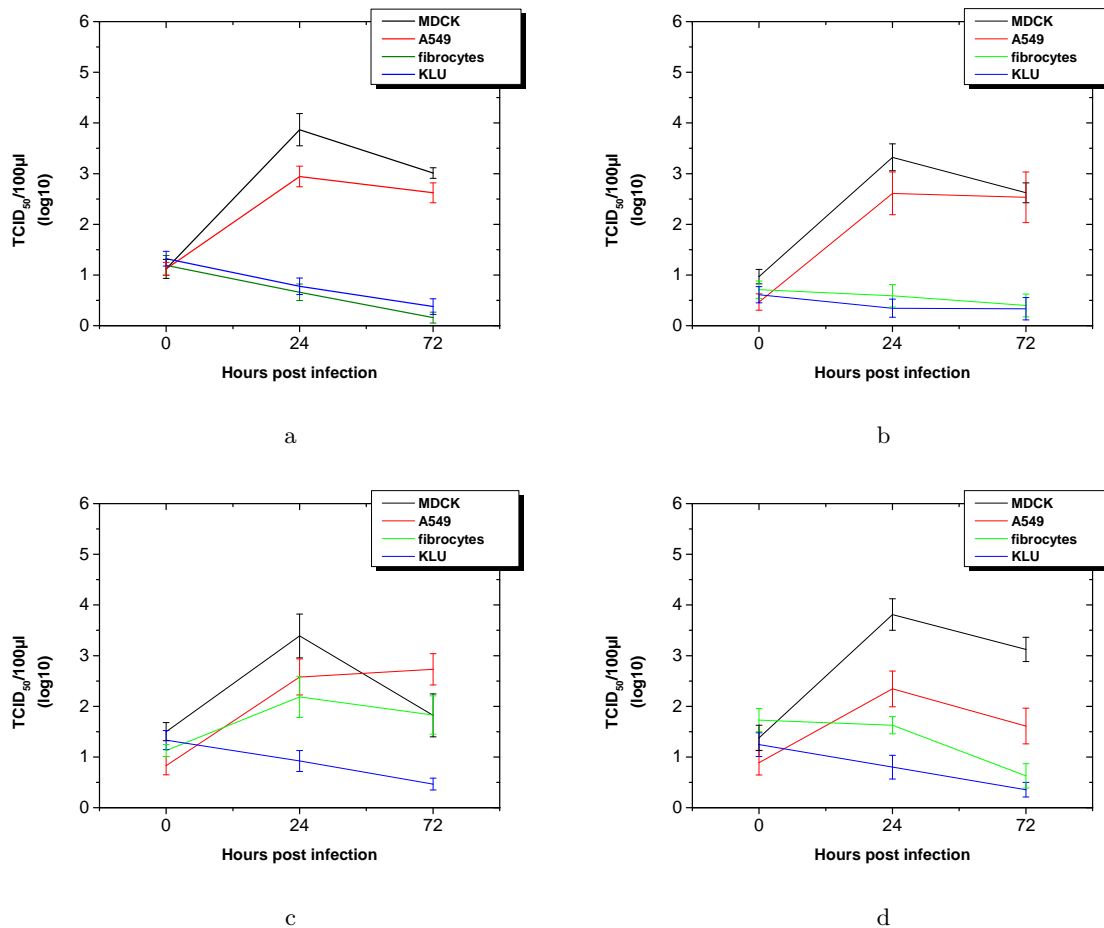


Figure 5.8: Comparative study of replication kinetics of current SIV isolates on MDCK, A549, KLU-2-R cells and porcine fibrocytes - cell associated infectivity. At 0h, 24h, and 72h p.i. supernatants were removed and cell associated viral titers were determined. Results are expressed as TCID₅₀/100µl ± standard error of the mean (SEM) of at least nine independent experiments using three individual isolates for each IAV subtype. Mean virus titers of subtype (a)H1N1, (b)H1N2, (c)H3N2, (d)pdmH1N1, pdmH1N2 on MDCK, A549, KLU-2-R cells and porcine fibrocytes.

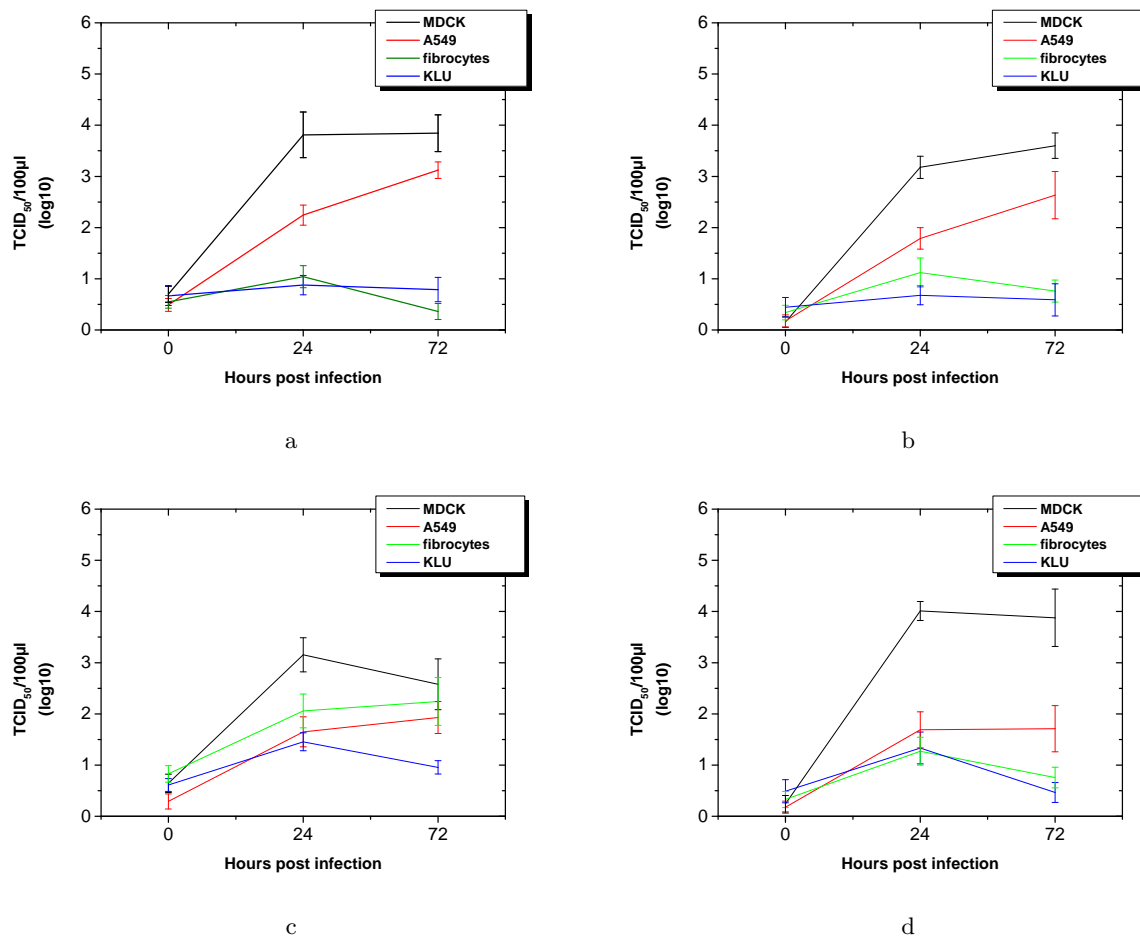


Figure 5.9: Comparative study of replication kinetics of current SIV isolates on MDCK, A549, KLU-2-R cells and porcine fibrocytes - supernatant associated infectivity. At 0h, 24h, and 72h p.i. supernatants were collected and their viral titers were determined. Results are expressed (TCID₅₀/100µl) ± standard error of the mean (SEM) of at least nine independent experiments using three individual isolates for each IAV subtype. Mean virus titers of subtype (a)H1N1, (b)H1N2, (c)H3N2, (d)pdmH1N1, pdmH1N2 on MDCK, A549, KLU-2-R cells and porcine fibrocytes.

5.3 Dynamics of viral RNA loads after infection of MDCK, A549, KLU-2-R cells, and porcine fibrocytes with current isolates of porcine IAV

The dynamics of viral genome loads were assessed as a second parameter to address in vitro phenotypes of current SIV isolates. They were investigated to get information about viral RNA multiplication in infected cells and to look for correlations between kinetics of viral titers and viral RNA loads. The dynamics of viral RNA loads over the 72h of incubation after infection with twelve different virus isolates were assessed by real time RT-PCR. For this purpose, the infected cells and supernatants (Section 4.2.4) were harvested at 0h, 24h, and 72h p.i. Total RNA and DNA were extracted separately from supernatants and cells as described in Section 4.1.1. Subsequently, a real time RT-PCR protocol (Table 3.5) with probe and primers (Section 3.6.1), targeting the matrix-gene of IAV, was used to measure the presence of viral RNA. Amplifications were carried out in 96-well plates using the Biorad C1000Touch Thermal Cycler and analyzed with the Bio-Rad CFX Manager 3.0 software. The retrieved c_q values were compared between individual PCR-experiments using identical analysis settings. According to the detection limit and sensitivity of the PCR technique used, c_q values >39 were rated as not specific, or not relevant, respectively. Because no absolute quantification was done, the respective c_q values were directly compared and not put into relation to genome copy numbers. However, c_q values represent the number of cycles until an increase in fluorescence signal is detected. Since a lower number of cycles before this increase directly represents a higher load of specific input RNA, the c_q value can be taken as measurement for the viral RNA level in a sample. Therefore, a higher c_q value indicates a lower viral RNA load, while smaller values represent higher viral RNA loads.

5.3.1 Dynamics of viral RNA loads in SIV infected MDCK cells

Irrespective of the input virus, the cell associated c_q values ranged between 25.7 and >39 at 0h p.i. and in most experiments the values were higher than 29. This cell associated RNA load resulted from bound or already internalized viral particles. The mean c_q values in supernatants were comparable at this point of time, indicating residual input virus RNA. Since a markedly decrease of c_q values between 6 and 15 levels was observed within the first 24h of incubation in the cells, genome replication and/or mRNA transcription was clearly demonstrated for all isolates in MDCK cells within this time-frame.

For most samples, the detected mean c_q values in supernatants indicated a wide variance and hence a large standard error of the mean (SEM). Therefore, most differences observed between the individual points in time had to be regarded as not significant. The reason for this is most probably the production and release of infectious virus progeny from cells into the supernatants. Another reason for these results may be the detachment of just lightly cell-bound virus particles from cell surfaces into the supernatants.

Accordingly, end-point c_q values detected in MDCK cells at 72h p.i. also varied notably. A possibility would be the influence of the degree of cell destruction, resulting in transfer of already replicated RNA and/or mRNA into the supernatants. In addition, the instability of viral RNA upon prolonged incubation at 37°C has to be taken into account.

5.3.2 Dynamics of viral RNA loads in SIV infected A549 cells

The mean c_q values detected in A549 cells at 0h p.i. were comparable to those found in MDCK cells. Irrespective of the virus isolate the notable decrease of c_q values in supernatants and associated with cells indicated a replication of viral genomes and/or viral RNA transcription after 24h p.i. After 72h p.i. the observed mean c_q values differed for the individual isolates, as

depicted in Figure 5.11. RNA loads either increased or decreased or even remained at constant values over the time of incubation, with no noteworthy correlations between them.

The c_q values in supernatants at the early times were comparable to the ones associated with the cells. However, as c_q values markedly decreased in supernatants, over the 72h of incubation, a clear increase in extracellular viral RNA was demonstrated. This is most probably due to the production and release of infectious virus progeny into supernatants. In addition, the possibility of viral RNA originating from disrupted cell membranes may explain these findings as described for similar results in MDCK cells (Section 5.3.1).

Summing up, viral genome replication and/or mRNA production was clearly demonstrated for all isolates in A549 cells within 24h, correlating with results observed in MDCK.

5.3.3 Dynamics of viral RNA loads in SIV infected KLU-2-R cells

In contrast to the results reported for RNA loads measured in infection assays on MDCK and A549 cells (Sections 5.3.1 and 5.3.2), the obtained mean end-point values in the M-gene real time RT-PCR of KLU-2-R infections, did not vary as much. As shown in Figure 5.12, detected c_q values were around 30 at 0h p.i. and did not alter significantly over the observed time intervals. Only the isolates i101 (H3N2), i225 (H1N2) and i42 (pdmH1N2) showed a slight decrease, usually less than 5 c_q values in average. A difference of 3 c_q values simply reflects variations between individual replicates within an experimental setting. Therefore, these small differences were considered as not significant.

End-point values in supernatants again had comparable c_q values around 30 and showed no marked difference over the 72h of incubation. This fact might indicate, that viral RNA loads detected in supernatants resulted from residual input virus RNA.

Taken together, no genome replication and or mRNA production was observed after infecting KLU-2-R cells with all twelve different SIV isolates.

5.3.4 Dynamics of viral RNA loads in SIV infected porcine fibrocytes

Irrespective of the virus isolate, the mean c_q values ranged between 26.7 and 35.5 at 0h p.i. In two out of ten infections mean c_q values below 29 were reached. Interestingly, real time RT-PCR results demonstrated a replication of viral RNA and/or mRNA production in fibrocytes infected with the H3N2 and pandemic H1 containing strains. Respective assays indicated a distinct decrease of 5 to 10 c_q values within the first 24h (Figure 5.13 g, h, k, and m). In contrast, the mean end-point viral RNA loads obtained at 72h p.i. demonstrated a significant increase of c_q values, indicating a loss of detectable viral RNA. Associated supernatants showed similar dynamics in c_q values. However, among the H1N1 and H1N2 strains only one out of three isolates, revealed a decrease in c_q value at 24h p.i. (i199 & i114 Figure 5.13 a and e). Furthermore, respective mean c_q values decreased only by four, which could still be simply due to variations between replicate experiments. For the latter isolates, dynamics in c_q values at 72h p.i. were similar to those attained for H3N2 strains, namely an increase in c_q values was noted. Infections with any of the four other H1N1 and H1N2 isolates resulted in c_q values without significant variance over the investigated incubation time. In conclusion, not all isolates were able to induce a viral genome replication and/or mRNA transcription in porcine fibrocytes.

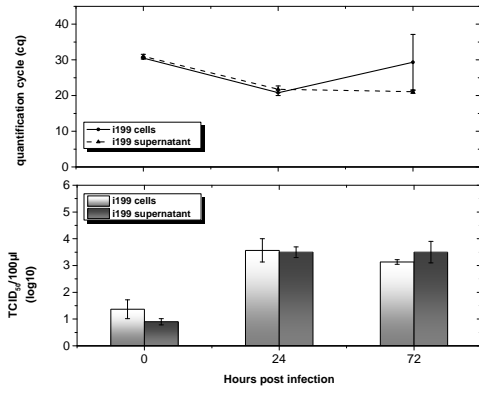
5.3.5 RNA load dynamics in correlation with the detection of infectious titers

The employed real time RT-PCR allows to set specific c_q values by plotting the measured level of fluorescence against the number of cycles. For this purpose, an assay-specific baseline was defined and used for analyses of every PCR assay in this study. The baseline defines the value for detection of a specific increase in fluorescence levels. The number of amplification cycles

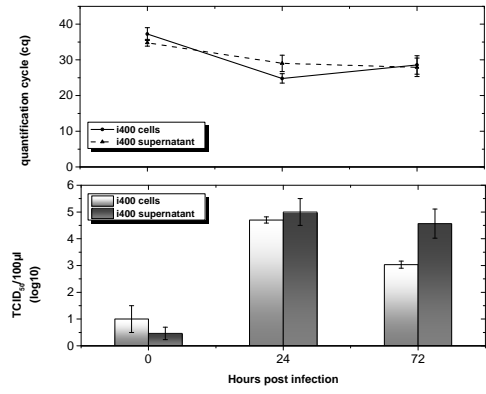
needed until the fluorescence curve crosses the baseline, defines the c_q of every sample. Hence, the c_q value does not indicate absolute genome copy numbers, but an increase or decrease of viral RNA loads can be compared relatively.

In most cases the c_q values - and therefore detected viral RNA-loads - reflected the findings concerning infectious viral titers considerably well in the performed assays.

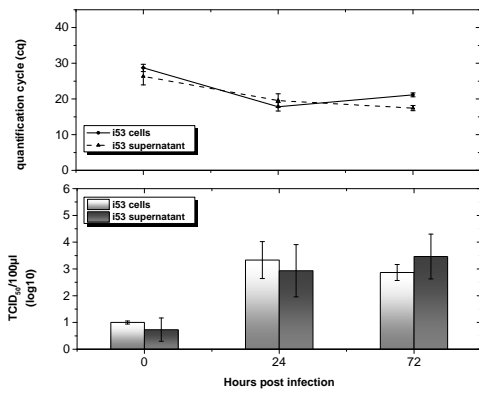
In replication-competent cells the viral titers mostly increased notably within the first 24h after infection. This titer increase was always reflected by an increase in viral RNA loads. Since no absolute quantification was done, the c_q value differences cannot be put in quantitative, direct context with the increase in viral titers. Nevertheless, when comparing to the viral RNA loads at 0h p.i., the c_q values clearly decreased in permissive cells, which mirrors the rise of viral titers. Surprisingly, individual assays showed a decrease of c_q values, even in some assays on porcine fibrocytes where no production of virus progeny could be detected in the infectivity assays (Figure 5.13 h, k, and m). This indicates an RNA multiplication and/or mRNA transcription combined with an impaired replication at some point in the replication cycle, without resulting in infectious virus progeny. To differentiate between the latter options further analyses, such as assessing the production of viral proteins, became necessary.



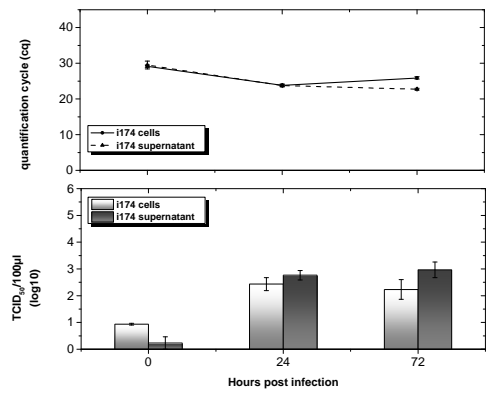
a



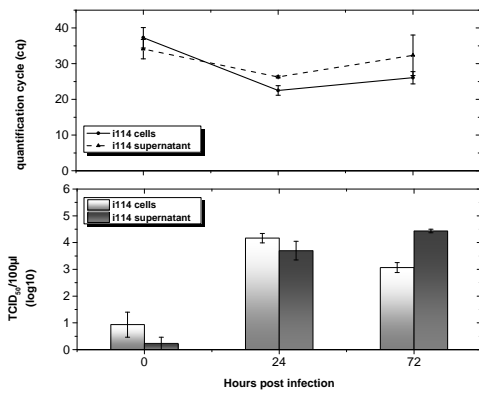
b



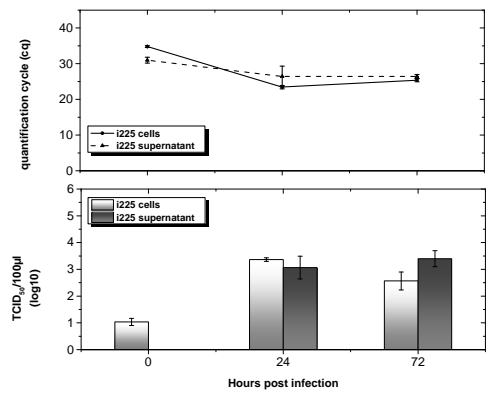
c



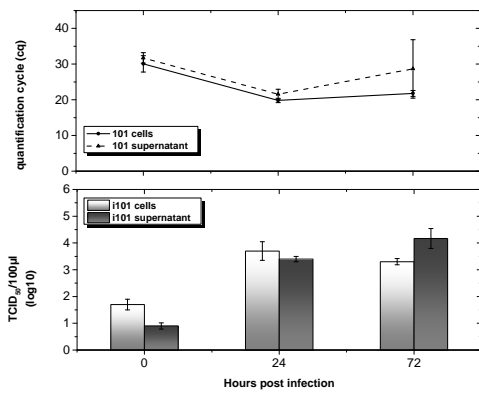
d



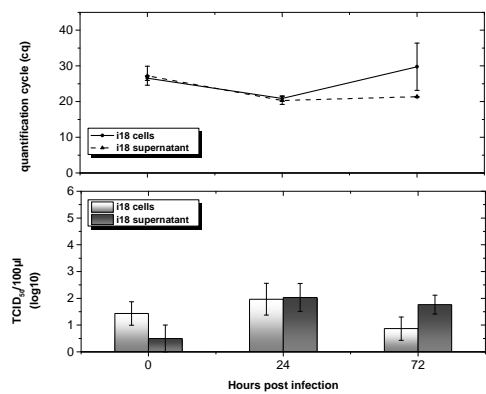
e



f



g



h

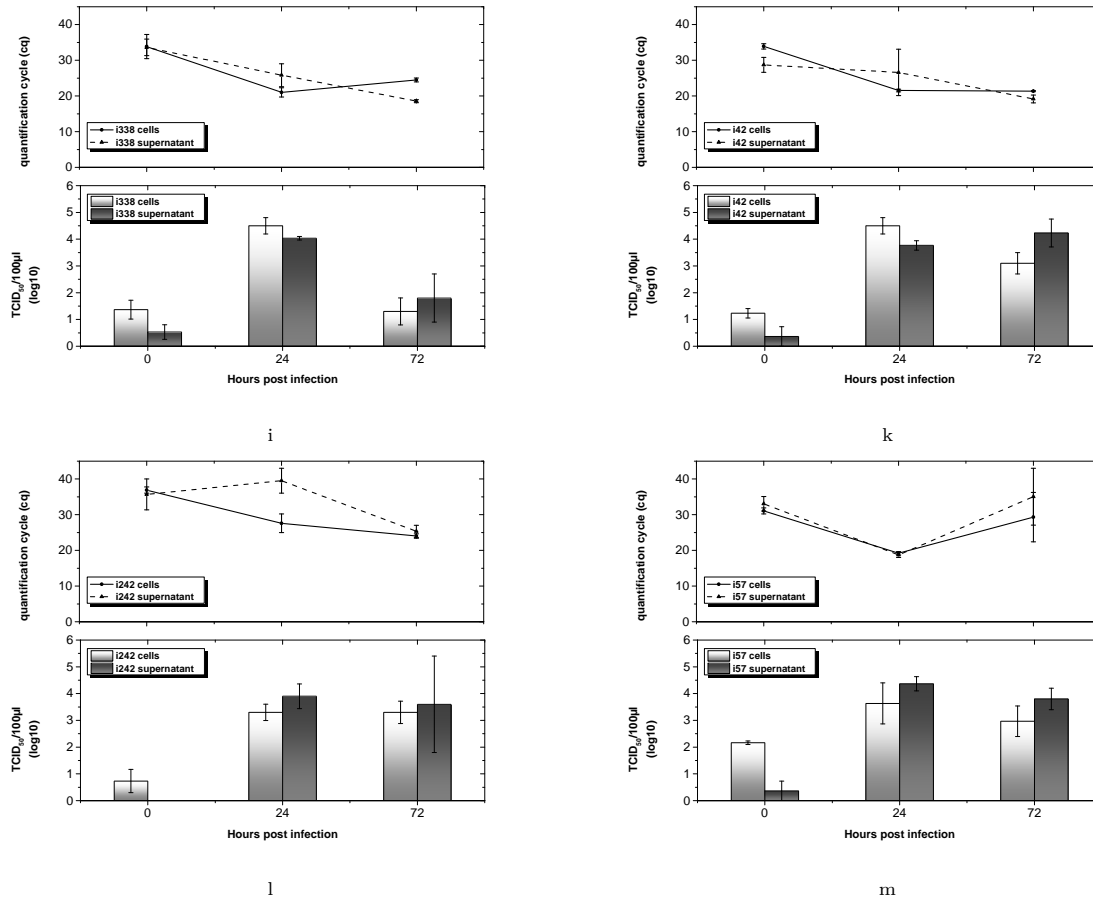
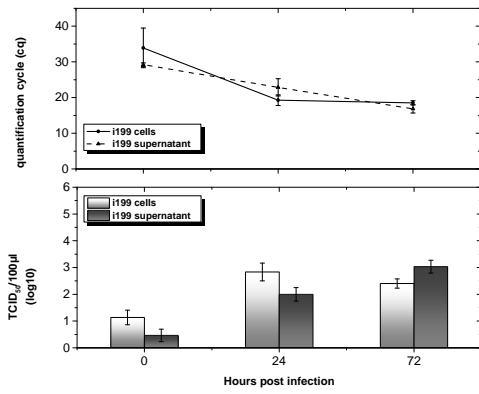
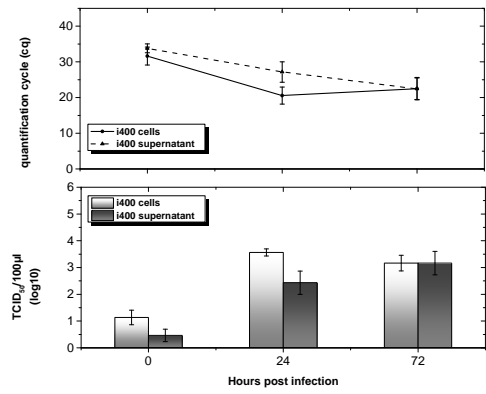


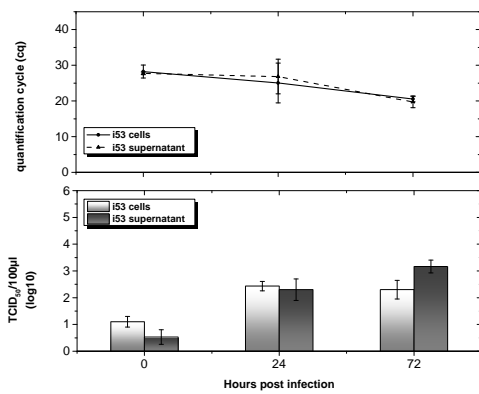
Figure 5.10: SIV replication in MDCK cells infected with twelve different isolates at 0h, 24h, and 72h p.i. Virus titers and viral genome loads in supernatants of infected cells as well as associated with cells are given for the assessed points of time. Mean viral titers ($TCID_{50}/100\mu l$) were determined as described in 4.2.4 and 5.2. In parallel viral genome loads were compared by real time RT-PCR targeting sequences within the Matrix gene and are given as mean c_q values \pm SEM. The following virus isolates were used: (a) A/swine/Bavaria/199002/2014(H1N1), (b) A/swine/Bavaria/400001/2013(H1N1), (c) A/swine/Bavaria/53002/2014(H1N1), (d) A/swine/Bavaria/174002/2014(H1N2), (e) A/swine/Bavaria/114003/2010(H1N2), (f) A/swine/Bavaria/225002/2011(H1N2), (g) A/swine/Bavaria/101001/2013(H3N2), (h) A/swine/Bavaria/18002/2013(H3N2), (i) A/swine/Bavaria/338011/2012(H3N2), (k) A/swine/Bavaria/42001/2014(pdmH1N2), (l) A/swine/Bavaria/242001/2013(pdmH1N2), (m) A/swine/Bavaria/57002/2013(pdmH1N1).



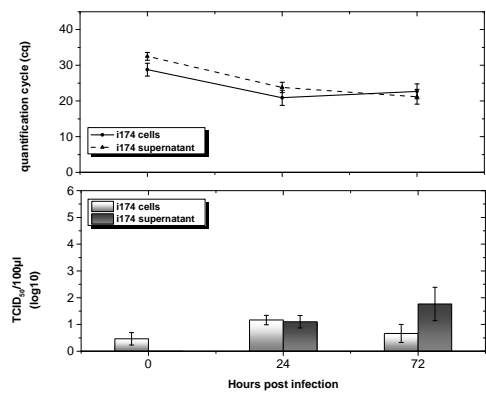
a



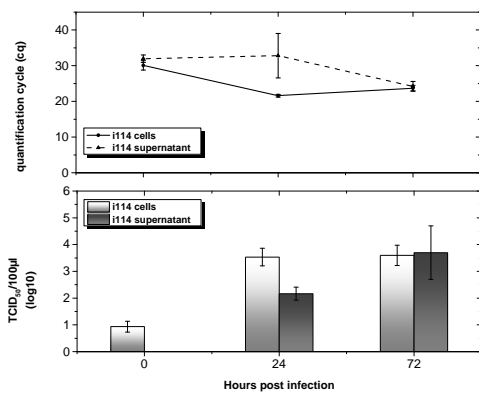
b



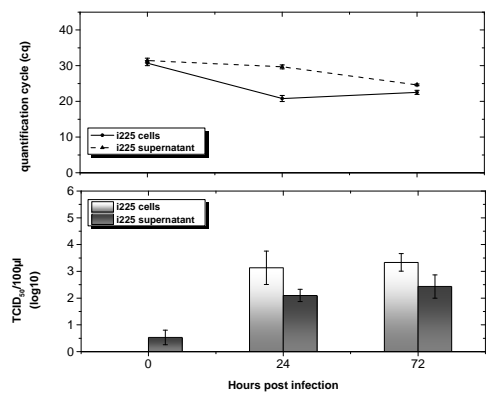
c



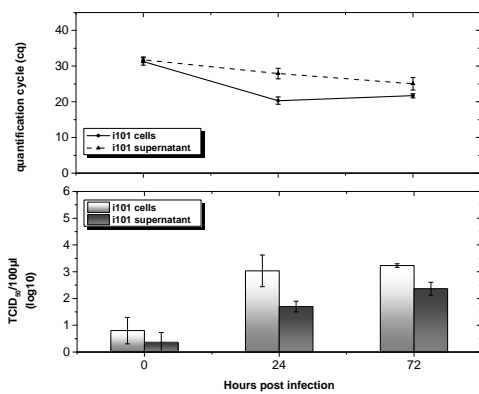
d



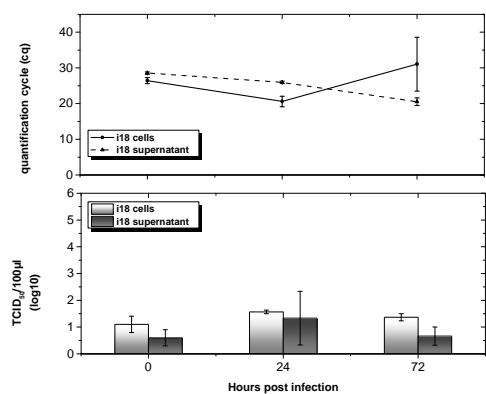
e



f



g



h

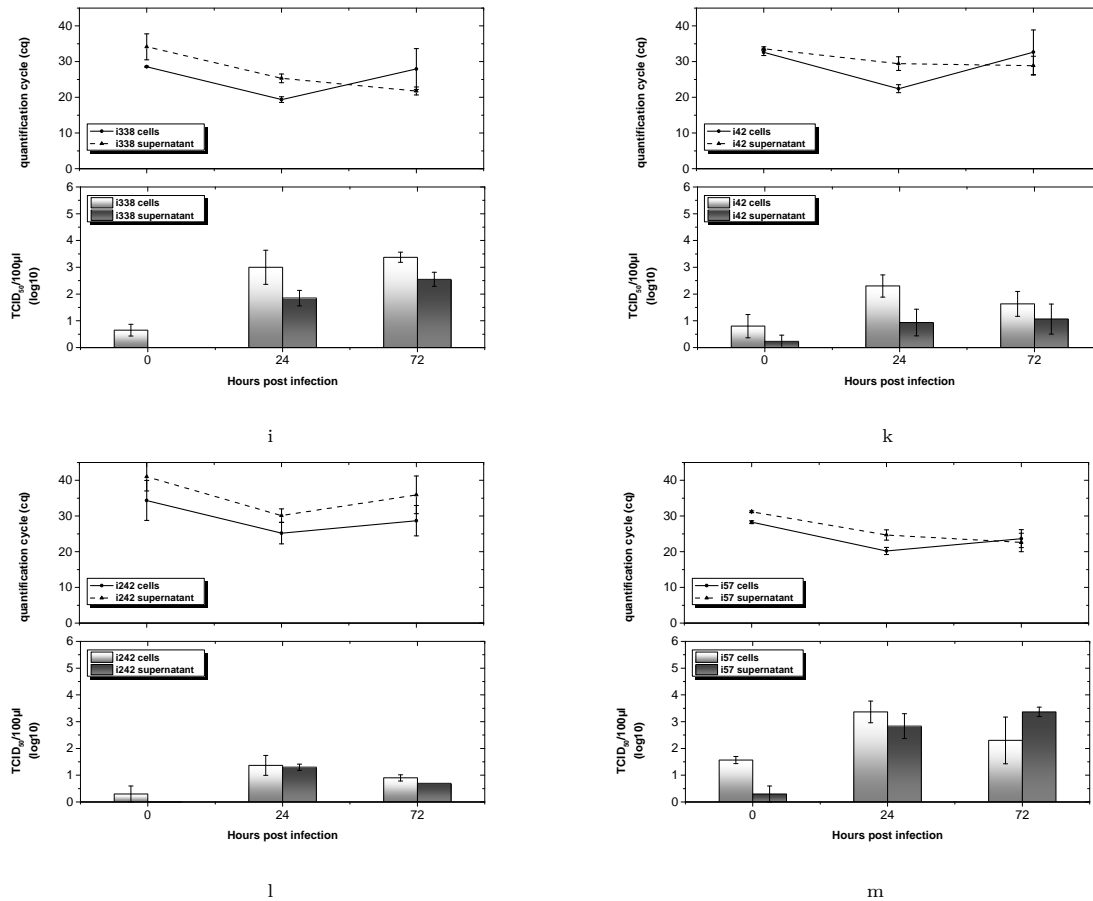
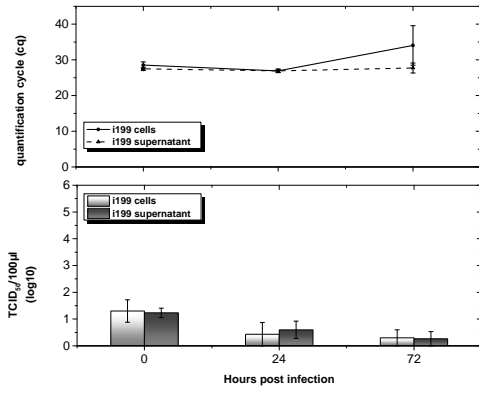
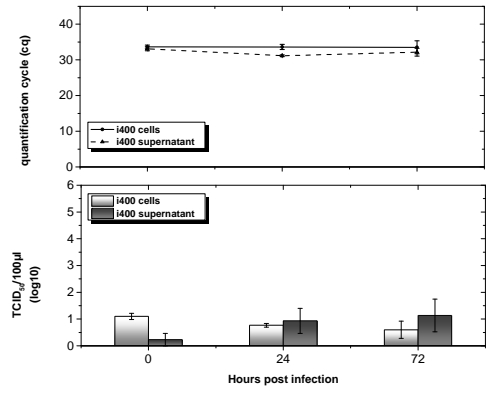


Figure 5.11: SIV replication in A549 cells infected with twelve different isolates at 0h, 24h, and 72h p.i. Virus titers and viral genome loads in supernatants of infected cells as well as associated with cells are given for the assessed points of time. Mean viral titers ($TCID_{50}/100\mu l$) were determined as described in 4.2.4 and 5.2. In parallel viral genome loads were compared by RT-PCR targeting sequences within the Matrix gene and are given as mean c_q values \pm SEM. The following virus isolates were used:

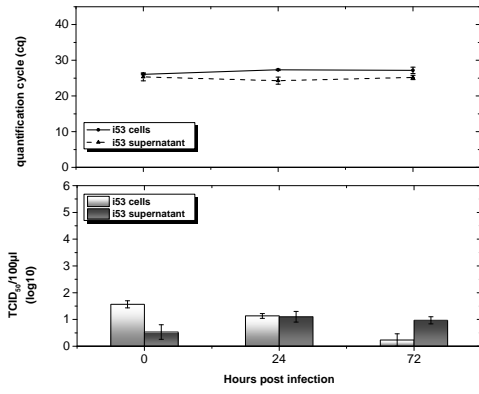
(a) A/swine/Bavaria/199002/2014(H1N1), (b) A/swine/Bavaria/400001/2013(H1N1), (c) A/swine/Bavaria/53002/2014(H1N1), (d) A/swine/Bavaria/174002/2014(H1N2), (e) A/swine/Bavaria/114003/2010(H1N2), (f) A/swine/Bavaria/225002/2011(H1N2), (g) A/swine/Bavaria/101001/2013(H3N2), (h) A/swine/Bavaria/18002/2013(H3N2), (i) A/swine/Bavaria/338011/2012(H3N2), (k) A/swine/Bavaria/42001/2014(pdmH1N2), (l) A/swine/Bavaria/242001/2013(pdmH1N2), (m) A/swine/Bavaria/57002/2013(pdmH1N1).



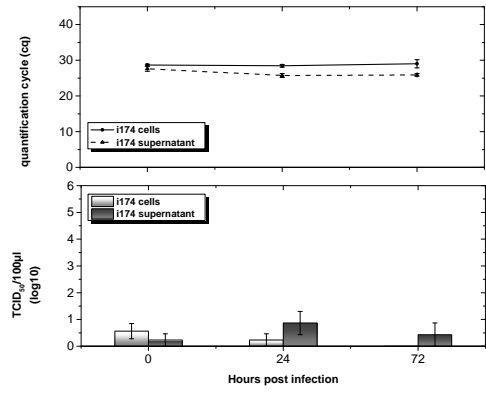
a



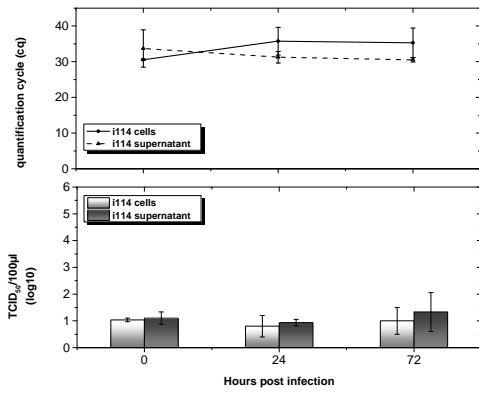
b



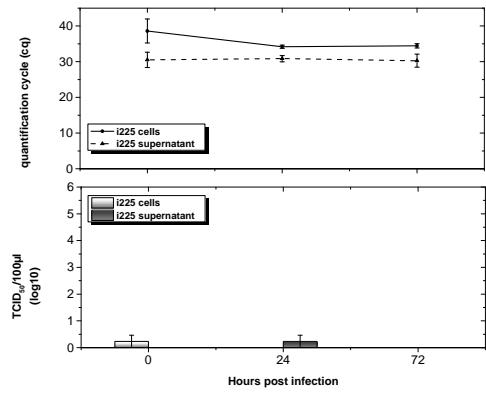
c



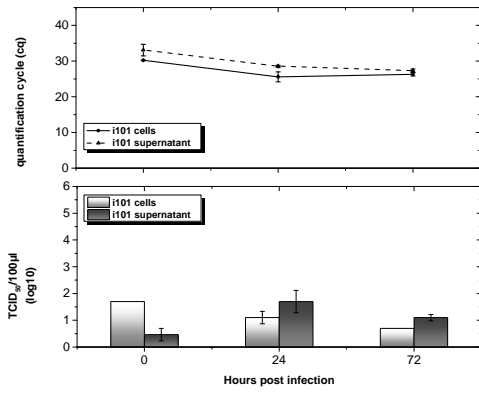
d



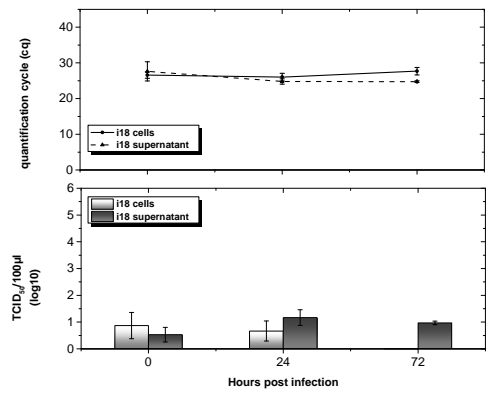
e



f



g



h

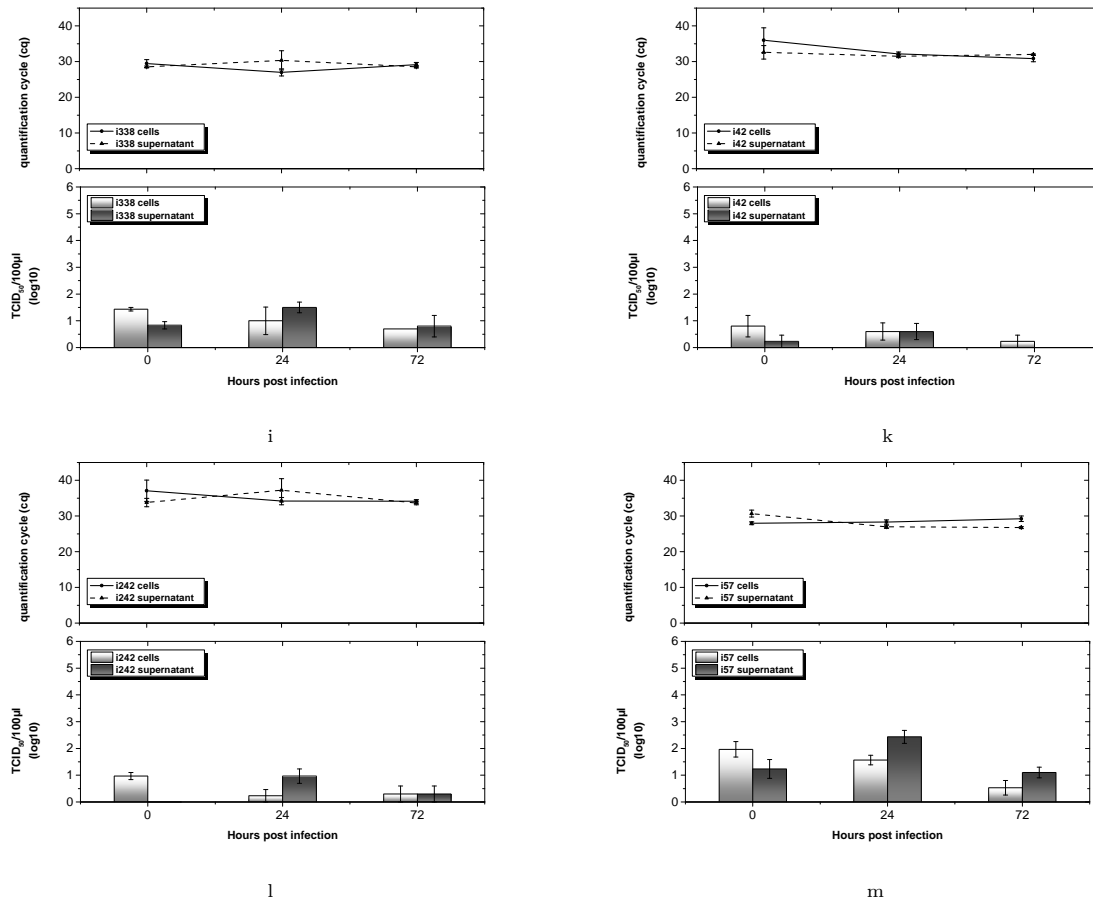
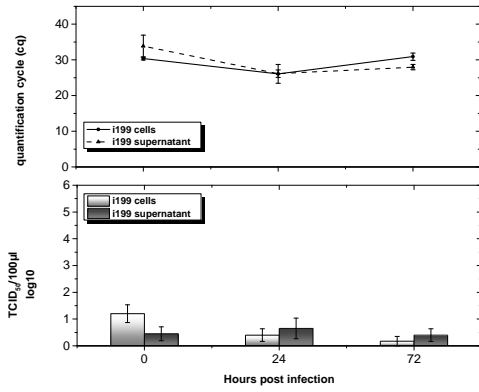
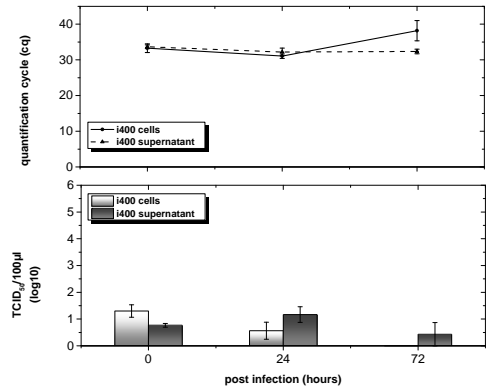


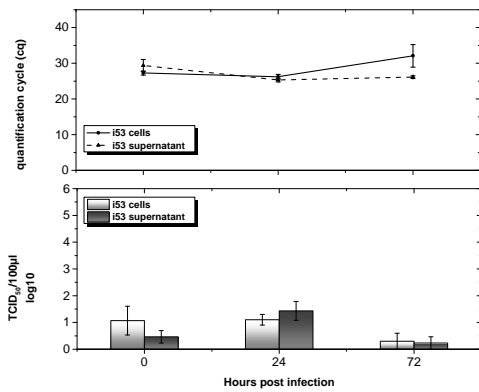
Figure 5.12: SIV replication in KLU-2-R cells infected with twelve different isolates at 0h, 24h, and 72h p.i. Virus titers and viral genome loads in supernatants of infected cells as well as associated with cells are given for the assessed points of time. Mean viral titers (TCID₅₀/100µl) were determined as described in 4.2.4 and 5.2. In parallel viral genome loads were compared by RT-PCR targeting sequences within the Matrix gene and are given as mean c_q values \pm SEM. The following virus isolates were used: (a) A/swine/Bavaria/199002/2014(H1N1), (b) A/swine/Bavaria/400001/2013(H1N1), (c) A/swine/Bavaria/53002/2014(H1N1), (d) A/swine/Bavaria/174002/2014(H1N2), (e) A/swine/Bavaria/114003/2010(H1N2), (f) A/swine/Bavaria/225002/2011(H1N2), (g) A/swine/Bavaria/101001/2013(H3N2), (h) A/swine/Bavaria/18002/2013(H3N2), (i) A/swine/Bavaria/338011/2012(H3N2), (k) A/swine/Bavaria/42001/2014(pdmH1N2), (l) A/swine/Bavaria/242001/2013(pdmH1N2), (m) A/swine/Bavaria/57002/2013(pdmH1N1).



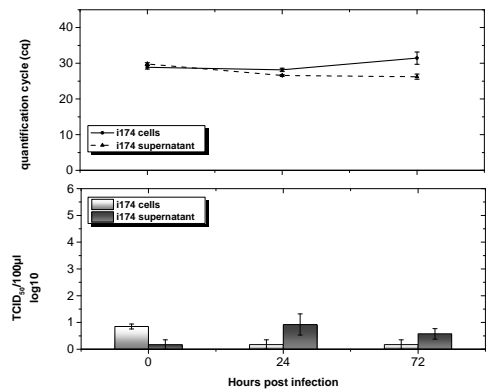
a



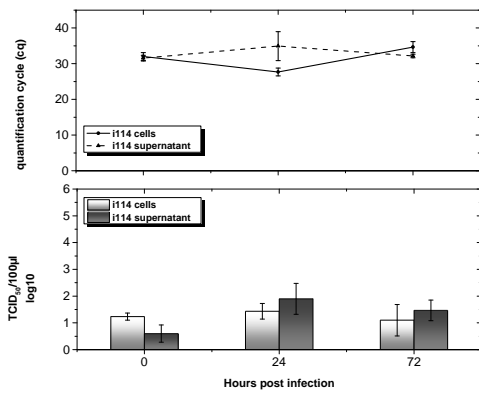
b



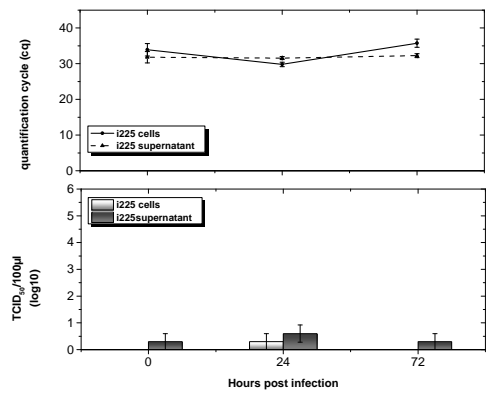
c



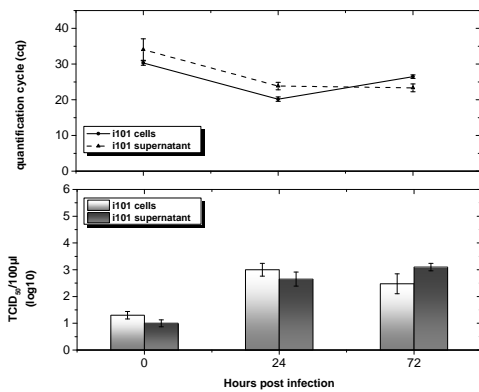
d



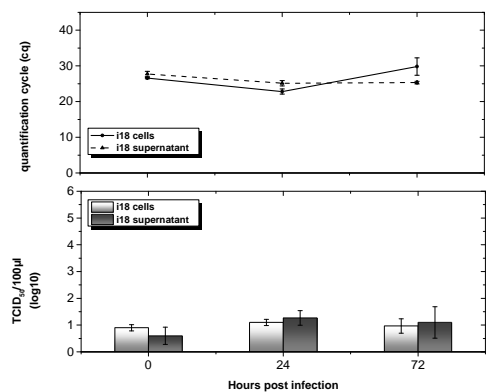
e



f



g



h

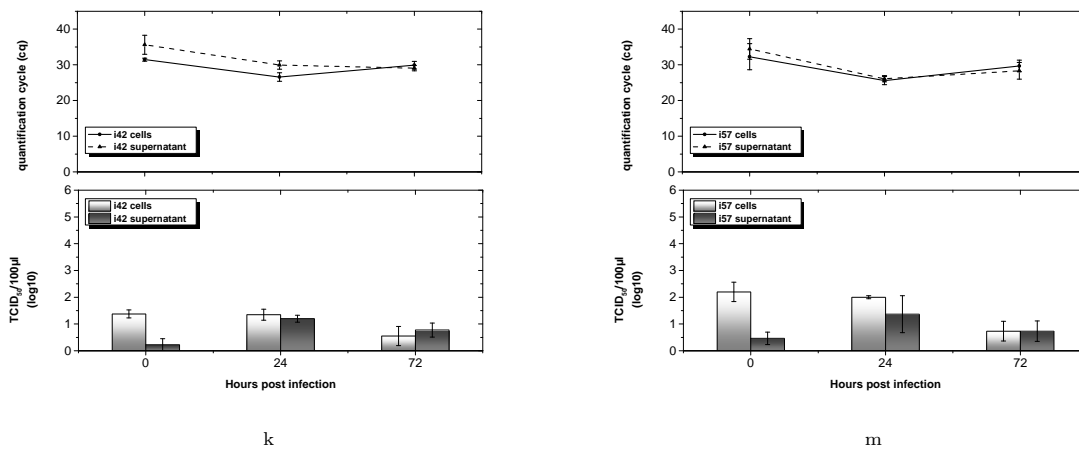


Figure 5.13: SIV replication in porcine fibrocytes infected with twelve different isolates at 0h, 24h, and 72h p.i. Virus titers and viral genome loads in supernatants of infected cells as well as associated with cells are given for the assessed points of time. Mean viral titers (TCID₅₀/100µl) were determined as described in 4.2.4 and 5.2. In parallel viral genome loads were compared by RT-PCR targeting sequences within the Matrix gene and are given as mean c_q values \pm SEM. The following virus isolates were used: (a) A/swine/Bavaria/199002/2014(H1N1), (b) A/swine/Bavaria/400001/2013(H1N1), (c) A/swine/Bavaria/53002/2014(H1N1), (d) A/swine/Bavaria/174002/2014(H1N2), (e) A/swine/Bavaria/114003/2010(H1N2), (f) A/swine/Bavaria/225002/2011(H1N2), (g) A/swine/Bavaria/101001/2013(H3N2), (h) A/swine/Bavaria/18002/2013(H3N2), (k) A/swine/Bavaria/42001/2014(pdmH1N2), (m) A/swine/Bavaria/57002/2013 (pdmH1N1).

5.4 Distribution of the SIV nucleoprotein (NP) and the matrix 1 protein (M1) in *in vitro* infected cells

In addition to the infectivity assays described in Sections 5.2 and 5.3, the expression of viral proteins in the different cell types was evaluated. The intracellular localization of the viral nucleoprotein (NP) and viral matrix protein 1 (M1) was investigated by indirect immunofluorescence microscopy to determine and compare the protein expression and distribution patterns. The cultured cells were inoculated and prepared as described in Sections 4.2.2 and 4.2.5. The detection and distribution of viral proteins were evaluated directly after rinsing off inoculating virus suspensions, which was done after 2h of incubation at 35°C (0h p.i.) and 24h p.i. The samples were analyzed by scanning laser confocal microscopy and the triple channel mode was used for the immunofluorescence analyses. Z-stacks through individual cells were collected in six optical Sections with a thickness of approximately 0.4µm. Furthermore, the individual assays were analyzed by immunofluorescence microscopy, using a 10x PlanApoλ NA 0.45 (WD 4.00) objective lens. The specific antibodies for the NP and M1-proteins were used as described in Section 3.9. The differences in viral protein expression between individual isolates or cell systems, were reflected best by the NP specific fluorescence in cell nuclei, which is why the amount of NP fluorescence positive nuclei were determined for all cell types (Table 5.5). NP localization is shown by green-colored fluorescence, M1 in red. DNS was visualized using the intercalating, blue fluorescing dye DAPI. It is incidental that the protein expression - and hence the fluorescence intensity - differed from cell type to cell type. An improvement of the individual pictures for every cell system, would go hand in hand with a lack of comparability between the different cell types. Therefore, picture settings were determined in initial experiments, and kept constant to ensure the necessary comparability of the experiments. The individual picture settings are described in Section 4.2.6.

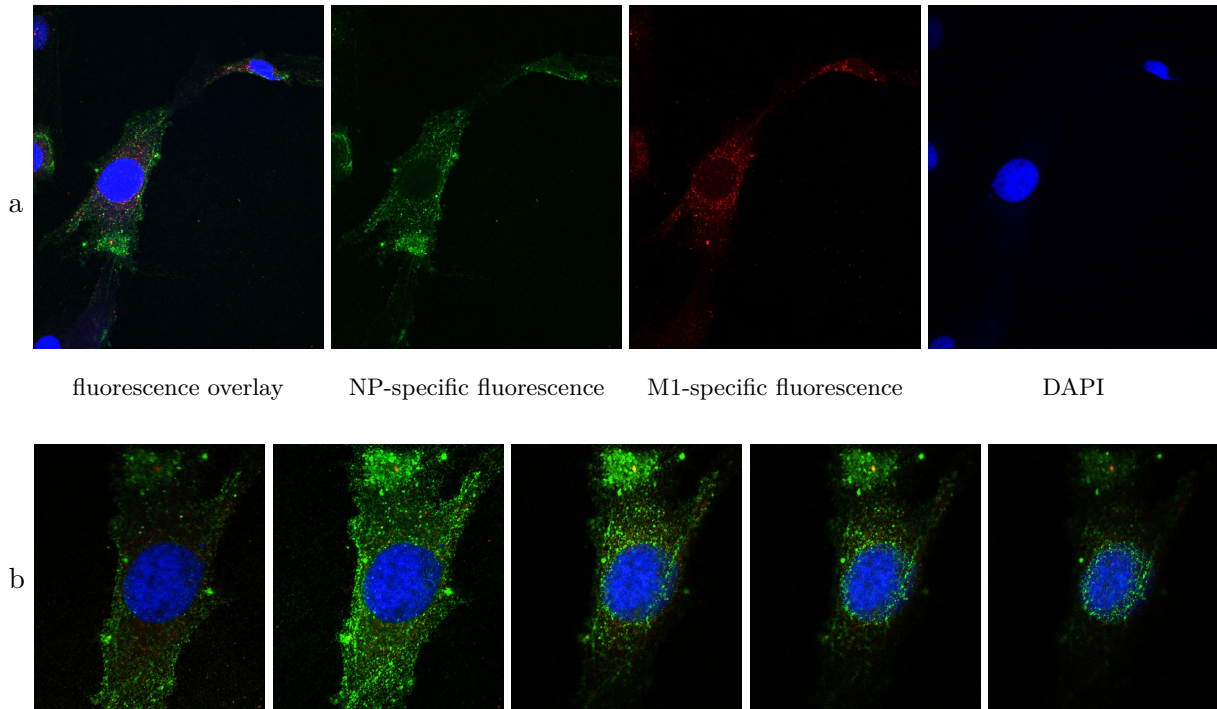


Figure 5.14: Viral proteins detected at 0 h p.i. in KLU-2-R cells infected with i53(H1N1): (a) The cytoplasmic localization of NP and M1 proteins is shown. The pictures represent a Section through a KLU-2-R cell infected with SIV isolate i53 (H1N1) at 0h p.i. (b) Images of a Z-stack through the same KLU-2-R cell infected with SIV isolate i53 (H1N1) at 0h p.i. The individual images show overlays of NP-specific fluorescence (green), M1-specific fluorescence (red) and DAPI visualized nuclei (blue).

5.4.1 Viral NP and M1 protein detection in *in vitro* infected cells at 0h p.i.

All respective isolates (i199, i400, i53 (H1N1); i174, i114, i225 (H1N2); i101, i18, i338 (H3N2); i42, i242 (pdmH1N2), i57 (pdmH1N1)) were used for infections at the same MOI (0.5) as in replication assays (Section 5.2), to allow for comparison between those assays. Again, the infectivity of the used virus suspension was confirmed after the infection was done. Thereby, used MOIs were calculated to vary between 0.2 and 1.1.

Indirect immunofluorescence analyses using antibodies to NP and M1 were employed to determine and compare the distribution of viral proteins at 0h p.i. (Section 5.4).

Within the vast majority of cell-virus combinations no structural protein - neither NP, nor M1 - was detectable. As long as endocytosed viral particles are still intact, the antibodies might have limited access to the internal interacting structural proteins. Therefore, viral antigen detection might be hindered in early stages. When released into the cytosol, the dissociation of M1 from the RNP may increase accessibility of antibodies to the structure [12]. In addition, the used MOI were relatively low, hence the amounts of incoming protein were rather low and thus hard to demonstrate.

However, viral proteins were detectable in MDCK, A549, PEL, and porcine fibrocytes infected with isolates i53 (H1N1), i114 (H1N2), and i225 (H1N2). As depicted in Figure 5.16 in cells infected with the respective isolates only NP was present in the cytoplasm, while M1 was not detectable. In KLU-2-R cells only after infection with isolate i53 (H1N1) and only within few individual cells viral antigen (NP and M1) was detectable (Figure 5.14). The fact, that viral protein was observable in three out of four *in vitro* cell systems for exclusively three out of twelve isolates, and actually for one in all cell types (i53(H1N1)), indicates an individual penetration or replication efficiency for individual SIV strains. Since three of these isolates are of two different subtypes - H1N1 (i53) and H1N2 (i114, i225) - observations seem to be not specific for the subtype. Notably, these observations prove evidence, that some SIV strains were able to penetrate porcine fibrocytes, while the immunofluorescence assay turned out negative for any viral protein 24h later in infection (Section 5.4.2.4). All NP detected was predominantly cytoplasmic at this early point of time. Mostly, NP localized to the cells' periphery and within the nuclei no antigen-antibody reaction was observed. In KLU-2-R cells NP appeared to be distributed in a grainy pattern throughout the cell as exemplarily shown in Figure 5.14.

The number of cells in which NP could be detected, varied between the different cell types. Notably, viral protein was detected in a vast majority of A549 cells, while in MDCK and PEL cells only few individual cells were positive for cytoplasmic NP. Additionally, within A549 cells not only the respective three isolates, but also viruses i400 (H1N1), i174 (H1N2) and i18 (H3N2) exhibited detectable NP at 0h p.i., in at least two out of three individual experiments (Figure 5.15). These results might suggest a faster uncoating process of influenza A virions in A549 cells than in the other cell types tested.

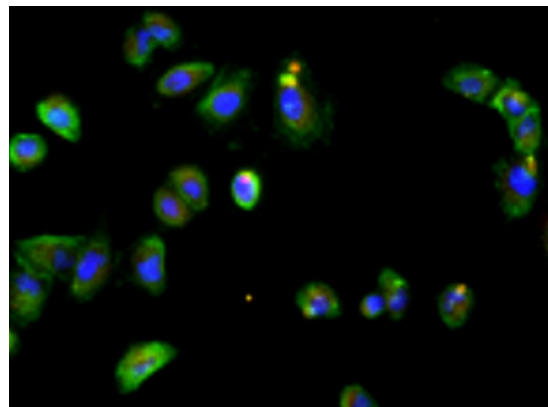


Figure 5.15: Cytoplasmic NP localization exemplarily shown for i400 (H1N1) infected A549 cells at 0h p.i. Nuclei are visualized by DAPI staining. NP fluorescence is shown in green.

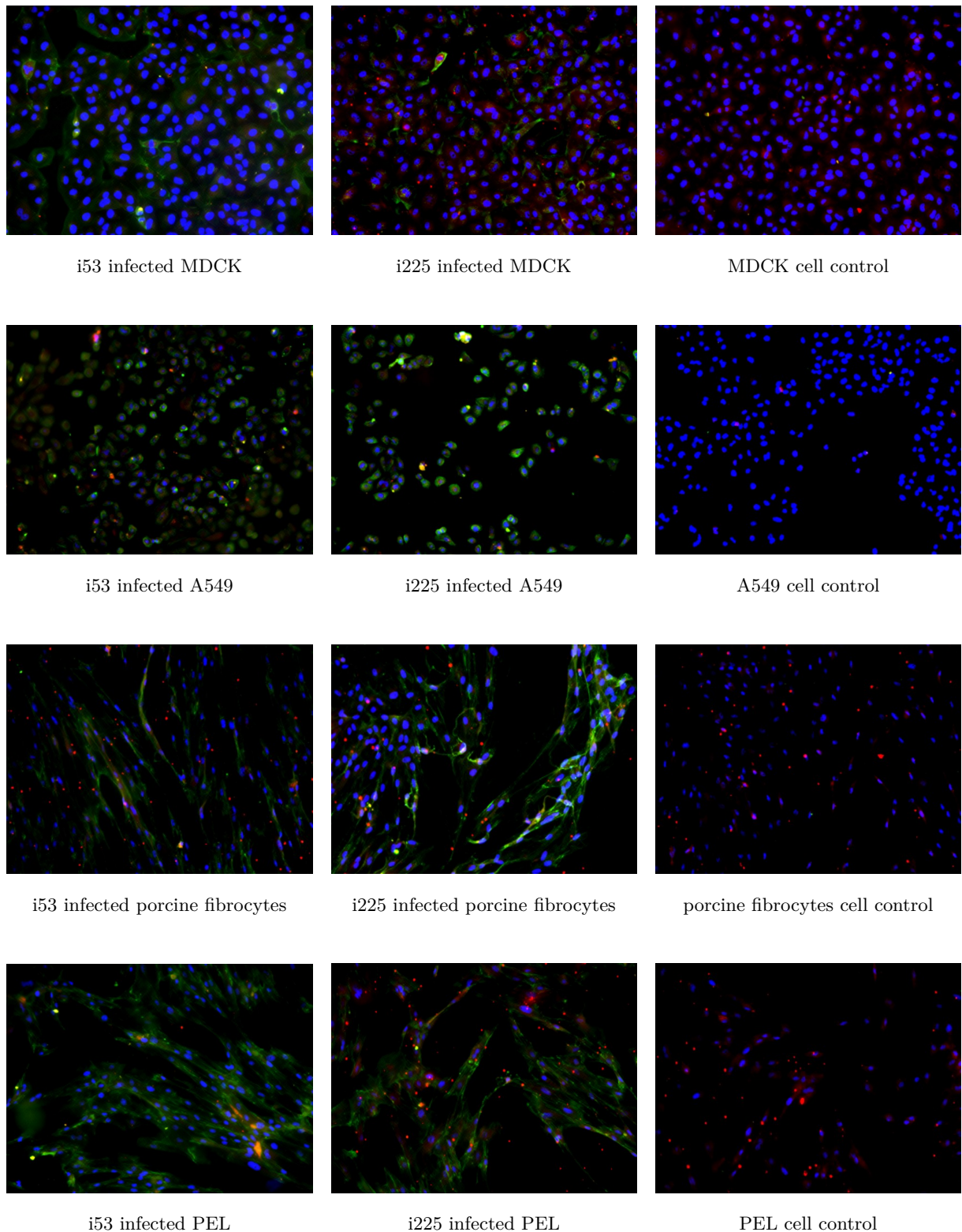


Figure 5.16: Immunofluorescence analysis of MDCK, A549, porcine fibroblasts and PEL cells at early times after infection (0h p.i.) with porcine IAV isolates i53 (H1N1) and i225 (H1N2). NP-specific fluorescence is shown in green and M1 in red. Nuclei are visualized using DAPI (blue).

5.4.2 Viral NP and M1 protein detection in *in vitro* infected cells at 24h p.i.

The following data indicate that viral proteins were detectable in high amounts in MDCK and A549, albeit in partially distinct distribution. All SIV strains were able to induce expression of NP and M1 proteins in both cell lines and moreover, also in PEL cells. Since infections of MDCK as well as A549 demonstrated a high susceptibility of these cells to SIV in the previous experiments, protein expression in PEL was also expected to be minor in comparison. Surprisingly, the H3N2 isolates were demonstrated to be exclusively capable of inducing viral protein expression in infected KLU-2-R cells and porcine fibrocytes. Accordingly, for no other strain than i114 (H1N2) and respective H3N2 isolates viral protein could be detected in those cells. In the following Section results of experiments addressing viral protein distribution in the different cell types are presented in more detail.

5.4.2.1 Distribution of SIV proteins NP and M1 in *in vitro* infected MDCK cells

Notable NP and M1 presence was demonstrated in the infected MDCK cells, irrespectively which virus strain was used. The analyzed point of time (24h p.i.) allows for the conclusion that the antigen detected corresponds to newly synthesized viral proteins (Section 2.2.1). In infectivity assays with H1N1, H1N2 and H3N2 viruses a high amount of MDCK cells showed viral antigen expression. In MDCK cells infected with the pdmH1N2 strains positive cells were more isolated and an overall lower amount of cells expressed viral protein (Figure 5.31). Since, the MOIs were comparable, the number of cells infected did not result from less input virus, but possibly due to a lower internalization efficiency of pandemic H1 containing viruses within MDCK cells. Additionally, a higher amount of cells showed exclusive M1-expression, indicating an impaired infection or replication process within these individual cells (Figures 5.20(b), 5.31(a)).

Generally, the intracellular distribution pattern varied between NP and M1. Even if cytoplasmic NP was detectable, the protein was predominantly localized to the nucleus. M1 showed a different behavior, being evenly distributed over the cytoplasm and the nucleus (Figure 5.17). Within the nucleus, M1 and NP appeared to disseminate homogeneously throughout the nucleoplasm, without being detectable in the nucleoli (Figure 5.18). In a large part of the infected cells, NP and M1 exhibited granular, presumably vesicular aggregations in the cytoplasm, predominantly close by the nucleus. This finding was comprehensive for all virus isolates. Furthermore, those highly concentrated aggregations often showed a co-localization of NP and M1 (Figures 5.18 and 5.20). Possibly, these aggregations could reflect protein producing cell compartments, such as the ribosomes, the endoplasmic reticulum and/or the Golgi-complex. They could also indicate M1 bound to new RNP complexes transported from the nucleus to the cell surface.

As opposed to the comprehensive general variations of M1 and

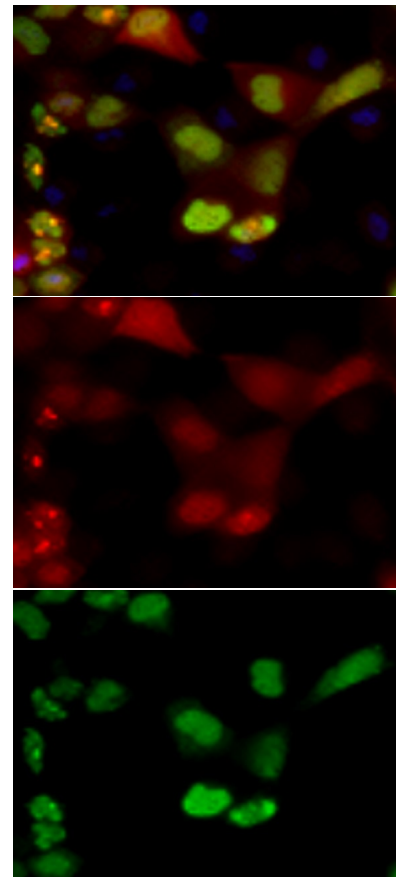


Figure 5.17: NP and M1 protein localizations in i400 (H1N1) infected MDCK cells at 24h p.i. The individual images show an overlay (first picture) of NP-specific fluorescence (green second picture) and M1-specific fluorescence (red last picture). Nuclei are visualized by DAPI staining.

NP localization in cells infected with any of the virus strains, a difference in NP expression could be observed between the individual SIV subtypes. Interestingly, NP of H3N2 isolates concentrated almost exclusively to the nuclei, while for all other strains the nuclear NP-expression was combined with a distinct cytoplasmic NP localization. Furthermore, NP was present in more than 90% of the cells' nuclei when infected with any of the H3N2 isolates (Figure 5.21). In correlation with these findings, M1 was not as evenly distributed between the nucleus and cytosol in H3N2 infected samples as reported above, in contrast to all other isolates used (Figure 5.19). Compared to other virus strains, a delay in M1 synthesis in respective H3N2 infected cells could be the reason for the NP accumulation. Since M1 mediates the export of RNP bound NP, a smaller amount of nuclear M1 (Figure 5.21) would corroborate this interpretation. Taken together, the immunofluorescence experiments in MDCK cells indicate that NP proteins were newly synthesized in the cytoplasm and a large fraction was transported back to the nucleus. The observation of these important steps in replication confirmed that all virus isolates were capable of productively infecting MDCK cells and to induce expression of viral structural proteins. Individual differences in the proteins' distribution patterns were observed, probably demonstrating the different stages in the viral replication cycle in MDCK. The presumable variation in the internalization process of the input virus poses an important factor for this result.

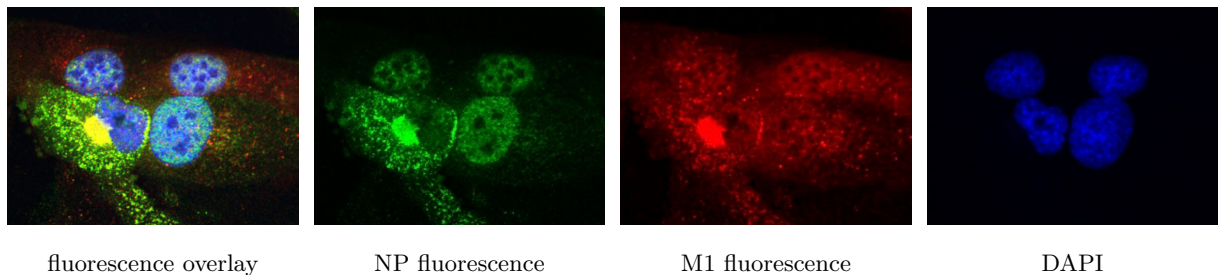


Figure 5.18: NP and M1 protein distribution exemplary shown for i114 (H1N1) infected MDCK cells at 24h p.i. The individual images of a confocal laser scanning analysis show NP-specific fluorescence (green) and M1-specific fluorescence (red) and an overlay of both including DAPI visualized nuclei. The arrowheads indicate the concentrated aggregations were detected as co-localization of NP and M1, localized close by the nucleus.

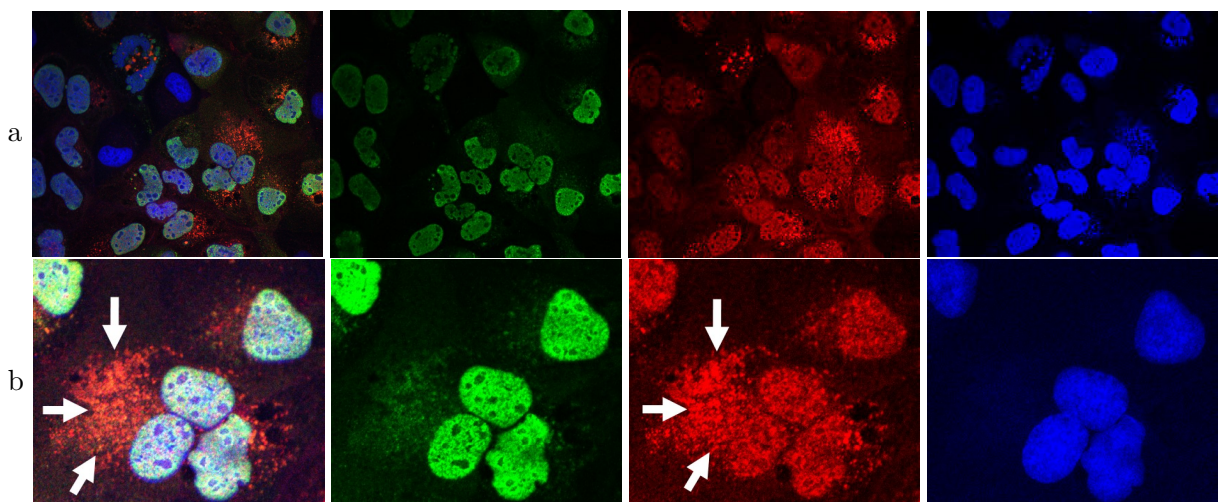


Figure 5.19: Confocal laser scanning analysis of MDCK cells infected with i101 (H3N2) at 24h p.i. (a) NP-specific fluorescence is shown in green and M1 in red, the nuclei are visualized with DAPI and shown in blue. The overlay of all detected signals are given as first picture of the row. (b) An enlarged section of (a) is shown. The arrows indicate the notable cytoplasmic localization of M1.

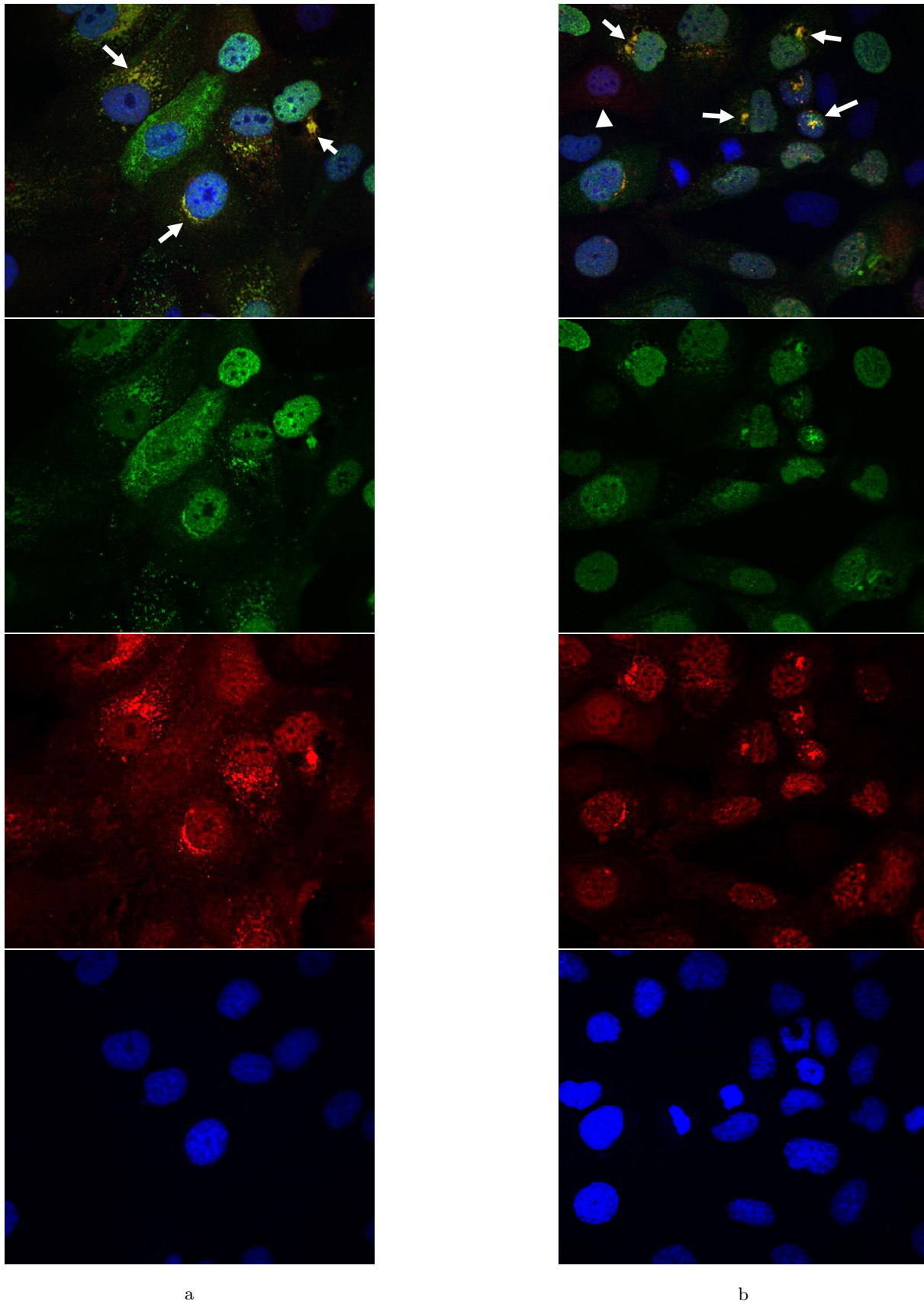


Figure 5.20: Confocal laser scanning analysis of MDCK cells infected with (a)i114 (H1N2) and (b)i57 (pdmH1N1) at 24h p.i. The individual images show an overlay (see first picture) of NP-specific fluorescence (see second picture, green) and M1-specific fluorescence (see third picture, red). The nuclei were visualized using DAPI and therefore show blue (see last picture, blue). The white arrows demonstrate for highly concentrated aggregations of co-localized NP and M1. Arrowhead shows exclusive M1-expression in cells.

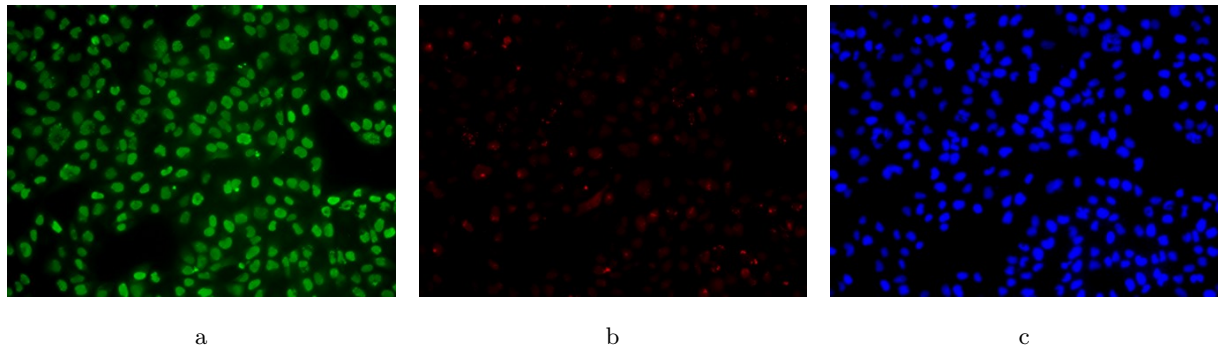


Figure 5.21: Analysis of NP and M1 protein localizations exemplary shown for i101 (H3N2) infected MDCK cells at 24h p.i. NP-specific fluorescence is shown in green (a) and M1 in red (b), the nuclei are visualized with DAPI and shown in blue (c).

Table 5.5: Immunofluorescence at 24h post infection. NP expressing cell nuclei were counted. Levels ranged from no nucleus (= N) to more than 75%. Numbers indicate: N=negative; 1=<10%; 2=10-25%; 3=25-50%; 4=50-75%; 5=>75%

Cells	H1N1			H1N2			H3N2			pdmH1		
	i199	i400	i53	i174	i114	i225	i101	i18	i338	i57	i42	i242
MDCK	2	3	3	2	4	2	5	5	4	4	3	1
A549	4	3	3	3	3	3	5	5	4	3	1	1
KLU-2-R	N	N	N	N	1	N	2	2	2	N	N	N
Fibrocytes	N	N	N	N	1	N	2	2	-	N	N	-
PEL	1	1	1	1	2	1	2	2	2	1	1	1

5.4.2.2 Distribution of SIV proteins NP and M1 in *in vitro* infected A549 cells

The performed immunofluorescence assays demonstrated that SIV viruses were able to infect a high amount of A549 cells and efficiently express new viral proteins. Over 50% of the cells showed antigen expression for infecting viruses of H1N1, H1N2 and the pdmH1N1 strain i57 (Table 5.5). For the pdmH1N2 isolates, the number of protein positive cells was notably lower. Correlating with observations in MDCK cells, NP detection in H3N2 infected cells was almost exclusively restricted to nuclear NP staining, in fact in over 90% of the cells. The same trends of the overall viral protein distribution pattern, as in MDCK, could be observed in A549 cells, irrespective of the infecting virus. While cytoplasmic NP could also be detected most of the time, NP was predominantly found in the nuclei. It is noteworthy that NP often concentrated to the periphery of the nucleus. This observation was unique for A549 cells, compared to the other tested cell systems, but not distinctive for any individual virus strain (Figures 5.23, 5.24 and 5.25). In general, in A549 cells, the M1-specific fluorescence signals were not as intense as observed in other cell types. Conclusive distinctions in M1 expression between subtypes - as observed in MDCK - were therefore hardly notable. Only in few cells of this cell system an exclusive M1 expression could be observed, in contrast to other cell types, where more

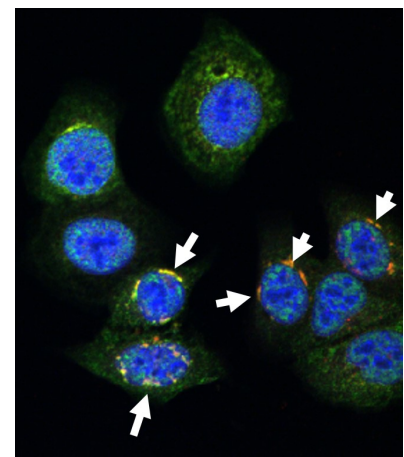


Figure 5.22: Cytoplasmic NP localization exemplary shown for i400 (H1N1) infected A549 cells at 24h p.i. NP is visualized in green, M1 in red and the nuclei in blue. The white arrows demonstrate co-localizations of NP and M1, located near by the nucleus.

frequently exclusive M1 detection was noted. This indicates, that a high amount of immunofluorescence positive cells was successfully infected, since exclusive M1 observation is an indication for inefficient virus replication. Additionally, vesicular co-localizations of viral protein NP and M1 were detected in A549 (Figure 5.22). These co-localizations were not as large as in MDCK cells.

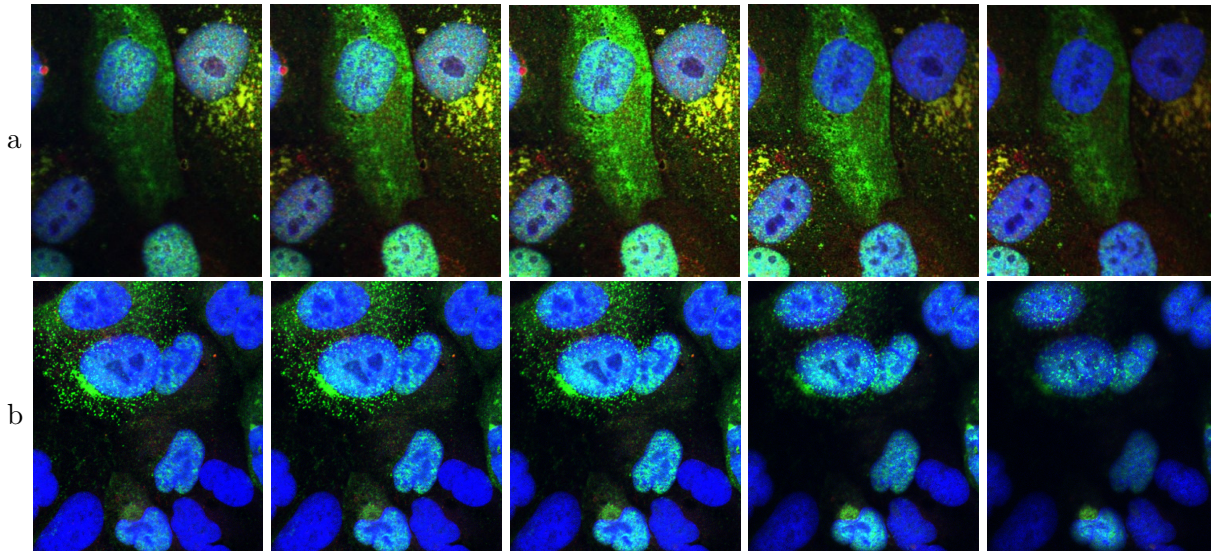


Figure 5.23: Confocal laser scanning analysis of MDCK and A549 cells 24h after infection with porcine IAV isolate i114 (H1N2). The present illustration show images of a Z-stack through (a)MDCK and (b) A549 cells infected with SIV isolate i114 (H1N1) at 24h p.i. The individual images show overlays of NP-specific fluorescence (green), M1-specific fluorescence (red) and DAPI visualized nuclei (blue).

5.4.2.3 Distribution of SIV proteins NP and M1 in *in vitro* infected KLU-2-R cells

Since replication assays were negative for any viral titer, it was not expected to detect high amounts of viral protein expressing cells in KLU-2-R cell assays. Surprisingly, distinct nuclear NP signals were observed in single cells infected with H3N2 isolates at 24h p.i. (Figure 5.32). The total amount of immunofluorescence positive cells in H3N2 assays was not comparable to the protein expression observed in MDCK or A549 cells (Table 5.5). Nevertheless, NP revealed the same almost exclusively nuclear localization. M1 could also be detected in infected cells, being predominantly cytoplasmic. Co-localization in vesicular aggregations could not be detected in infected KLU-2-R cells. Interestingly, some isolated cells, infected with isolate i114 (H1N2), also expressed NP (Figure 5.33). However, both other H1N2 samples were negative for antigen expression. Accordingly, KLU-2-R cells expressed no observable NP or M1 neither in cells infected with H1N1, nor with pandemic isolates at 24h p.i. (Figure 5.29,5.31 and 5.30). This includes the isolate i53 (H1N1), where NP-specific signals had been detected at 0h p.i.

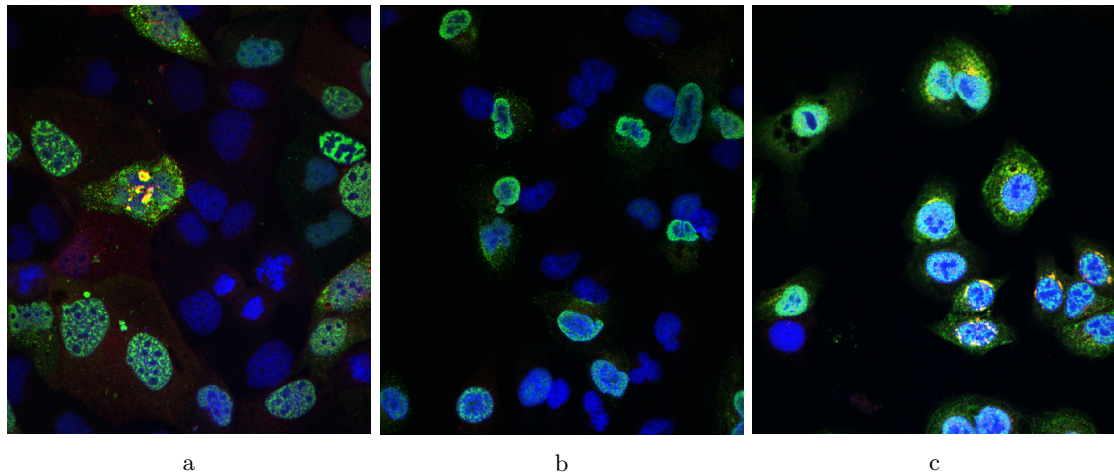


Figure 5.24: Confocal laser scanning analysis of NP and M1 localization in MDCK and A549 cells 24h p.i. The individual images show the distinct NP localization patterns (green) in (a) MDCK and (b),(c) A549 cells infected with SIV isolate i400 (H1N1). M1-specific fluorescence is red and nuclei are visualized with DAPI (blue).

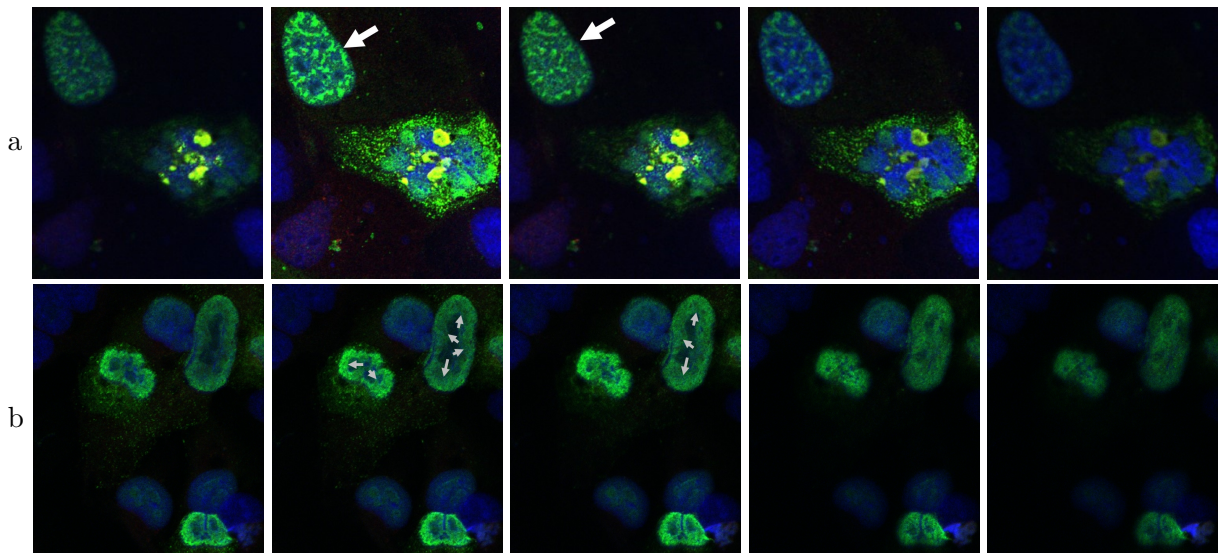


Figure 5.25: Confocal laser scanning analysis of MDCK and A549 cells 24h after infection with porcine IAV isolate i114 (H1N2). Images of a Z-stack through (a)MDCK and (b) A549 cells infected with SIV isolate i114 (H1N1) at 24h p.i. are shown. The overview images are given in Figure 5.24. The individual images are combined overlays of NP-specific fluorescence (green), M1-specific fluorescence (red) and DAPI visualized nuclei (blue).

5.4.2.4 Distribution of SIV proteins NP and M1 in *in vitro* infected porcine fibrocytes

Porcine fibrocytes showed a similar antigen detection pattern as reported for KLU-2-R cells. Cells infected with strains of H1N1, H1N2 or pandemic H1 containing viruses revealed no viral antigens (Figures 5.29, 5.31 and 5.30). These findings seemed rather surprising after detecting NP at 0h p.i. in cells infected with isolates i53 (H1N1), i114 (H1N2) and i225 (H1N2) (Section 5.4.1).

Again, H3N2 was exceptional. As presented in Table 5.5, H3N2 SIV isolates were capable to induce detectable NP synthesis, localizing predominantly in the nucleus. The majority of

NP positive nuclei also expressed M1, indicating a successful infection and some level of protein expression in porcine fibrocytes. Yet, highly concentrated co-localizations of both proteins lacked in porcine fibrocytes (Figure 5.26).

In correlation with the findings in KLU-2-R, the isolate i114 (H1N2) behaved differently to the other H1N2 isolates by exhibiting NP-specific fluorescence in cells. Nevertheless, the fluorescence detection clearly differed from the antigen distribution pattern observed in H3N2 infected cells as depicted in Figures 5.32 and 5.33.

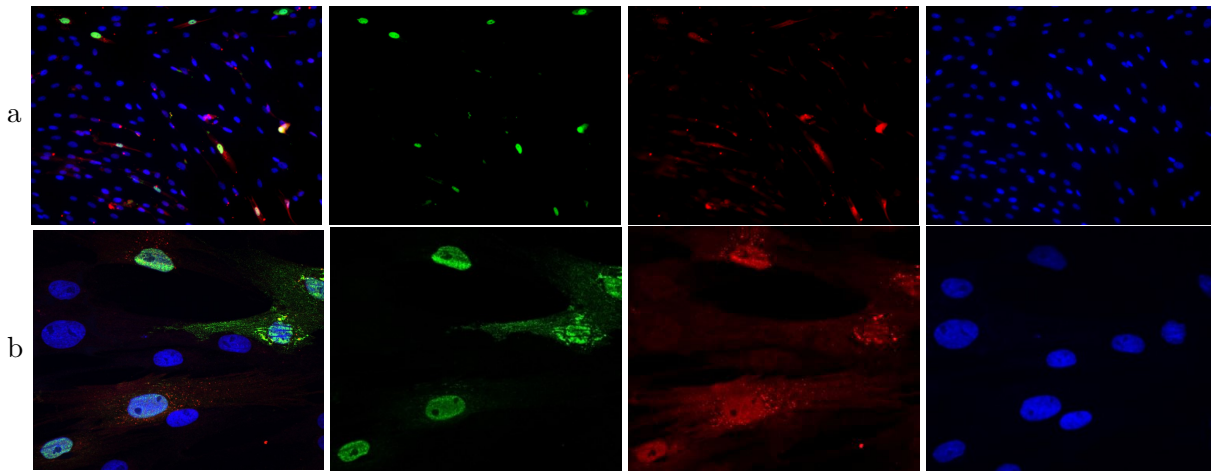


Figure 5.26: Immunofluorescence analysis of porcine fibrocytes at 24h after infection with porcine IAV isolate i18 (H3N2): (a) Illustration of the localization of NP and M1 protein. (b) The individual images show an overlay (see first picture) of NP-specific fluorescence (see second picture) and M1-specific fluorescence (see third picture). The nuclei were visualized using DAPI and therefore show blue (see last picture)

5.4.2.5 Distribution of SIV proteins NP and M1 in *in vitro* infected PEL cells

The immunofluorescence assays in PEL demonstrated some of the same trends as observed in MDCK and A549, but also some distinct differences. On the one hand the amount of viral protein expressing cells was crucially different, since not more than 25% of PEL cells were positive. On the other hand, the number of infected cells by an individual isolate (ranked by nuclear NP detection), clearly showed parallels to results in MDCK (Table 5.5). As for all other cell types, H3N2 showed the highest amount of fluorescence positive cells and isolate i242 (pdmH1N2) showed the lowest. Additionally, M1 and NP exhibited co-localization in vesicular aggregations in the cytoplasm (Figure 5.27). Notably, several cells exhibited exclusively M1, which again might indicate an impaired infection process within these cells (Figure 5.27(b)).

The next distinct observation relates to the intracellular protein distribution. Although both structural proteins could be found nuclear as well as cytoplasmic, NP was not detected predominantly in the cell nuclei, as shown for other cell types. In contrast, the structural protein was distributed evenly between nucleus and cytoplasm, including the cells infected with the H3N2 viruses.

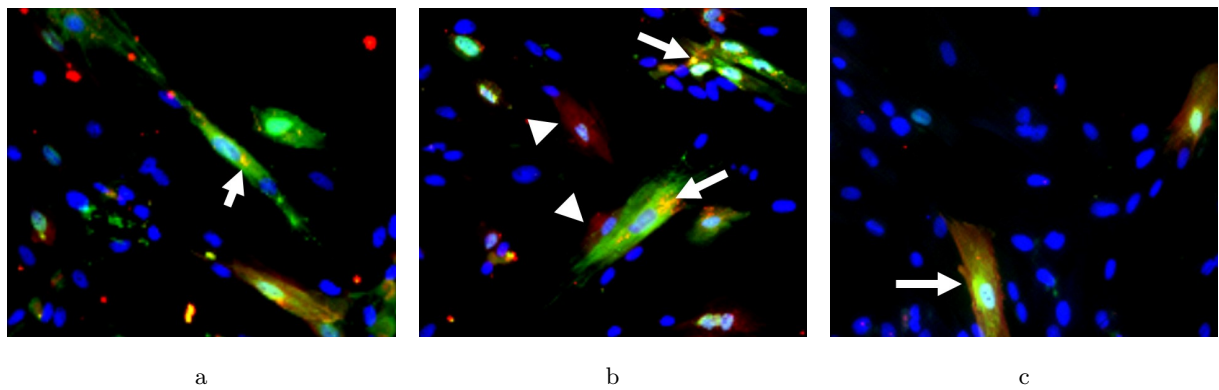


Figure 5.27: NP and M1 protein localizations exemplary shown for i18 (H3N2) and i400 (H1N1) infected PEL cells at 24h p.i. The individual images (a) and (b) show PEL cells infected with isolate i101 (H3N2) and (c) isolate i400 (H1N1). NP-specific fluorescence is green, M1-specific fluorescence red and DAPI visualized nuclei blue. The white arrows demonstrate co-localizations in vesicular aggregations of M1 and NP. Exclusive M1 expression is indicated by arrowheads.

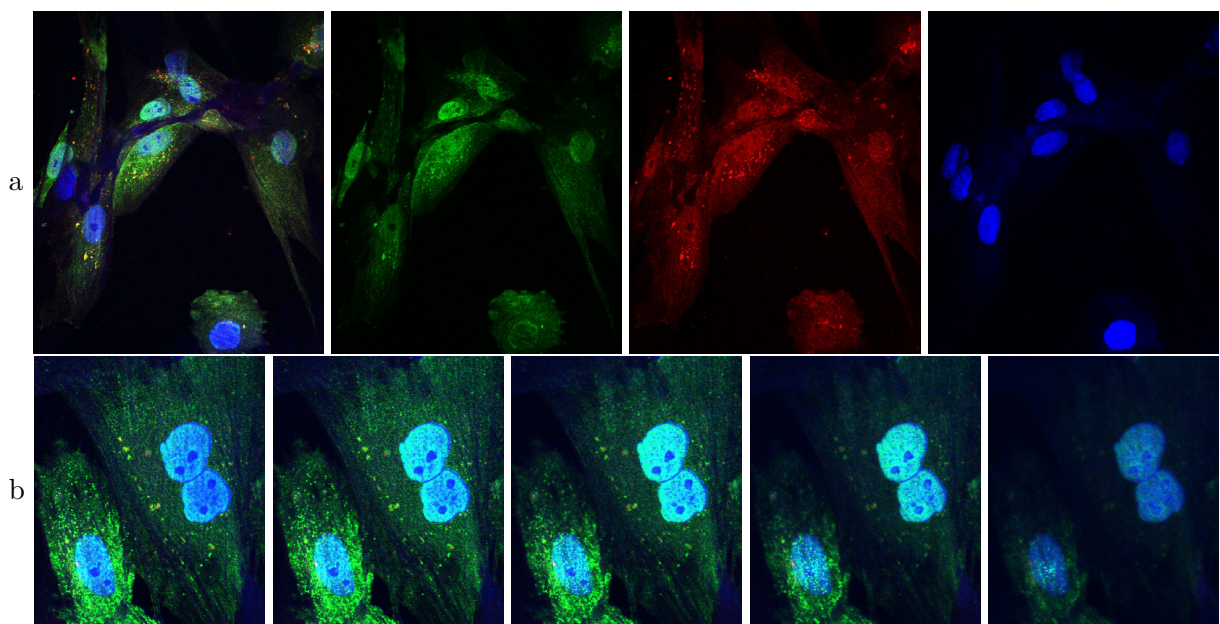


Figure 5.28: Confocal laser scanning analysis of PEL cells infected with i101 (H3N2) at 24h p.i. (a)The individual images show an overlay (first picture) of NP-specific fluorescence (second picture, green) and M1-specific fluorescence (third picture, red). The nuclei were visualized in blue using DAPI (last picture, blue). (b)Images of a Z-stack through PEL cells infected with SIV isolate i101 (H3N2) at 24h p.i. The individual images show overlays of NP-specific fluorescence (green), M1-specific fluorescence (red) and DAPI visualized nuclei (blue).

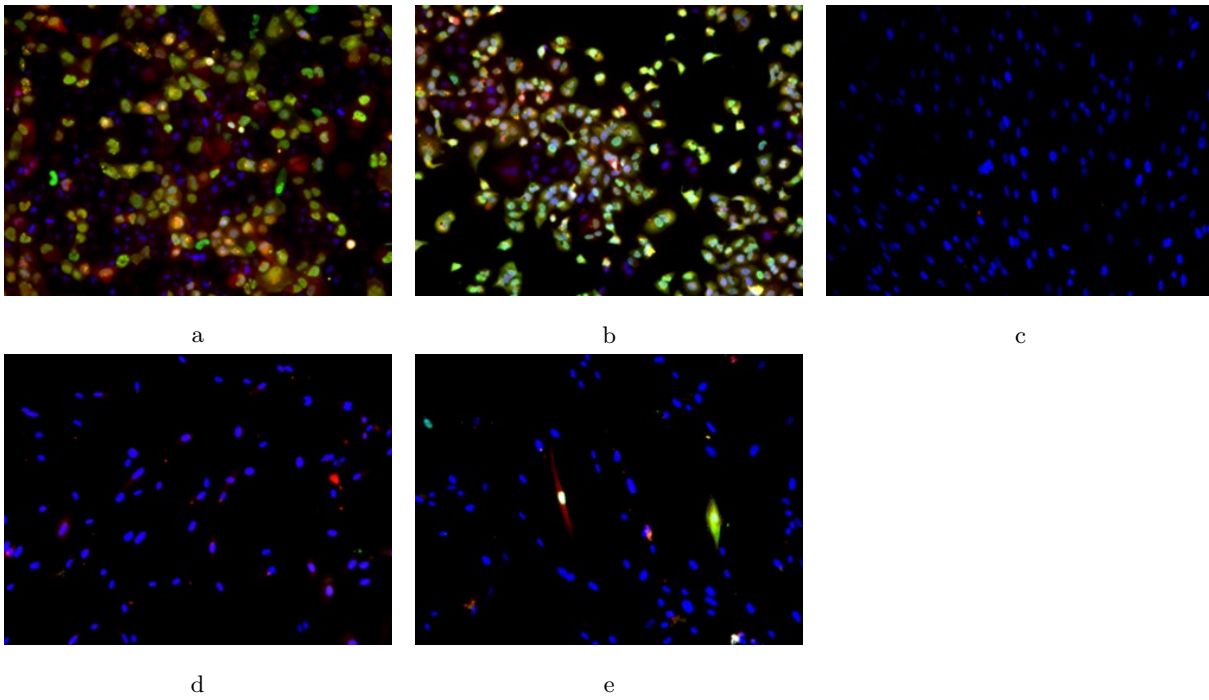


Figure 5.29: NP and M1 protein localizations exemplary shown for isolate i400 (H1N1) infected cell systems at 24h p.i. The individual images show NP-specific fluorescence (green), M1-specific fluorescence (red), and DAPI visualized nuclei (blue) in (a)MDCK, (b)A549, (c)KLU-2-R, (d)porcine fibrocytes and (e)PEL cells.

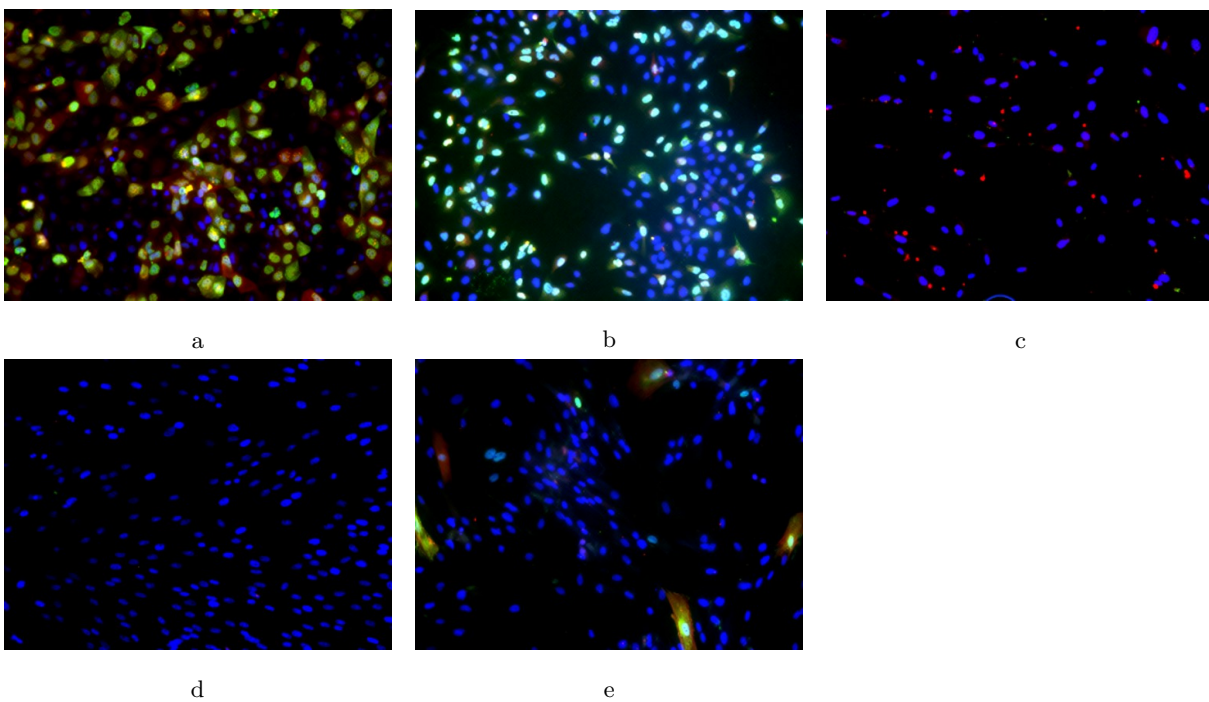


Figure 5.30: NP and M1 protein localizations exemplary shown for isolate i225 (H1N2) infected cell systems at 24h p.i. The individual images show NP-specific fluorescence (green), M1-specific fluorescence (red), and DAPI visualized nuclei (blue) in (a)MDCK, (b)A549, (c)KLU-2-R, (d)porcine fibrocytes and (e)PEL cells.

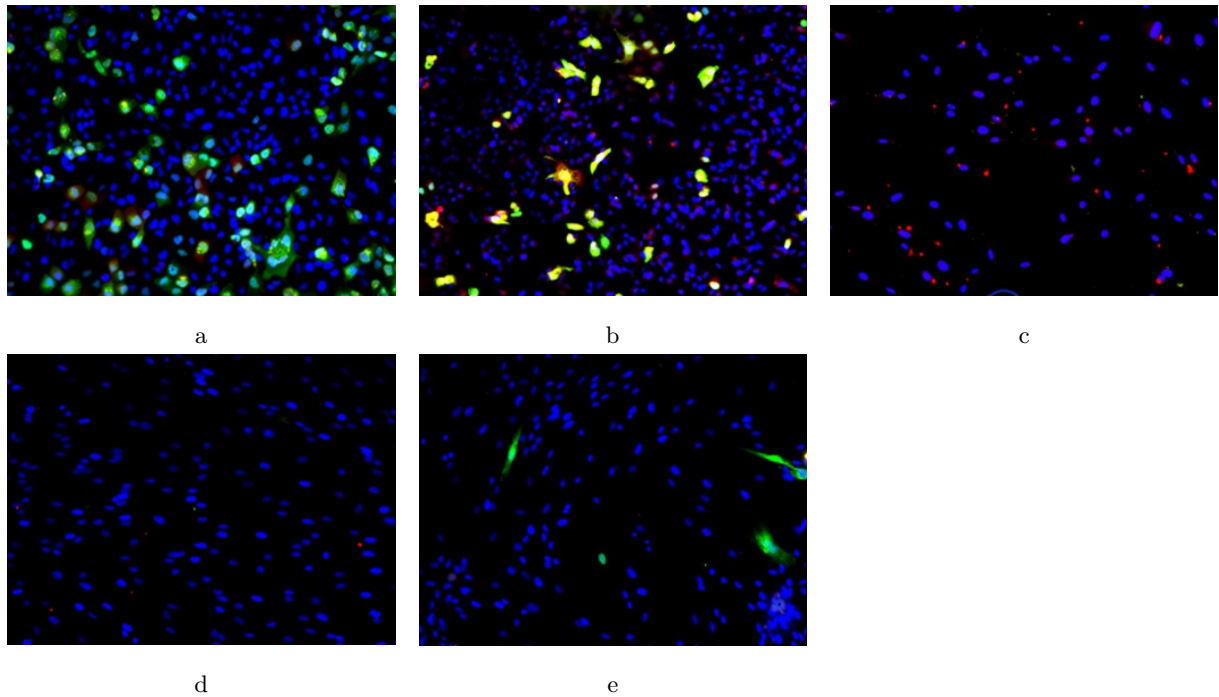


Figure 5.31: NP and M1 protein localizations exemplary shown for isolate i42 (pdmH1N1/pdmH1N2) infected cell systems at 24h p.i. The individual images show NP-specific fluorescence (green), M1-specific fluorescence (red), and DAPI visualized nuclei (blue) in (a)MDCK, (b)A549, (c)KLU-2-R, (d)porcine fibrocytes and (e)PEL cells.

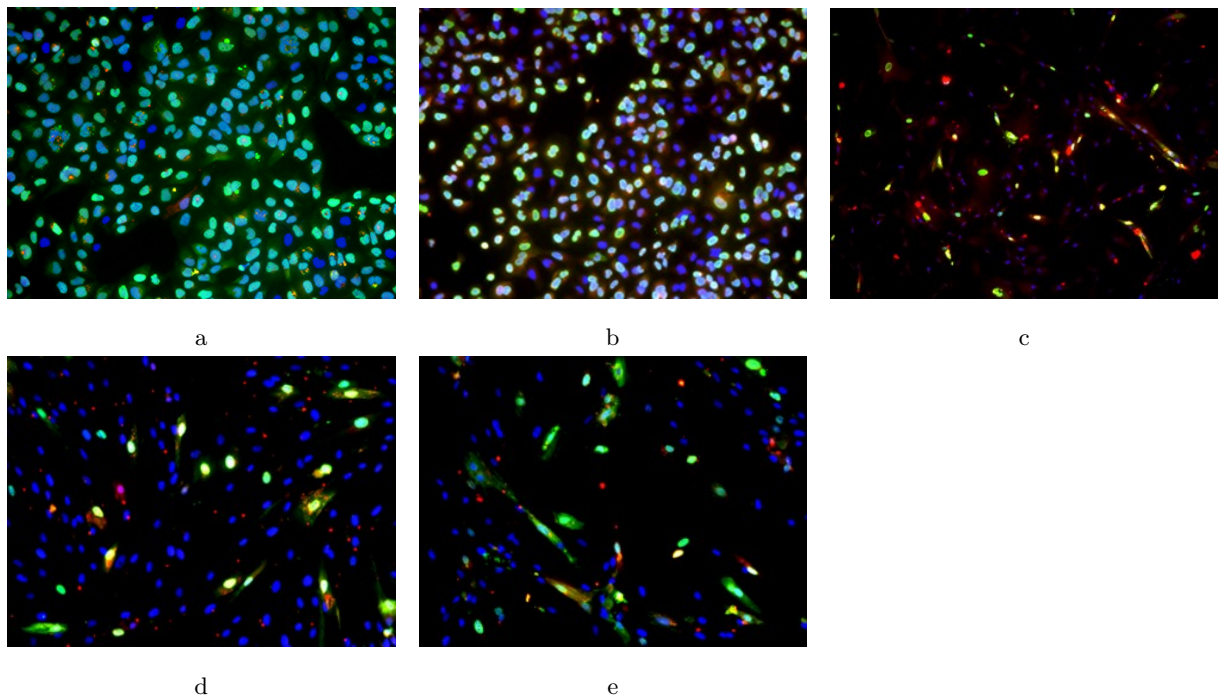


Figure 5.32: NP and M1 protein localizations exemplary shown for isolate i18 (H3N2) infected cell systems at 24h p.i. The individual images show NP-specific fluorescence (green), M1-specific fluorescence (red), and DAPI visualized nuclei (blue) in (a)MDCK, (b)A549, (c)KLU-2-R, (d)porcine fibrocytes and (e)PEL cells.

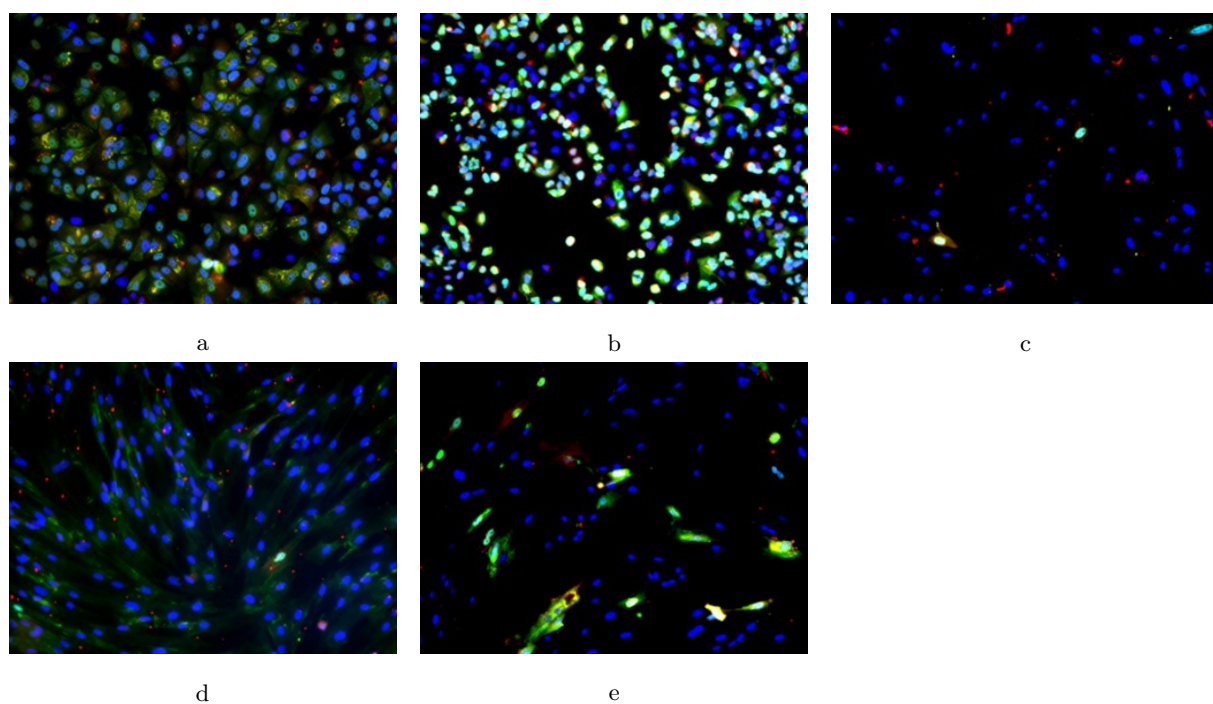


Figure 5.33: NP and M1 protein localizations exemplary shown for isolate i114 (H1N2) infected cell systems at 24h p.i. The individual images show NP-specific fluorescence (green), M1-specific fluorescence (red), and DAPI visualized nuclei (blue) in (a)MDCK, (b)A549, (c)KLU-2-R, (d)porcine fibrocytes and (e)PEL cells.

Discussion and Conclusion

The aim of the presented comprehensive study was the comparison of infectivity, replication and production of infectious virus progeny of current SIV isolates from Southern Germany *in vitro*. Therefore, the parameters chosen for analyses were cytopathic effects (cpe), infectious virus titers, viral protein expression and viral genome loads (Chapter 5). Twelve individual and independent isolates of porcine influenza A virus, classified as subtypes H1N1 (n=3), H1N2 (n=3), H3N2 (n=3) and pdmH1 containing reassortant viruses (n=3) were used (Section 3.1). To compare phenotypic characteristics five different cell systems, MDCK, A549, KLU-2-R, PEL cells, and porcine fibrocytes, were selected. Since MDCK cells are one of the most widely used cell systems for efficient IAV propagation, they were included as reference cells to compare to. A549 cells have mainly been used for isolation of human derived IAV but also in previous studies for SIV replication, posing an important reference for a respiratory epithelial cell line of human origin. The bovine derived cell line KLU-2-R was selected, since it should prove less efficient for SIV replication. Swine derived cells were included systems, originated from the natural host, in contrast to the established cell systems for IAV propagation. Since fibrocytes play a role in the mediated immune system, it was of great interest whether SIV strains would behave differently compared to the other cell systems (Section 4.2.2).

An input MOI of 0.5 was used throughout the infectivity assays described in Chapter 5. During the course of the individual experiments, the infectivity of the input virus suspensions were controlled by titration on MDCK cells (Sections 4.2.3.3 and 4.2.4). Reassessed viral titers indicated minimal variation between 0.1 and 0.8 of input MOI, thereby confirming the comparability of the individual assays. In addition, Abdoli et al. (2012) and Rimmelzwaan et al. (1998) established that IAV showed little difference in replication kinetics for a wide variance in MOI (1-0.0001). Input virus with a MOI of 1-0.1 showed a significant increase of viral titers (expressed in TCID₅₀/100 μ l) within the first 24h p.i. Latest 48h p.i., the maximal titers were reached for these MOIs in MDCK cells and stayed at this level for the next 24h. Therefore, the selected points of time for harvesting the cells and supernatants were at 24h and 72h p.i. for the current experiments. Hence, the outcome of the individual assays was not dependent on large variations in input MOI, but rather on viral phenotypes and cellular systems. In addition all experiments were done at least three times with independent settings.

The immunofluorescence assays showed that infection of MDCK and A549 cells with any of the tested SIV strains resulted in expression of the structural proteins NP and M1. Furthermore, they were able to form progeny infectious virions in MDCK and A549 cells, clearly demonstrated by an increase of infectious viral titers. In striking contrast, at 24h p.i in KLU-2-R cells, no protein expression was observed, except when infected with any of the three H3N2 viruses. Furthermore, no significant increase of infectious virus titers was noted throughout incubation. Interestingly, also porcine fibrocytes infected with H3N2 strains demonstrated viral protein ex-

pression at 24h p.i., in contrast to the other subtypes. In the following Chapter, the results of the study are discussed in detail.

6.1 SIV replication in MDCK and A549 cells is isolate independent and productive

MDCK and A549 pose cell types, which are confirmed to support replication of various influenza A viruses [99][33]. In both cell lines virus replication showed a significant increase within the first 24h of incubation, indicating the peak of progeny production to be around this time for the vast majority of the virus strains. The time-infectivity-kinetics were similar for all isolates in these cells (Figure 5.8 and 5.9). On average, determined viral titers in MDCK cells exceeded the ones in A549 by one order at 24h p.i. (Figure 5.8). The highest infectious mean titers of all compared assays could be obtained in MDCK cells (Figure 5.4 b), which correlates with reported findings [1][59][64][114]. Relative high viral loads were also detected in A549 (Figure 5.5). This was consistent with findings of efficient viral replication of SIV in respiratory tract tissue of different hosts [59][23][61]. Considering the fact that primary target cells for SIV are respiratory epithelium cells, it seems striking that MDCK yielded higher infectious titers compared to A549 cells (Figure 5.8). However, the MDCK system has been used over a long time-period as one of the most efficient cell systems to propagate IAV [78][99] with resulting viral titers of 10^6 - 10^8 (TCID₅₀/ml) [1][64], while infection of A549 cells produced titers exceeding 10^6 only for avian H5N1 virus [59].

Previous studies demonstrated that the presence of exogenous trypsin supports a higher efficiency of plaque forming units, since trypsin supports the HA cleavage during the life-cycle of IAV [48][35]. Since no trypsin treatment was performed in this study, it was expected that detected titers would come below the previously published data that mainly used trypsin [59][114]. All together it was not the aim of this study to enhance the virus yield in a cell system. Adding trypsin to the system might mask strain specific properties in individual cell culture systems, wherefore the artificial trypsin treatment was omitted in the present study.

Taken together, the major production of virus progeny took place within the first 24h after infecting both cell lines with any virus strain, as reported [1][114][83]. Furthermore, there was no distinct difference in maximal virus titers between the individual subtypes, which is corresponding with the reported results of studies using several IAV types [59][64]. Also, obtained real time RT-PCR results demonstrated consistency with previous findings, by detecting viral RNA in every infected sample (Section 2.1.3.1). The real time RT-PCR detected dynamics of viral RNA loads correlated well with the measured production of infectious virus. There was a marked increase of viral protein encoding RNA for MDCK and A549 at 24h p.i., irrespective of the infecting isolate (Figure 5.10 and 5.11). Since both, the production of mRNA and progeny vRNA, might be the reason for this real time RT-PCR result, the RNA load multiplication can be directly associated with the production of new infectious virus, reflected in the titers in these cells (Section 5.3.1 and 5.3.2).

In conclusion, no significant differences concerning replication kinetics and viral RNA load dynamics were detectable between the various SIV subtypes.

In contrast, the observed protein expression in cells infected with the individual SIV strains revealed notable variances. The majority of immunofluorescence assays were negative at 0h p.i. for both structural proteins, NP and M1. However, in cells infected with three individual isolates i53 (H1N1), i114 (H1N2) and i225 (H1N2) viral antigen was observed. Interestingly, the infection with the respective three isolates resulted in detectable viral protein in both cell types, while in A549 actually three additional isolates, i400 (H1N1), i174 (H1N2), and i18 (H3N2), showed detectable NP expression at this point of time (Figure 5.16, Section 5.4.1). There are several reasons which could explain these findings:

1. Since, the virus suspension was inoculated for 2h before rinsing and preparing the cells (Section 4.2.5), this early NP detection could indicate newly synthesized viral protein. This explanation suggests, that proteins of the incoming virus are not detectable due to the relatively low MOI. Visible fluorescence signals depend on the amount of antibodies binding to their antigen and, therefore, on the amount of present proteins, which is clearly enhanced after the synthesis of new viral protein at the ribosomes in the cytoplasm. In consequence, the replication cycle must have started within the 2h of inoculation for early internalized virus particles. Regarding previous reports, IAV requires approximately 25 to 90min to penetrate a cell after adsorption at 37°C *in vitro* [1][50][62][67][34]. With a comparable experimental setting Abdoli et al. (2012) and Rimmelzwaan et al. (1998) detected first NP expression at 4h p.i., once the virus had incubated for 1h. Accordingly, in this study all immunofluorescence assays were negative, except for infections with the respective three (six in A549) isolates. This finding seems conclusive, considering the time that RNPs need to be transported into the nucleus, for transcription of mRNA and to synthesize new proteins at free ribosomes or the endoplasmic reticulum. Hence, this gives reason to assume the isolates i53 (H1N1), i114 (H1N2) and i225 (H1N2) to induce some of these steps more rapidly than all other tested isolates. The fact that NP was exclusively detected at 0h p.i. and that NP is synthesized early in the replication cycle, supports the assumption of visualizing new protein synthesis. Furthermore, input virus should cause M1-specific fluorescence as well. The exclusive cytoplasmic localization of the NP is another supporting argument for the outlined statement.

2. Another explanation could be, that virus particles adhered to the cells surface or were already internalized into the cytoplasm, were still intact at this early stage of replication cycle. As a consequence, the antibodies had limited access to the internal structural proteins and infected cells were not yet detectable. Martin et al. (1991) indicated: When released into the cytosol, the dissociation of M1 from the RNPs might increase accessibility of antibodies to the structure, while intact endosomal virus or particles bound to the surface cannot be detected with utilized antibodies to NP and M1. Koff et al. (1979) examined the kinetics of the uncoating process of IAV and revealed a lag of 15 to 20min after the viral adsorption period before uncoated virus could be detected. The results may indicate that the detected fluorescence represented only released RNPs, giving access to respective antibody binding sites. A supporting argument would again be the exclusive cytoplasmic localization of detected NP in the assays, implying an early stage after the uncoating of IAV into the cells. Nevertheless, obtained observations in this study give reason to some doubt to this thesis. In neither of the two cell types, M1 could be detected at 0h p.i. If the fluorescence signal was derived from incoming virus, this antigen would have been more accessible than NP and should therefore be detectable. Considering the previous studies, frequently reporting the time-frame, required for penetration and uncoating, [1][62][67][34][29] makes this explanation unlikely. Further analyses are needed to elucidate this hypothesis, e.g. with the additional usage of HA detecting antibodies. Since HA is localized at the viral surface, the detection of intact viral particles at any given time of infection would provide evidence if the amount of input virus is detectable at any MOI.

3. Additionally, the temperature fluctuation during inoculation of the viruses could make a difference. As described in previous studies, IAV requires approximately 25 to 90min to penetrate a cell after adsorption at 37°C [1][50][62][67][34]. Youil et al. (2004) and Li et al. (2009) showed in their experiments a delay of replication for IAV at lower temperatures (32°C-33°C) in MDCK cells. Since this delay was observed via viral titers at 24h p.i., it is hardly applicable for protein expression at this earlier time after infection. It seems not probable, but further investigations, whether or not incubation temperatures of 35°C, as used in this study, and 37°C result in a

notable difference of the required times for virus penetration, would be of interest in this matter.

Considering the first explanation most conclusive, the obtained results indicate that SIV isolates i53 (H1N1), i114 (H1N2) and i225 (H1N2) are faster in early infection processes such as adsorption, penetration, uncoating and/or early protein expression, than the other isolates tested. Obviously, the phenomenon is not strictly subtype specific, since two different subtypes demonstrated this feature.

In A549 cells, additionally after infection with isolates i400 (H1N1), i174(H1N2), and i18 (H3N2) antigen was detected at 0h p.i., demonstrating that 6 out of 12 isolates replicate at a faster speed. This result might suggest a faster process in early steps of SIV replication in A549 compared to MDCK, due to a intrinsic cell factors. Since, respiratory epithelium cells are considered to be the target for SIV, it seems probable that some crucial steps in replication could be more efficient in A549 cells, leading to a faster synthesis of new NP. Since this observation was not reflected in the viral titers, when compared to MDCK, it could be assumed, that A549 cells support a more rapidly process only in early steps of replication, e.g. adsorption, penetration or/and uncoating or/and early protein expression. Further investigation into the processes of replication of SIV within A549, with respect to the early stage of infection, would be of interest. It is noteworthy, that the early NP expression in cells infected with the respective isolates (i53 (H1N1), i114 (H1N2) and i225 (H1N2)), were neither reflected by viral titers or viral RNA loads, nor was there a marked difference in the overall fluorescent distribution pattern of NP and M1 at 24h p.i. to other tested isolates (Section 5.4.2.1).

Regarding the time IAV needs to penetrate and replicate in a host cell, as outlined in previous studies [50][62][67], it can be assumed, that at 24 h p.i. the detected fluorescence signals emanate from newly synthesized viral proteins. The overall protein-distribution pattern observed at 24h p.i., illustrated a similar picture for H1N1 and H1N2 isolates in both cell lines (Figures 5.29 and 5.30). In general, NP was predominantly localized to the nucleus - unlike M1- which was evenly distributed within the cytoplasm and the nucleus (Figures 5.17 and 5.18). NP shuttles between the nucleus and the cytoplasm, while transporting RNPs in both directions [109]. Consequently, various steps in virus replication are reflected by the respective distribution of NP within an infected cell. A predominant nuclear NP indicates newly synthesized NP which is transported back to the nucleus. Within the nucleus NP is essential for the production of new vRNA and it interacts directly with the RNA-polymerase proteins to form RNPs progeny [80]. The fact that newly synthesized NP catalyzes the switch from transcription to synthesis of new vRNA [6][49], implies that the amount of NP in the nuclei correlates to the significant increment of viral RNA loads at 24h p.i.

Martin et al. (1991) demonstrated, that the transport of incoming M1 into the nucleus is not required for replication and transcription of viral RNA (Section 2.2.1.1). However, M1 is required to export RNPs from the nucleus to the cell surface membrane. Newly synthesized M1 diffuses into the nucleus and mediates the export by binding to the RNPs. Therefore, the combination of both proteins in the nucleus, increases the likelihood of viral RNPs being exported from the nucleus, hence increasing the amount of infectious progeny.

H1N1 and H1N2 viruses exhibited a clearly co-localized nuclear distribution as well as vesicular aggregations of both structural proteins in the cytoplasm in both cell lines (Figures 5.20 and 5.22). Those vesicular co-localizations represent a promising indicator for a high load of protein synthesis in the producing cell compartments and presumably accumulations of M1 bound RNPs. These cytoplasmic accumulations of both viral proteins were also observed in cells infected with H3N2 and pandemic H1 containing strains.

However, a notable difference was found in immunofluorescence assays with H3N2 viruses. In over 90% of the cells infected with H3N2 isolates, the detected NP concentrated almost ex-

clusively to the nuclei (Table 5.5). This was observed in both cell types, MDCK and A549. Furthermore, in cells infected with H3N2 isolates M1 was mostly cytoplasmic in contrast to H1N1, H1N2 and pandemic H1 containing strains. As previously outlined, NP accumulates and remains in the nucleus until M1 mediates their export, bound to the vRNPs. Since exclusively newly synthesized M1 migrates to the nucleus (Section 2.2.1.3), the findings indicate M1 being not as efficiently produced or shuttled at this point of time for H3N2 strains as in other strains. A delay in some earlier steps in the replication cycle, such as entry events, RNPs transportation, transcription and/or protein synthesis of H3N2 subtypes could be an explanation for this surprising result. In order to determine, if the described observations are based on an altered replication cycle of H3N2 subtypes, shorter temporal intervals ought to be investigated in future studies.

On average, pandemic H1 containing subtypes did not exhibit an uniform distribution of immunofluorescent positive cells in MDCK and A549, as strains of H1N2, H3N2 and H1N1 did. As depicted in Figure 5.31, infected cells appeared more isolated than in other samples. The respective assays included more frequently cells with only a specific fluorescence for either M1 or NP. Especially exclusive expression of M1 could indicate an impaired infection of those cells. Whether other viral proteins degraded or if only M1 was efficiently produced in the cells, could not be determined in this study. But the amount of viral protein degradation seems to be higher for these pandemic strains, than for the 'classic' SIV subtypes. Infection with the pdmH1N1 isolate (i57) resulted in comparatively higher levels of specific fluorescence for both structural proteins, than the pdmH1N2 strains. In addition mean infectious titers of the latter were below the maximal titers of the pdmH1N1 isolate i57 (Figures 5.4 m and 5.5 m). Again, these findings largely corresponded between MDCK and A549 cells.

In conclusion, the performed immunofluorescence experiments in MDCK and A549 cells demonstrated the synthesis of new viral proteins, which was reflected in various individual stages of replication in the cells at 24h p.i. Several interesting differences could be defined between H3N2, pandemic H1 containing strains and the isolates of subtypes H1N1 and H1N2. However, the respective differences in protein expression were neither reflected by the mean viral titers detected for the individual isolates, nor could they be associated with specific genome replication dynamics. It has to be noted, that respective variations evolved similarly in A549 and MDCK.

6.2 SIV is not replication-competent in KLU-2-R cells

The results obtained for KLU-2-R infectivity assays, corroborated the assumption of bovines not being hosts for influenza A viruses (Section 5.8, Figure 5.6). Accordingly, no production of virus progeny could be obtained in infected cells, irrespective of the isolate. All determined viral titers decreased within the 72h of incubation, indicating an impaired replication. In prospect of discussing the obtained results in KLU-2-R cells, it has to be emphasized that infection is not equitable with the capability to replicate. Important steps in replication, replication of viral genomes and mRNA production, are performed within the infected nuclei [36]. As also shown in this study, whenever the NP-entry into the nucleus is blocked, replication has to be inhibited. Evidence of a successful entry of RNPs into the nucleus is essential to prove the replication capability. Either this is performed by detecting viral RNA multiplication or observing viral protein expression in the nucleus. Furthermore, a successful infection of a cells' nucleus does not necessarily result in a complete replication cycle and thus in producing infectious progeny virions (Section 2.2.1).

In infectivity assays in KLU-2-R cell, the most interesting finding was the detectable NP-expression in H3N2 subtype infected cells at 24h p.i. (Section 5.4.2.3). Since NP was clearly located in the nucleus, it has to be concluded that H3N2 isolates successful infected the KLU-2-R cells. With regard to the time of 24h after infection, this NP most likely demonstrated

newly synthesized NP. In contrast, M1 proteins were rarely detected and were mostly localized in the cytoplasm (Section 5.4.2.3). However, neither infectious virus nor a distinct increase of viral RNA loads could be observed. The fact that no infectious virus was obtained leads to the conclusion that replication stopped during or after the protein synthesis.

One reason might have been an insufficient M1 synthesis. Since M1 is required for the export of new RNPs, a shortage might inhibit this transport [63] (Section 2.2.1.3). Horisberger et al. (1988) showed bovine interferon (IFN)- α to be very effective in reducing viral replication of influenza virus. The inhibition of IAV RNA transcription [52] or translation [40] are discussed to be sensitive steps for IFN action in bovine cells. Therefore, IFN- α inhibits the early protein synthesis, which does not correlate with the findings for H3N2 isolate infected cells (Section 5.4.2.3). An inhibition of transcribing cRNA and thus new vRNA might be one reason for the impairment of replication of H3N2 isolates in this study, since the determined c_q values decreased between 0h and 24h p.i. by not more than 4 levels, which is notable but minor. Obviously, no large amounts of viral RNA could be synthesized. Possibly the small increase in viral RNA load reflects some mRNA synthesis needed for the production of early proteins, such as NP. Since the used real time RT-PCR system cannot differentiate between mRNA and vRNA, there is no verification for this hypothesis.

In conclusion, the reported results show, that H3N2 strains do infect KLU-2-R cells to some extent but cannot complete their replication cycle, even if the synthesis of NP is successfully initiated (Figure 5.8 c, Section 5.4.2.3, Figure 5.32).

Accordingly, other subtypes were incapable of replicating until anew formation of virus particles in KLU-2-R cells, and therefore, viral titers decreased within the 72h of incubation. The highest infectious loads were detected at 0h p.i. (Figure 5.8).

On the one hand the increase of titer in supernatants at 24h p.i. in 9 out of 12 samples, could lead to the suggestion that viral particles only adhered to the cells' surface, but did not even penetrate. This could be the result of detached virus eluted in the supernatant.

On the other hand, the detection of highest titers at 0h p.i. in the cells, could mean an entry of the input virus, which is subsequently inhibited to infect the nucleus, resulting in a degradation of virus and hence a decrease in viral titer.

Besides the fact, that H3N2 isolates were clearly able to penetrate KLU-2-R cells, more observations support the hypothesis of abortive infection. Infection with isolate i114 (H1N2) also resulted in few single cells expressing NP (Figure 5.33), and for isolate i53 (H1N1) in fact both structural proteins were detected at 0h p.i. Real time RT-PCR results revealed a small c_q decrease (not more than 4 levels) in cells infected with isolate i225 (H1N2) and i42 (pdmH1N2) at 24h p.i. (Figure 5.12 f and k). However, due to the experimental settings, we consider a difference of up to 3 c_q values as ordinary variation, leading to the conclusion that these viral RNA load dynamics are indistinct. Therefore, the present results (Figures 5.12 and 5.14, Section 5.4.1) are not conclusive, whether all investigated isolates were capable of penetrating KLU-2-R cells - irrespective of further infection - or if just the particular strains (i53 (H1N1), i114 (H1N2), i101 (H3N2), i18 (H3N2) and i338 (H3N2)) were capable of entering the cells. Undeniably, in the majority of performed assays neither NP and M1-expression was found, nor markedly increased viral RNA loads nor prove of infectious virus production during incubation. Further experiments would be necessary, to conclude if only H3N2 subtypes and isolates i114 (H1N2) and i53 (H1N1), were able to penetrate KLU-2-R cells or if all influenza A viruses could enter the cells, without initiating any detectable marker for infection. The usage of a wider antibody range and shorter temporal intervals within experiments could give prospect for an accurate explanation in this matter.

As depicted in Figure 5.14, isolate i53 (H1N1) only induced detectable NP and M1 staining at 0h p.i. but not 24h later. This implies a degradation of viral protein, hence suggesting that the

infection was impaired at one crucial stage in the replication cycle.

In sum, this study proved SIV strains to be incapable of infecting KLU-2-R cells except for H3N2 subtype viruses, one H1N2 isolate (i114) and probably one H1N1 isolate (i53). No SIV virus is capable of infectious virus production in these cells, irrespective of infecting the cells or not.

6.3 Infection and replication of SIV in porcine fibrocytes is isolate specific

The results presented in Section 5.2.4 indicate that no SIV isolate, tested in this study, replicated in porcine fibrocytes (Figure 5.8), except one single H3N2 isolate. Only infection with i101 (H3N2) resulted in an increase in viral titers, of more than one order within the first 24h p.i. (Figure 5.7 g). Furthermore, real time RT-PCR results showed an increase of viral RNA loads in samples infected with i101 (H3N2). Viral protein expression was also detected at 24h p.i., completing the parameters investigated and necessary to judge an efficient infection and replication.

The results for other strains, were not as conclusive as for isolate i101 (H3N2). Corresponding with findings in KLU-2-R cells, the fibrocytes infected with H3N2 isolates and i114 (H1N2) were the only ones expressing antigen at 24h p.i. No fluorescence was detected at this point of time in cells infected with any of the other isolates, indicating that no other SIV isolate could efficiently induce protein expression. In H3N2 infected cells the distribution pattern for NP was predominantly nuclear whereas M1 was distributed evenly. Since this reflected most likely newly synthesized proteins [50][62][67], it corresponded with the distribution pattern observed in every other investigated cell types (Sections 6.1 and 6.2).

One isolate of H3N2 (i18) seemed to stop at one point in infection in porcine fibrocytes, whereas the other isolate used in these assays (i101) evidently completed the replication cycle. There was hardly any viral RNA multiplication detectable for isolate i18 in porcine fibrocytes over the 72h of incubation, implying, that replication stopped with the viral protein synthesis. Kistner et al. (1989) revealed the phosphorylation of the virus' NP to be crucial for efficient replication of IAV. This could indicate that the NP of isolate i101 (H3N2) was adequately phosphorylated, due to slight sequence variations ('antigenic drift'), while the NP of isolate i18 (H3N2) was not, thus being inhibited in subsequent replication. Further investigations in isolates of H3N2 and a detailed comparison of NP-sequences could elucidate the reasons for one isolate being able to replicate, while a closely related one was not.

Although antigen was detectable at 24h p.i., the distribution of NP and M1 differed clearly for isolate i114 (H1N2) from the H3N2 strains (Figures 5.32 and 5.33). Since the detected NP expression emanates most likely from newly synthesized proteins, H3N2 shows a strong ability to re-import NP into the nucleus, whereas for i114 (H1N2) NP was found predominantly outside the nucleus in the cytoplasm. Furthermore, basically no M1 was detected in i114 (H1N2) infected cells. Whether the re-import of NP into the nucleus is inhibited or whether the observation reflects an earlier stage in the production of NP in the cells' compartments could not be distinguished in this study.

Viral M-gene RNA detection was quite sensitive in revealing SIV H3N2 and isolate i114 to enter porcine fibrocytes (Figure 5.13 e, g, and h). Viral RNA of pdmH1 isolates was also found to multiply within the first 24h p.i. (Figure 5.13 k and m). Interestingly, the c_q values, did not correlate with protein expression (Section 5.4.2.4). Obviously pandemic H1 containing viruses multiplied RNA, but surprisingly, they were not able to induce synthesis of NP or M1, in contrast to H3N2 subtypes or i114 (H1N2). The detected replication of viral RNA, indicates that the respective viruses were capable of transporting RNPs to the nuclei and transcribe mRNA. The

DNA Polymerase, used in the real time RT-PCR system, is designed for a sensitive amplification of RNA molecules from either form of RNA - mRNA, cRNA and vRNA. Since free NP protein is required for a production of cRNA and new vRNA (Section 2.2.1), the c_q values assumingly based on the detection of viral mRNA for the pandemic H1 containing isolates. Since a clear increase of RNA load could be detected, but no protein expression, the replication is probably inhibited during or after transcribing the incoming vRNA into mRNA.

As described in Section 5.2.4, all infections of fibrocytes except of the ones with i101 (H3N2) showed a decrease in virus titers or remained at the level of the input virus titers at 0h p.i. In contrast, titers in supernatants increased between 0h and 24h p.i., irrespective of the subtype (Figure 5.9). This could be a result of virus first adhering to the cells surface, but being unable to penetrate and thereby, detaching from the surface in the first 24h of incubation. Balmelli et al. (2005) showed the efficient endocytosis capability of porcine fibrocytes. Therefore, it has to be considered, that SIV could enter porcine fibrocytes via unspecific endocytosis, instead of receptor mediated endocytosis as in ‘conventional’ infections. Further experiments are necessary to investigate a not receptor-mediated endocytosis process and its influence on the interpretation of our results.

It is notable, that the same isolates i53 (H1N1), i114 (H1N2) and i225 (H1N2) lead to NP expression at 0h p.i. as in MDCK, A549, and PEL cells. The potential explanations for this observation are discussed in Section 6.1.

6.4 Protein expression in PEL cells is comparable for all individual SIV isolates

Protein expression in infected PEL cells at 0h and 24h p.i. was assessed in three independent experiments, and NP and M1 expression in some, albeit not all cells were observable, irrespective of the infecting virus. This implies that all virus strains could to some extent enter the cells, transport RNPs to the nuclei and initiate viral protein synthesis. These findings were consistent with previous results, stating efficient IAV protein replication in porcine respiratory epithelia [81]. Although the amount of infected cells, varied notably (Table 5.5), the protein localization did not vary as much in respect of NP and M1 distribution, as it did in other cell systems (Section 6.1). Remarkably, the amount of NP expressing cells in H3N2 infected PEL cells was higher than for other SIV isolates, supporting previous results obtained in the other cell systems (Section 5.4.2.5). In PEL cells, virus replication could only be addressed once (Section 5.2.5)), due to the limited availability of PEL cells. In contrast, SIV replication in all other cell systems was determined in at least three individual and independent experiments. Due to the fact that PEL cells were used just once, it only allows the conclusion that most virus isolates were capable of full replication in these cells, albeit at very low levels (Table 5.4). In context with previous studies [64][23], the capability of SIV isolates to replicate in PEL was expected. Surprisingly, replication was not as efficient as anticipated, since titers of isolate i199 (H1N1) decreased notably, while i174 (H1N2) and i57 (pdmH1N1) showed no titer increment over the 72h of incubation. Further experiments are needed for detailed interpretation, because the assessed results may be influenced by the specific experimental setting.

6.5 Specific features of individual SIV isolates correspond in all cell systems tested

This study demonstrated a close correlation between specific subtypes of SIV and the capability of efficient infection and initiating structural protein expression of a virus. Clearly every H3N2 isolate could translate mRNA into new NP and M1 synthesis, irrespective in which cell type. Respective H3N2 isolates revealed an efficient protein expression, resulting in an almost exclusive nuclear NP localization, also found in every cell type infected. The strong ability to transcribe mRNA - which is translated to new NP - was reflected in the viral RNA dynamics detected with the real time RT-PCR system. KLU-2-R cells were the only exception wherein H3N2 isolates could neither replicate infectious viral progeny, nor initiate any significant decrease in c_q value. Kistner et al. (1989) studied NP and showed that the phosphorylation process of NP is a crucial step in the virus life-cycle. The phosphorylation is supposed to be one reason, why viral NP can interact with other proteins i.e. the M1 (Section 2.2.1.2). In previous studies Kistner et al. (1989) showed that the host-specific phosphokinases play an important modifying role in the process of this NP-phosphorylation. Therefore, it is reasonable to presume that different host cells might regulate the multiplication of a virus differently in this aspect. It could be speculated that replication was interrupted in KLU-2-R cells, due to a lack of interaction with cell-specific phosphokinases in these cells.

In porcine fibrocytes the replication was only partially inhibited, for isolate i18 (H3N2), since i101 (H3N2) evidently could complete the replication cycle.

Interestingly, the results obtained in experiments on MDCK and A549 cells, support the observation of isolate i18 being not as efficient in *in vitro* replication as H3N2 isolates i101 and i338 (Figures 5.4 to 5.7 g and i compared to h). Even in highly susceptible MDCK and A549 cells, infectious viral titers increased not more than $0.5\log_{10}$ in the first 24h p.i. infected with i18 (H3N2). A lower viral titer of this isolate at all investigated points in time, compared to the other H3N2 viruses, was a consistent finding, although protein expression did not differ between the individual isolates. As discussed in Section 6.3 this observation might result of sequence variations between the H3N2 viruses, enabling isolate i101 (H3N2) and i338 (H3N2) to replicate more efficiently. Individual ‘antigenic drift’, could be one reason why specifically isolate (i101) could replicate in porcine fibrocytes, while the second isolate (i18) tested was not able to. Results of phylogenetic analyses by Pippig et al. (2016) showed the close relationship between all Bavarian H3N2 viruses analyzed on the level of H and N sequences, other segments however still need to be analyzed. Hence, there is reason to assume that individual properties are not only SIV subtype dependent, but also due to individual variations, underlining the importance of investigating more than one isolate per subtype. One additional indicator for this assumption was revealed by analyzing SIV H1N2 subtype infected cells. Surprisingly, isolate i114 induced detectable NP/M1-expression in KLU-2-R cells and porcine fibrocytes, whereas for the other H1N2 strains no specific immunofluorescence could be observed in those two cell types. Interestingly, i225 (H1N2) revealed viral protein expression in all cell types (excluding KLU-2-R) at 0h p.i. The reason for the negative assays at 24h p.i. in porcine fibrocytes may also be a result of individual properties. In immunofluorescence assays of isolate i114 almost exclusively NP was observed for fibrocytes and KLU-2-R cells infected at 0h and 24h p.i., implying an insufficient M1 production. The replication was inhibited in both cell systems (porcine fibrocytes and KLU-2-R), but this study could not establish at which exact step the replication cycle was impaired (Sections 6.2 and 6.3).

The conclusion that individual SIV subtypes possess specific subtype-dependent characteristics is not invalidated by these data. Individual strains showing exclusive features in a variety of cells only implies that the phenotype of a single virus isolate can differ from others of the same subtype, due to mutations (Sections 2.1.3 and 2.1.4).

Furthermore, this study suggested that pandemic H1 containing viruses might have the potential of adapting to different cell systems, since a distinct increase of viral RNA loads in porcine fibrocytes was observed. Even if these pandemic H1 containing viruses could not express viral proteins or replicate new virus, they were able to transport viral RNA into nuclei and to initiate RNA multiplication. Interestingly enough, only H3N2 and the pandemic H1 containing strains were able to perform those first steps in replication in all tested cells (with the exception of KLU-2-R for pandemic H1 containing isolates) representing the two subtypes which are found in a lower prevalence in Southern Germany [79]. Virulence on the one hand and adaptation to host species on the other hand require complex multi-factorial interactions between virus and host, which are likely under individual selective pressure [98], which could be one explanation for this observation. The presented data on differences in *in vitro* phenotypes of SIV subtypes give rise to the assumption, that these phenotypes may result from different solutions to the problem of replication and transmission in a host. The accumulation of NP in the nuclei - observed in every tested cell type for H3N2 strains - suggest that M1 might not be as efficiently exporting RNPs as observed for other subtypes at 24h p.i. Porcine influenza viruses usually bud from a cell and reenter adjacent ones. An 'inadequate' time of the replication cycles could result in insufficient quantities of virus progeny to promote an efficient cell-to-cell spreading infection. In total, less virions could be released from the cells, thus also leading to a rather insufficient transmission between pigs. On the one hand utilizing this small advantage of a faster virus shedding, H1N1 and H1N2 may be transmitted more rapidly. This might be represented in the higher prevalence.

On the other hand, for strains replicating slower, like H3N2 viruses, the rather few opportunities for a transmission in pigs may result in a higher adaption capability to different host cells. The ability of infecting cells of the immune system (porcine fibrocytes), implies a specific potential of a subtype to adapt to their hosts, which was demonstrated in this study by H3N2 and pandemic viruses. Together with the findings in bovine cells (KLU-2-R) these indications point to an increased likelihood of H3N2 being capable of crossing species barriers efficiently.

6.6 Conclusion

Since the aim of the current study was the comparison of infectivity, replication, and production of infectious progeny virus of current SIV isolates, it is noteworthy that observed results actually indicated unique features for one SIV subtype, namely H3N2. The fact, that H3N2 strains were able to perform first steps in replication in all cells tested, demonstrated specific infectivity characteristics for this subtype, when compared to the other porcine IA viruses. The working theory of not all SIV subtypes being equal in their phenotypic properties was therefore proven. However, these findings are dependent on the *in vitro* system employed. As in many previous studies, the experiments in MDCK and A549 cells indicated no significant differences in the replication kinetics of different SIV subtypes. All investigated isolates multiplied significantly within the first 24h, irrespective of the subtype. These results are comparable to the findings of studies, investigating in IAV replication in these cell systems [1][59][64][114][83]. The measured c_q values of the real time RT-PCR confirmed results of virus infectivity assays, in terms of increasing RNA levels, when virus multiplied and no significant change in c_q values when replication was absent. Hence, investigations of titers and viral RNA loads, may not indicate a substantial difference between SIV subtypes, as performed in most previous studies in well established cell systems. Only the additional experiments in this study revealed that characteristics detected in one or two cell systems do not necessarily allow for conclusions about comprehensive characteristics of a porcine IAV subtype in general. Though individual SIV isolates will represent genetic variations, and may thus additionally differ in their phenotypes, the results of the presented study suggest, that certain properties are indeed depending on the SIV subtype.

Whether these *in vitro* observations can be reflected by specific pathogenic properties of these viruses *in vivo*, would be of high interest for future studies. In addition, those findings could suggest that especially porcine H3N2 viruses might have an enhanced zoonotic potential and therefore, would have to be thoroughly watched in future surveillance.

Summary

Influenza is an acute respiratory disease of pigs, caused by swine influenza A viruses (SIV). Three different subtypes, avH1N1, huH1N2 and ‘human-like’ swine H3N2 virus, were stably prevalent in pig populations in Germany until the incursion of the new pdmH1N1 virus in 2009. Its ever since co-circulation with endemic SIV, has yielded new reassortant viruses some of which have already established stable infection chains. Specific phenotypic characteristics, especially of these new emerging reassortant viruses are largely unknown.

The aim of the present study was to address whether in southern Germany currently circulating SIV vary in their phenotypes *in vitro*. Therefore, a comparison of selected steps in the SIV life cycle was performed by analyzing expression of individual viral proteins and kinetics of viral RNA loads within infected cells. In addition, the production of virus progeny was compared quantitatively at different times after infection. Twelve individual and independent isolates of porcine influenza A virus, classified as subtypes H1N1 (n=3), H1N2 (n=3), H3N2 (n=3) and pdmH1 containing, reassortant viruses (n=3) were used in these investigations. To compare phenotypic characteristics, five different cell systems, MDCK, A549, KLU-2-R, PEL, and porcine fibrocytes, were selected.

Expectedly, efficient replication and production of infectious progeny was noted for all twelve SIV isolates in MDCK, A549, and PEL cells. MDCK cells and the A549 cells, derived from human lung, are well known to support replication of various influenza A viruses. In these established systems no noteworthy differences between the replication kinetics of the twelve viruses were observed. Surprisingly, infection and replication was not as efficient as anticipated in the porcine embryonic lung cells (PEL). However, the replication kinetics were comparable between all isolates. Since, bovine KLU-2-R cells derived from calf lung should hardly be subject of IAV infection, as expected, no infectious virus progeny was replicated in these cells, irrespective of the isolate used. Hence, assessing *in vitro* viral titers and viral RNA loads in ‘standard’ cell systems, such as well established MDCK or A549 cells, may not allow to define distinct differences between phenotypes of SIV subtypes. In contrast, in porcine fibrocytes only one single virus isolate of SIV subtype H3N2 was able to produce virus progeny, providing the first indication that differences might nevertheless exist. Furthermore, for pandemic H1 containing viruses viral RNA multiplication was detected in porcine fibrocytes, while neither virus progeny, nor viral protein expression was observed. These results might suggest, that in those cases mRNA was produced, but further steps of replication were impaired. However, pandemic H1 containing isolates clearly infected porcine fibrocytes, while other isolates were incapable of doing so.

Surprisingly, protein expression and distribution patterns varied not only between the different cell systems but also between individual SIV subtypes. In all five cell lines infected with any of the H3N2 isolates, NP was almost exclusively found in the nuclei at 24h p.i. In contrast, when

infected with H1N1, H1N2 or the pandemic H1 containing isolates the observed NP-distribution was more cytoplasm associated in MDCK, A549, and PEL cells. For these strains no indication of protein expression was found at all in porcine fibrocytes or KLU-2-R cells.

In summary, the presented data indicate unique features for SIV subtype H3N2 *in vitro*. The results also suggest that individual isolate characteristics occur within a specific subtype, since one out of the three H1N2 isolates displayed some distinctive features. Furthermore, some variations between the individual H3N2 isolates were noted. Hence, it was demonstrated that assessing the phenotypic properties of one single strain of SIV does not necessarily allow for conclusions about the corresponding subtype or even about SIV in general. It was clearly shown in this study that present SIV isolates are not only genetically but also phenotypically divergent. Further investigations will be necessary to examine the observations of this study in more detail and to determine the *in vivo* relevance of the specific virus characteristics observed in this study.

Summary (German)

Influenza ist eine akute respiratorische Erkrankung des Schweines, verursacht durch porcine Influenza A Viren (pIAV). Drei Subtypen, avH1N1, huH1N2, sowie 'human-like' swine H3N2 bildeten eine stabile Mehrheit der vorkommenden pIAV in Deutschland, bis 2009 ein neues pdmH1N1 Virus in den Schweinepopulationen auftrat. Dessen Ko-Zirkulation mit endemisch verbreiteten porcinen Subtypen brachte neue, reassortierte Viren hervor, die bereits eigenständige Infektionslinien etablieren konnten. Spezifische phänotypische Charakteristika, besonders dieser neu reassortierten Viren, sind weitestgehend unbekannt.

Diese Studie beschäftigte sich mit der Frage, ob in Süddeutschland gegenwärtige pIAV in ihren phänotypischen Eigenschaften *in vitro* variieren. Dazu wurden einige entscheidende Schritte im Infektionszyklus von pIAV, mittels Analyse der viralen Proteinexpression und der Kinetik viraler RNA-Lasten in infizierten Zellen, verglichen. Die Produktion infektiöser Tochterviren wurde zu verschiedenen Zeitpunkten nach der Infektion quantitativ verglichen. Zwölf individuell unabhängige Isolate der porcinen Virussubtypen H1N1 (n=3), H1N2 (n=3), H3N2 (n=3) und reassortierte, pandemisches H1 beinhaltende Viren (n=3), wurden in den Experimenten genutzt. Um die phänotypischen Charakteristika zu vergleichen, wurden fünf verschiedene Zellsysteme, MDCK-, A549-, KLU-2-R-Zellen, porcine embryonale Lungenzellen und porcine Fibrozyten ausgewählt.

Wie zu erwarten replizierten alle zwölf Isolate effizient infektiöses Virus in MDCK, A549 und PEL Zellen. MDCK Zellen und die von menschlichem Lungengewebe gewonnenen A549 eignen sich bekanntlich zur produktiven Influenza A Virus Reproduktion. In diesen etablierten Zellsystemen wurden keine auffälligen Unterschiede in der Replikationskinetik zwischen den zwölf Isolaten beobachtet. Infektion und Replikation waren in porcinen embryonalen Lungen Zellen (PEL) überraschenderweise weniger effizient als erwartet. Allerdings waren die Replikationskinetiken zwischen den Isolaten auch hier vergleichbar. Es wurde erwartet, dass Bovine KLU-2-R Zellen nur schlecht infizierbar sein würden. Entsprechend wurde in diesen Zellen keine infektiösen Nachkommenviren gebildet, unabhängig vom verwendeten Virusisolat. Die in den Standard-Zellsystemen, z.B. MDCK und A549, bestimmten viralen Titer und RNA-Lasten, waren nicht geeignet, spezifische Unterschiede der phänotypischen Eigenschaften zwischen pIAV Subtypen herauszuarbeiten. Im Gegensatz dazu war nur ein einzelnes Isolat des Subtyps H3N2 fähig in porciner Fibrozyten neue Viren zu produzieren, was den ersten Hinweis für unterschiedliche Eigenschaften der Subtypen lieferte. Für pandemische H1 enthaltende Isolate war zwar eine merkliche RNA Vermehrung in porcinen Fibrozyten nachweisbar, ein Anstieg der infektiösen Titer, oder die Expression von viralen Proteinen jedoch nicht. Diese Ergebnisse lassen vermuten, dass in diesen Fällen eine Produktion von mRNA stattfand, während die weiteren Schritte der Replikation beeinträchtigt waren. Allerdings wurde somit gezeigt, dass pandemische Isolate por-

eine Fibrozyten infizieren konnten, während andere Isolate dazu nicht fähig waren.

Überraschenderweise konnten in der Proteinexpression wesentliche Unterschiede sowohl zwischen den verschiedenen Zellarten, als auch zwischen den einzelnen Subtypen gezeigt werden. In allen fünf Zelllinien, die mit Isolaten des Subtyps H3N2 infiziert waren, wurde NP 24h nach Infektion fast ausschließlich in den Kernen gefunden. Im Gegensatz dazu wiesen A549, MDCK und PEL Zellen, die mit H1N1, H1N2 und den pandemischen H1 enthaltenden Viren infiziert wurden, eine eher zytoplasmatische Verteilung des NP auf. Weder in porcinen Fibrozyten, noch in KLU-2-R Zellen wurde zu diesem Zeitpunkt für diese Virusstämme Hinweise auf eine virale Proteinexpression detektiert.

Zusammengefasst deuten die Daten darauf hin, dass kürzlich in Bayern isolierte Schweineinfluenza Viren des Subtyps H3N2 *in vitro* spezielle, phänotypische Merkmale besitzen. Außerdem weisen die Ergebnisse darauf hin, dass individuelle Charakteristika auch innerhalb eines spezifischen Subtyps auftreten können, da eines der drei Isolate des Subtyps H1N2 deutlich abweichende Eigenschaften zu den anderen zeigte. Außerdem konnten Variationen zwischen den einzelnen H3N2 Isolaten festgestellt werden. Folglich können auch innerhalb eines bestimmten IAV Subtyps weitere Isolat-spezifische Charakteristika auftreten. Dies verdeutlicht, dass einzelne phänotypische Eigenschaften nicht zwangsläufig auf den gesamten Subtyp generalisiert werden dürfen und daher auch nicht für pIAV im Allgemeinen. Diese Studie zeigte, dass sich aktuelle in Bayern isolierte pIAV nicht nur genetisch sondern auch phänotypisch unterscheiden. Um die Beobachtungen dieser Studie detaillierter zu untersuchen und die *in vivo* Relevanz zu klären, werden weiterführende Untersuchungen benötigt.

Bibliography

- [1] ABDOLI, A., SOLEIMANJAH, H., TAVASSOTI KHEIRI, M., JAMALI, A., AND JAMAATI, A. Determining influenza virus shedding at different time points in madin-darby canine kidney cell line. *Cell* 15, 2 (2013), 130–5.
- [2] AKARSU, H., BURMEISTER, W. P., PETOSA, C., PETIT, I., MÜLLER, C. W., RUIGROK, R. W. H., AND BAUDIN, F. Crystal structure of the M1 protein-binding domain of the influenza A virus nuclear export protein (NEP/NS2). *The EMBO Journal* 22, 18 (2003), 4646–55.
- [3] AVALOS, R. T., YU, Z., AND NAYAK, D. P. Association of influenza virus NP and M1 proteins with cellular cytoskeletal elements in influenza virus-infected cells. *Journal of Virology* 71, 4 (1997), 2947–58.
- [4] BALMELLI, C., ALVES, M. P., STEINER, E., ZINGG, D., PEDUTO, N., RUGGLI, N., GERBER, H., MCCULLOUGH, K., AND SUMMERFIELD, A. Responsiveness of fibrocytes to toll-like receptor danger signals. *Immunobiology* 212, 9 (2008), 693–699.
- [5] BALMELLI, C., RUGGLI, N., MCCULLOUGH, K., AND SUMMERFIELD, A. Fibrocytes are potent stimulators of anti-virus cytotoxic T cells. *Journal of Leukocyte Biology* 77, 6 (2005), 923–933.
- [6] BEATON, A. R., AND KRUG, R. M. Transcription antitermination during influenza viral template RNA synthesis requires the nucleocapsid protein and the absence of a 5' capped end. *Proceedings of the National Academy of Sciences of the United States of America* 83, 17 (1986), 6282–6.
- [7] BLUMENTHAL, H. T., GREIFF, D., PINKERTON, H., AND DEWITT, R. Influenza I. The hemagglutination and infectivity titre curves of PR8 influenza virus cultivated in embryonated eggs at different temperatures. *The Journal of Experimental Medicine* 91, 3 (1950), 321–329.
- [8] BOSCH, F., ORLICH, M., KLENK, H.-D., AND ROTT, R. The structure of the hemagglutinin, a determinant for the pathogenicity of influenza viruses. *Virology* 95, 1 (1979), 197–207.
- [9] BOUVIER, N. M., AND PALESE, P. The Biology of Influenza Viruses. *Vaccine* 26, Suppl 4 (2008), D49–53.

- [10] BROWN, I., HARRIS, P., MCCAULEY, J., AND ALEXANDER, D. Multiple genetic reassortment of avian and human influenza A viruses in European pigs, resulting in the emergence of an H1N2 virus of novel genotype. *Journal of General Virology* 79, 12 (1998), 2947–2955.
- [11] BUCALA, R., SPIEGEL, L., CHESNEY, J., HOGAN, M., AND CERAMI, A. Circulating fibrocytes define a new leukocyte subpopulation that mediates tissue repair. *Molecular Medicine* 1, 1 (1994), 71.
- [12] BUI, M., WILLS, E. G., HELENIUS, A., AND WHITTAKER, G. R. Role of the influenza virus M1 protein in nuclear export of viral ribonucleoproteins. *Journal of Virology* 74, 4 (2000), 1781–6.
- [13] CASTRUCCI, M. R., DONATELLI, I., SIDOLI, L., BARIGAZZI, G., KAWAOKA, Y., AND WEBSTER, R. G. Genetic reassortment between avian and human influenza A viruses in Italian pigs. *Virology* 193, 1 (1993), 503–506.
- [14] CHAMORRO, S., REVILLA, C., ALVAREZ, B., ALONSO, F., EZQUERRA, A., AND DOMINGUEZ, J. Phenotypic and functional heterogeneity of porcine blood monocytes and its relation with maturation. *Immunology* 114, 1 (2005), 63–71.
- [15] CHESNEY, J., BACHER, M., BENDER, A., AND BUCALA, R. The peripheral blood fibrocyte is a potent antigen-presenting cell capable of priming naive T cells in situ. *Proceedings of the National Academy of Sciences of the United States of America* 94, 12 (1997), 6307–6312.
- [16] CHOI, Y., GOYAL, S., KANG, S., FARNHAM, M., AND JOO, H. Detection and subtyping of swine influenza H1N1, H1N2 and H3N2 viruses in clinical samples using two multiplex RT-PCR assays. *Journal of Virological Methods* 102, 1 (2002), 53–59.
- [17] CLAAS, E. C., OSTERHAUS, A. D., VAN BEEK, R., DE JONG, J. C., RIMMELZWAAN, G. F., SENNE, D. A., KRAUSS, S., SHORTRIDGE, K. F., AND WEBSTER, R. G. Human influenza A H5N1 virus related to a highly pathogenic avian influenza virus. *The Lancet* 351, 9101 (1998), 472–477.
- [18] COCCIA, E. M., SEVERA, M., GIACOMINI, E., MONNERON, D., REMOLI, M. E., JULKUNEN, I., CELLA, M., LANDE, R., AND UZÉ, G. Viral infection and Toll-like receptor agonists induce a differential expression of type I and λ interferons in human plasmacytoid and monocyte-derived dendritic cells. *European Journal of Immunology* 34, 3 (2004), 796–805.
- [19] DE JONG, J., VAN NIEUWSTADT, A., KIMMAN, T., LOEFFEN, W., BESTEBROER, T., BIJLSMA, K., VERWEIJ, C., OSTERHAUS, A., AND CLAAS, E. Antigenic drift in swine influenza H3 haemagglutinins with implications for vaccination policy. *Vaccine* 17, 11 (1999), 1321–1328.
- [20] DIGARD, P., ELTON, D., BISHOP, K., MEDCALF, E., WEEDS, A., AND POPE, B. Modulation of nuclear localization of the influenza virus nucleoprotein through interaction with actin filaments. *Journal of Virology* 73, 3 (1999), 2222–31.
- [21] EASTERDAY, B., AND VAN REETH, K. *Swine influenza*, 8th ed. Wiley, 1999, pp. 277–290.
- [22] FERREIDOUNI, S. R., HARDER, T. C., GAIDET, N., ZILLER, M., HOFFMANN, B., HAMMOUMI, S., GLOBIG, A., AND STARICK, E. Saving resources: avian influenza surveillance using pooled swab samples and reduced reaction volumes in real-time RT-PCR. *Journal of Virological Methods* 186, 1 (2012), 119–125.

- [23] FERRARI, M., SCALVINI, A., LOSIO, M., CORRADI, A., SONCINI, M., BIGNOTTI, E., MILANESI, E., AJMONE-MARSAN, P., BARLATI, S., AND BELLOTTI, D. Establishment and characterization of two new pig cell lines for use in virological diagnostic laboratories. *Journal of Virological Methods* 107, 2 (2003), 205–212.
- [24] FOUCHIER, R. A., BESTEBROER, T. M., HERFST, S., VAN DER KEMP, L., RIMMELZWAAN, G. F., AND OSTERHAUS, A. D. Detection of influenza A viruses from different species by PCR amplification of conserved sequences in the matrix gene. *Journal of Clinical Microbiology* 38, 11 (2000), 4096–4101.
- [25] FRANK, A. L., COUCH, R. B., GRIFFIS, C. A., AND BAXTER, B. D. Comparison of different tissue cultures for isolation and quantitation of influenza and parainfluenza viruses. *Journal of Clinical Microbiology* 10, 1 (1979), 32–6.
- [26] FREYMAN, M., TAMM, I., AND GREEN, R. Growth curves of influenza virus based on hemagglutination titers in individual embryonated eggs. *The Yale journal of biology and medicine* 23, 4 (1951), 269.
- [27] GARTEN, R. J., DAVIS, C. T., RUSSELL, C. A., SHU, B., LINDSTROM, S., BALISH, A., SESSIONS, W. M., XU, X., SKEPNER, E., AND DEYDE, V. Antigenic and genetic characteristics of swine-origin 2009 A (H1N1) influenza viruses circulating in humans. *Science* 325, 5937 (2009), 197–201.
- [28] GAUSH, C. R., HARD, W. L., AND SMITH, T. F. Characterization of an established line of canine kidney cells (MDCK). *Experimental Biology and Medicine* 122, 3 (1966), 931–935.
- [29] GAUSH, C. R., AND SMITH, T. F. Replication and plaque assay of influenza virus in an established line of canine kidney cells. *Applied Microbiology* 16, 4 (1968), 588–594.
- [30] GOMEZ-PUERTAS, P., ALBO, C., PEREZ-PASTRANA, E., VIVO, A., AND PORTELA, A. Influenza virus matrix protein is the major driving force in virus budding. *Journal of Virology* 74, 24 (2000), 11538–47.
- [31] GREEN, I. J. Serial propagation of influenza B (Lee) virus in a transmissible line of canine kidney cells. *Science* 138, 3536 (1962), 42–43.
- [32] HARDER, T. C., GROSSE BEILAGE, E., LANGE, E., MEINERS, C., DÖHRING, S., PESCH, S., NOÉ, T., GRUND, C., BEER, M., AND STARICK, E. Expanded cocirculation of stable subtypes, emerging lineages, and new sporadic reassortants of porcine influenza viruses in swine populations in Northwest Germany. *Journal of Virology* 87, 19 (2013), 10460–10476.
- [33] HAYMAN, A., COMELY, S., LACKENBY, A., MURPHY, S., MCCAULEY, J., GOODBOURN, S., AND BARCLAY, W. Variation in the ability of human influenza A viruses to induce and inhibit the IFN- β pathway. *Virology* 347, 1 (2006), 52–64.
- [34] HENLE, W., AND LIU, O. C. Studies on host-virus interactions in the chick embryo-influenza virus system VI. Evidence for multiplicity reactivation of inactivated virus. *The Journal of Experimental Medicine* 94, 4 (1951), 305–322.
- [35] HERMAN MARGOT, HAUGERUD SIGRUN, M. Y. S. G. S. M. Improved In Vitro Cultivation of Swine Influenza Virus. *International Journal of Applied Research Volume* 13, Number 2 (2005).

- [36] HERZ, C., STAVNEZER, E., KRUG, R. M., AND GURNEY JR, T. Influenza virus, an RNA virus, synthesizes its messenger RNA in the nucleus of infected cells. *Cell* 26, 3, Part 1 (1981), 391–400.
- [37] HINSHAW, V., WEBSTER, R., EASTERDAY, B., AND BEAN, W. J. Replication of avian influenza A viruses in mammals. *Infection and Immunity* 34, 2 (1981), 354–361.
- [38] HIROMOTO, Y., UCHIDA, Y., TAKEMAE, N., HAYASHI, T., TSUDA, T., AND SAITO, T. Real-time reverse transcription-PCR assay for differentiating the Pandemic H1N1 2009 influenza virus from swine influenza viruses. *Journal of Virological Methods* 170, 12 (2010), 169–172.
- [39] HOFFMANN, B., HARDER, T., LANGE, E., KALTHOFF, D., REIMANN, I., GRUND, C., OEHME, R., VAHLENKAMP, T. W., AND BEER, M. New real-time reverse transcriptase polymerase chain reactions facilitate detection and differentiation of novel A/H1N1 influenza virus in porcine and human samples. *Berliner und Münchener Tierärztliche Wochenschrift* 7, 7-8 (2010), 286–292.
- [40] HORISBERGER, M. The action of recombinant bovine interferons on influenza virus replication correlates with the induction of two Mx-related proteins in bovine cells. *Virology* 162, 1 (1988), 181–186.
- [41] HOWARD, W. A., ESSEN, S. C., STRUGNELL, B. W., RUSSELL, C., BARASS, L., REID, S. M., AND BROWN, I. H. Reassortant pandemic (H1N1) 2009 virus in pigs, United Kingdom. *Emerging Infectious Diseases Journal* 17, 6 (2011), 1049–1052.
- [42] HUANG, Y. T., AND TURCHEK, B. M. Mink lung cells and mixed mink lung and A549 cells for rapid detection of influenza virus and other respiratory viruses. *Journal of Clinical Microbiology* 38, 1 (2000), 422–423.
- [43] HUBERT, J. *Spearman-Kärber method*, vol. 2nd edition. Hunt Publishing, Dubuque (Iowa), 1984, book section 65-66.
- [44] HUSAIN, M., AND GUPTA, C. Interactions of viral matrix protein and nucleoprotein with the host cell cytoskeletal actin in influenza viral infection. *Current Science* 73, 1 (1997), 40–47.
- [45] ITO, T., COUCEIRO, J. N. S., KELM, S., BAUM, L. G., KRAUSS, S., CASTRUCCI, M. R., DONATELLI, I., KIDA, H., PAULSON, J. C., AND WEBSTER, R. G. Molecular basis for the generation in pigs of influenza A viruses with pandemic potential. *Journal of Virology* 72, 9 (1998), 7367–7373.
- [46] KISTNER, O., MÜLLER, K., AND SCHOLTISSEK, C. Differential phosphorylation of the nucleoprotein of influenza A viruses. *Journal of General Virology* 70, 9 (1989), 2421–2431.
- [47] KISTNER, O., MULLER, H., BECHT, H., AND SCHOLTISSEK, C. Phosphopeptide fingerprints of nucleoproteins of various influenza A virus strains grown in different host cells. *Journal of General Virology* 66 (Pt 3) (1985), 465–72.
- [48] KLENK, H.-D., ROTT, R., ORLICH, M., AND BLÖDORN, J. Activation of influenza A viruses by trypsin treatment. *Virology* 68, 2 (1975), 426–439.
- [49] KOBAYASHI, M., TOYODA, T., ADYSHEV, D. M., AZUMA, Y., AND ISHIHAMA, A. Molecular dissection of influenza virus nucleoprotein: deletion mapping of the RNA binding domain. *Journal of Virology* 68, 12 (1994), 8433–8436.

- [50] KOFF, W. C., AND KNIGHT, V. Inhibition of influenza virus uncoating by rimantadine hydrochloride. *Journal of Virology* 31, 1 (1979), 261–3.
- [51] KOTHALAWALA, H., TOUSSAINT, M., AND GRUYS, E. An overview of swine influenza. *Veterinary Quarterly* 28, 2 (2006), 45–53.
- [52] KRUG, R. M., SHAW, M., BRONI, B., SHAPIRO, G., AND HALLER, O. Inhibition of influenza viral mRNA synthesis in cells expressing the interferon-induced Mx gene product. *Journal of Virology* 56, 1 (1985), 201–6.
- [53] KUNTZ-SIMON, G., AND MADEC, F. Genetic and antigenic evolution of swine influenza viruses in Europe and evaluation of their zoonotic potential. *Zoonoses and Public Health* 56, 6-7 (2009), 310–325.
- [54] LAMB, R. A. *Genes and proteins of the influenza viruses*. Springer, 1989, pp. 1–87.
- [55] LAMB, R. A., AND CHOPPIN, P. W. The gene structure and replication of influenza virus. *Annual Review of Biochemistry* 52 (1983), 467–506.
- [56] LANDOLT, G. A., KARASIN, A. I., PHILLIPS, L., AND OLSEN, C. W. Comparison of the pathogenesis of two genetically different H3N2 influenza A viruses in pigs. *Journal of Clinical Microbiology* 41, 5 (2003), 1936–1941.
- [57] LANGE, E., KALTHOFF, D., BLOHM, U., TEIFKE, J. P., BREITHAUPT, A., MARESCH, C., STARICK, E., FERREIDOUNI, S., HOFFMANN, B., AND METTENLEITER, T. C. Pathogenesis and transmission of the novel swine-origin influenza virus A/H1N1 after experimental infection of pigs. *Journal of General Virology* 90, 9 (2009), 2119–2123.
- [58] LANGE, J., GROTH, M., SCHLEGEL, M., KRUMBHOLZ, A., WIECZOREK, K., ULRICH, R., KOPPEN, S., SCHULZ, K., APPL, D., SELBITZ, H. J., SAUERBREI, A., PLATZER, M., ZELL, R., AND DURRWALD, R. Reassortants of the pandemic (H1N1) 2009 virus and establishment of a novel porcine H1N2 influenza virus, lineage in Germany. *Veterinary Microbiology* 167, 3-4 (2013), 345–56.
- [59] LI, I. W., CHAN, K. H., TO, K. W., WONG, S. S., HO, P. L., LAU, S. K., WOO, P. C., TSOI, H. W., CHAN, J. F., CHENG, V. C., ZHENG, B. J., CHEN, H., AND YUEN, K. Y. Differential susceptibility of different cell lines to swine-origin influenza A H1N1, seasonal human influenza A H1N1, and avian influenza A H5N1 viruses. *Journal of Clinical Virology* 46, 4 (2009), 325–30.
- [60] MAIER, S. *Interaktion von Influenza A Virus Subtypen mit primären porcinen Fibrozyten*. Thesis, 2011.
- [61] MAINES, T. R., JAYARAMAN, A., BELSER, J. A., WADFORD, D. A., PAPPAS, C., ZENG, H., GUSTIN, K. M., PEARCE, M. B., VISWANATHAN, K., AND SHRIVER, Z. H. Transmission and pathogenesis of swine-origin 2009 A (H1N1) influenza viruses in ferrets and mice. *Science* 325, 5939 (2009), 484–487.
- [62] MARTIN, K., AND HELENIUS, A. Transport of incoming influenza virus nucleocapsids into the nucleus. *Journal of Virology* 65, 1 (1991), 232–44.
- [63] MARTIN, K., AND HELENIUS, A. Nuclear transport of influenza virus ribonucleoproteins: the viral matrix protein (M1) promotes export and inhibits import. *Cell* 67, 1 (1991), 117–130.

- [64] MASSIN, P., KUNTZ-SIMON, G., BARBEZANGE, C., DEBLANC, C., OGER, A., MARQUET-BLOUIN, E., BOUGEARD, S., VAN DER WERF, S., AND JESTIN, V. Temperature sensitivity on growth and/or replication of H1N1, H1N2 and H3N2 influenza A viruses isolated from pigs and birds in mammalian cells. *Veterinary Microbiology* 142, 3 (2010), 232–241.
- [65] MATIKAINEN, S., SIRÉN, J., TISSARI, J., VECKMAN, V., PIRHONEN, J., SEVERA, M., SUN, Q., LIN, R., MERI, S., AND UZÉ, G. Tumor necrosis factor alpha enhances influenza A virus-induced expression of antiviral cytokines by activating RIG-I gene expression. *Journal of Virology* 80, 7 (2006), 3515–3522.
- [66] MATROSOVICH, M. N., MATROSOVICH, T. Y., GRAY, T., ROBERTS, N. A., AND KLENK, H.-D. Human and avian influenza viruses target different cell types in cultures of human airway epithelium. *Proceedings of the National Academy of Sciences of the United States of America* 101, 13 (2004), 4620–4624.
- [67] MEYER, T., AND HORISBERGER, M. A. Combined action of mouse alpha and beta interferons in influenza virus-infected macrophages carrying the resistance gene Mx. *Journal of Virology* 49, 3 (1984), 709–16.
- [68] NAGARAJAN, M. M., SIMARD, G., LONGTIN, D., AND SIMARD, C. Single-step multiplex conventional and real-time reverse transcription polymerase chain reaction assays for simultaneous detection and subtype differentiation of Influenza A virus in swine. *Journal of veterinary diagnostic investigation* 22, 3 (2010), 402–408.
- [69] NEUMANN, G., CASTRUCCI, M. R., AND KAWAOKA, Y. Nuclear import and export of influenza virus nucleoprotein. *Journal of Virology* 71, 12 (1997), 9690–700.
- [70] NEUMANN, G., NODA, T., AND KAWAOKA, Y. Emergence and pandemic potential of swine-origin H1N1 influenza virus. *Nature* 459, 7249 (2009), 931–939.
- [71] OFFICIAL WEBSITE OF INTERNATIONAL COMMITTEE ON TAXONOMY OF VIRUSES. (<http://www.ictvonline.org/virusTaxonomy.asp>). 01/2016.
- [72] OFFICIAL WEBSITE OF PAUL-EHRLICH-INSTITUT. (<http://www.pei.de>). 01/2016.
- [73] OFFICIAL WEBSITE OF WORLD HEALTH ORGANIZATION. (<http://www.who.int>). 01/2016.
- [74] ONDRACKOVA, P., MATIASOVIC, J., VOLF, J., DOMINGUEZ, J., AND FALDYNA, M. Phenotypic characterisation of the monocyte subpopulations in healthy adult pigs and Salmonella-infected piglets by seven-colour flow cytometry. *Research in Veterinary Science* 94, 2 (2013), 240–5.
- [75] O’NEILL, R. E., TALON, J., AND PALESE, P. The influenza virus NEP (NS2 protein) mediates the nuclear export of viral ribonucleoproteins. *The EMBO Journal* 17, 1 (1998), 288–296.
- [76] OSTERHAUS, A., RIMMELZWAAN, G., MARTINA, B., BESTEBROER, T., AND FOUCHIER, R. Influenza B virus in seals. *Science* 288, 5468 (2000), 1051–1053.
- [77] PENZAERT, M., OTTIS, K., VANDEPUTTE, J., KAPLAN, M. M., AND BACHMANN, P. Evidence for the natural transmission of influenza A virus from wild ducks to swine and its potential importance for man. *Bulletin of the World Health Organization* 59, 1 (1981), 75.

- [78] PESCHEL, B., FRENTZEL, S., LASKE, T., GENZEL, Y., AND REICHL, U. Comparison of influenza virus yields and apoptosis-induction in an adherent and a suspension MDCK cell line. *Vaccine* 31, 48 (2013), 5693–9.
- [79] PIPPIG J, RITZMANN M, B. M. N.-J. A. Influenza A Viruses Detected in Swine in Southern Germany after the H1N1 Pandemic in 2009. *Zoonoses and Public Health in press* (2016).
- [80] PORTELA, A., AND DIGARD, P. The influenza virus nucleoprotein: a multifunctional RNA-binding protein pivotal to virus replication. *Journal of General Virology* 83, Pt 4 (2002), 723–34.
- [81] PUNYADARSANIYA, D., LIANG, C.-H., WINTER, C., PETERSEN, H., RAUTENSCHLEIN, S., HENNIG-PAUKA, I., SCHWEGMANN-WESSELS, C., WU, C.-Y., WONG, C.-H., AND HERRLER, G. Infection of differentiated porcine airway epithelial cells by influenza virus: differential susceptibility to infection by porcine and avian viruses. *PLoS One* 6, 12 (2011), e28429.
- [82] REINA, J., FERNANDEZ-BACA, V., BLANCO, I., AND MUNAR, M. Comparison of Madin-Darby canine kidney cells (MDCK) with a green monkey continuous cell line (Vero) and human lung embryonated cells (MRC-5) in the isolation of influenza A virus from nasopharyngeal aspirates by shell vial culture. *Journal of Clinical Microbiology* 35, 7 (1997), 1900–1901.
- [83] RIMMELZWAAN, G. F., BAARS, M., CLAAS, E. C., AND OSTERHAUS, A. D. Comparison of RNA hybridization, hemagglutination assay, titration of infectious virus and immunofluorescence as methods for monitoring influenza virus replication in vitro. *Journal of Virological Methods* 74, 1 (1998), 57–66.
- [84] ROCHA, E. P., XU, X., HALL, H. E., ALLEN, J. R., REGNERY, H. L., AND COX, N. J. Comparison of 10 influenza A (H1N1 and H3N2) haemagglutinin sequences obtained directly from clinical specimens to those of MDCK cell-and egg-grown viruses. *Journal of general virology* 74, 11 (1993), 2513–2518.
- [85] SAKAGUCHI, A., HIRAYAMA, E., HIRAKI, A., ISHIDA, Y.-I., AND KIM, J. Nuclear export of influenza viral ribonucleoprotein is temperature-dependently inhibited by dissociation of viral matrix protein. *Virology* 306, 2 (2003), 244–253.
- [86] SANCHEZ, C., DOMENECH, N., VAZQUEZ, J., ALONSO, F., EZQUERRA, A., AND DOMINGUEZ, J. The porcine 2A10 antigen is homologous to human CD163 and related to macrophage differentiation. *Journal of Immunology* 162, 9 (1999), 5230–7.
- [87] SCHILD, G., OXFORD, J., DE JONG, J., AND WEBSTER, R. Evidence for host-cell selection of influenza virus antigenic variants. *Nature* 303, 5919 (1983), 706–709.
- [88] SCHOLTISSEK, C., HINSHAW, V., AND OLSEN, C. *Influenza in pigs and their role as the intermediate host*. Blackwell Healthcare Communications, Oxford, 1998, pp. 137–145.
- [89] SCHORR, E., WENTWORTH, D., AND HINSHAW, V. Use of polymerase chain reaction to detect swine influenza virus in nasal swab specimens. *American Journal of Veterinary Research* 55, 7 (1994), 952–956.
- [90] SIECZKARSKI, S., AND WHITTAKER, G. *Viral entry*. Springer, 2005, pp. 1–23.

- [91] SIMON, G., LARSEN, L. E., DÜRRWALD, R., FONI, E., HARDER, T., VAN REETH, K., MARKOWSKA-DANIEL, I., REID, S. M., DAN, A., AND MALDONADO, J. European Surveillance Network for Influenza in Pigs: Surveillance Programs, Diagnostic Tools and Swine Influenza Virus Subtypes Identified in 14 European Countries from 2010 to 2013. *PloS One* 9, 12 (2014), e115815.
- [92] STARICK, E., LANGE, E., FEREIDOUNI, S., BUNZENTHAL, C., HÖVELER, R., KUCZKA, A., GROSSE BEILAGE, E., HAMANN, H.-P., KLINGELHÖFER, I., AND STEINHAEUER, D. Reassorted pandemic (H1N1) 2009 influenza A virus discovered from pigs in Germany. *Journal of General Virology* 92, 5 (2011), 1184–1188.
- [93] STARICK, E., LANGE, E., GRUND, C., GROSSE BEILAGE, E., DÖHRING, S., MAAS, A., NOÉ, T., BEER, M., AND HARDER, T. C. Reassortants of pandemic influenza A virus H1N1/2009 and endemic porcine HxN2 viruses emerge in swine populations in Germany. *Journal of General Virology* 93, 8 (2012), 1658–1663.
- [94] STEINHAEUER, D. A. Role of hemagglutinin cleavage for the pathogenicity of influenza virus. *Virology* 258, 1 (1999), 1–20.
- [95] ÖSTERLUND, P., VECKMAN, V., SIRÉN, J., KLUCHER, K. M., HISCOTT, J., MATIKAINEN, S., AND JULKUNEN, I. Gene expression and antiviral activity of alpha/beta interferons and interleukin-29 in virus-infected human myeloid dendritic cells. *Journal of Virology* 79, 15 (2005), 9608–9617.
- [96] STRAUSS-AYALI, D., CONRAD, S. M., AND MOSSER, D. M. Monocyte subpopulations and their differentiation patterns during infection. *Journal of Leukocyte Biology* 82, 2 (2007), 244–52.
- [97] SUBBARAO, K., KLIMOV, A., KATZ, J., REGNERY, H., LIM, W., HALL, H., PERDUE, M., SWAYNE, D., BENDER, C., AND HUANG, J. Characterization of an avian influenza A (H5N1) virus isolated from a child with a fatal respiratory illness. *Science* 279, 5349 (1998), 393–396.
- [98] TAUBENBERGER, J. K., AND KASH, J. C. Influenza virus evolution, host adaptation, and pandemic formation. *Cell Host & Microbe* 7, 6 (2010), 440–451.
- [99] TOBITA, K., SUGIURA, A., ENOMOTE, C., AND FURUYAMA, M. Plaque assay and primary isolation of influenza A viruses in an established line of canine kidney cells (MDCK) in the presence of trypsin. *Medical Microbiology and Immunology* 162, 1 (1975), 9–14.
- [100] TONG, S., LI, Y., RIVAILLER, P., CONRARDY, C., CASTILLO, D. A. A., CHEN, L.-M., RECUENCO, S., ELLISON, J. A., DAVIS, C. T., AND YORK, I. A. A distinct lineage of influenza A virus from bats. *Proceedings of the National Academy of Sciences of the United States of America* 109, 11 (2012), 4269–4274.
- [101] TONG, S., ZHU, X., LI, Y., SHI, M., ZHANG, J., BOURGEOIS, M., YANG, H., CHEN, X., RECUENCO, S., GOMEZ, J., CHEN, L. M., JOHNSON, A., TAO, Y., DREYFUS, C., YU, W., MCBRIDE, R., CARNEY, P. J., GILBERT, A. T., CHANG, J., GUO, Z., DAVIS, C. T., PAULSON, J. C., STEVENS, J., RUPPRECHT, C. E., HOLMES, E. C., WILSON, I. A., AND DONIS, R. O. New world bats harbor diverse influenza A viruses. *PLoS Pathogens* 9, 10 (2013), e1003657.
- [102] VAN REETH, K. Avian and swine influenza viruses: our current understanding of the zoonotic risk. *Veterinary Research* 38, 2 (2007), 243–260.

- [103] VAN REETH, K., NAUWYNCK, H., AND PENSAERT, M. Bronchoalveolar interferon- α , tumor necrosis factor- α , interleukin-1, and inflammation during acute influenza in pigs: A possible model for humans? *Journal of Infectious Diseases* 177, 4 (1998), 1076–1079.
- [104] VAN REETH, K., VAN GUCHT, S., AND PENSAERT, M. Correlations between lung proinflammatory cytokine levels, virus replication, and disease after swine influenza virus challenge of vaccination-immune pigs. *Viral Immunology* 15, 4 (2002), 583–594.
- [105] VECKMAN, V., ÖSTERLUND, P., FAGERLUND, R., MELÉN, K., MATIKAINEN, S., AND JULKUNEN, I. TNF- α and IFN- α enhance influenza-A-virus-induced chemokine gene expression in human A549 lung epithelial cells. *Virology* 345, 1 (2006), 96–104.
- [106] WEBBY, R., AND WEBSTER, R. *Influenza viruses in animal wildlife populations*. Springer, 2007, pp. 67–83.
- [107] WEBER, F., KOCHS, G., GRUBER, S., AND HALLER, O. A classical bipartite nuclear localization signal on Thogoto and influenza A virus nucleoproteins. *Virology* 250, 1 (1998), 9–18.
- [108] WEBSTER, R. G., BEAN, W. J., GORMAN, O. T., CHAMBERS, T. M., AND KAWAOKA, Y. Evolution and ecology of influenza A viruses. *Microbiological Reviews* 56, 1 (1992), 152–179.
- [109] WHITTAKER, G., BUI, M., AND HELENIUS, A. Nuclear trafficking of influenza virus ribonucleoproteins in heterokaryons. *Journal of Virology* 70, 5 (1996), 2743–56.
- [110] WHITTAKER, G., KEMLER, I., AND HELENIUS, A. Hyperphosphorylation of mutant influenza virus matrix protein, M1, causes its retention in the nucleus. *Journal of Virology* 69, 1 (1995), 439–45.
- [111] YANG, Z. Y., WEI, C. J., KONG, W. P., WU, L., XU, L., SMITH, D. F., AND NABEL, G. J. Immunization by Avian H5 Influenza Hemagglutinin Mutants with Altered Receptor Binding Specificity. *Science* 317, 5839 (2007), 825–8.
- [112] YE, Z., LIU, T., OFFRINGA, D. P., MCINNIS, J., AND LEVANDOWSKI, R. A. Association of influenza virus matrix protein with ribonucleoproteins. *Journal of Virology* 73, 9 (1999), 7467–73.
- [113] YE, Z., ROBINSON, D., AND WAGNER, R. R. Nucleus-targeting domain of the matrix protein (M1) of influenza virus. *Journal of Virology* 69, 3 (1995), 1964–70.
- [114] YOUIL, R., SU, Q., TONER, T. J., SZYMKOWIAK, C., KWAN, W. S., RUBIN, B., PETRUKHIN, L., KISELEVA, I., SHAW, A. R., AND DiSTEFANO, D. Comparative study of influenza virus replication in Vero and MDCK cell lines. *Journal of Virological Methods* 120, 1 (2004), 23–31.
- [115] ZELL, R., MOTZKE, S., KRUMBHOLZ, A., WUTZLER, P., HERWIG, V., AND DÜRRWALD, R. Novel reassortant of swine influenza H1N2 virus in Germany. *Journal of General Virology* 89, 1 (2008), 271–276.
- [116] ZELL, R., SCHOLTISSEK, C., AND LUDWIG, S. Genetics, evolution, and the zoonotic capacity of European Swine influenza viruses. *Curr Top Microbiol Immunol* 370 (2013), 29–55.

- [117] ZHU, Y.-D., KOO, K., BRADSHAW, J. D., SUTTON, W. F., KULLER, L., BUCALA, R., ANDERSON, D., MOSSMAN, S. P., VILLINGER, F., AND HAIGWOOD, N. L. Macaque blood-derived antigen-presenting cells elicit SIV-specific immune responses. *Journal of Medical Primatology* 29, 3-4 (2000), 182–192.

DANKSAGUNG

An dieser Stelle möchte ich mich bei all jenen bedanken, die zur Entstehung dieser Arbeit beigetragen haben.

Als Erstes möchte ich Frau PD Dr. Antonie Neubauer-Juric für die Möglichkeit, diese Arbeit in der Abteilung der Veterinärvirologie des LGL Bayern auszuführen, danken. Dabei konnte ich mich immer auf umfassende Unterstützung und viele Denkanstöße während der gesamten Zeit verlassen.

Auch bei Herrn Prof. Dr. Mathias Ritzmann möchte ich mich für die freundliche und unkomplizierte Zusammenarbeit bedanken und die Vertretung dieser Arbeit vor dem Promotionsausschuss.

Der gesamten Veterinärvirologie im LGL Oberschleißheim danke ich für eine wirklich schöne Zeit mit angenehmer Arbeitsatmosphäre. Isa, Patricia, Manu, Susi, Birgit, Petra P., Sonja, Rebecca, Anita, Franziska, Simone, Petra S., Gabi, Nicki, Steffi, Anne und Eva, ihr alle habt mir den Laboralltag (nicht nur mit viel Kuchen) versüßt und die Latte für zukünftige Teamkollegen sehr hoch gehängt!

Ich danke ganz besonders Isabella Dzijan, für die geduldige Hilfe bei kleinen und großen Problemen, bei welchen sie mir nicht nur mit Rat, sondern auch mit sehr viel Tat (durch 363 Titrationsplatten hindurch!) zur Seite stand. Außerdem bedanke ich mich bei Birgit von Köln-Braun für die guten Tipps bezüglich meiner 'Zell-Kinder'. Großer Dank geht auch an Heike Lang, für die tatkräftige Unterstützung bei der Anzucht der Fibrozyten und den regen Austausch im Labor.

Des Weiteren möchte ich mich auch bei Herrn Prof. Dr. Büttner für die Zusammenarbeit und Bereitstellung von Daten und meines Laborarbeitsplatzes bedanken.

Außerdem danke ich Sandra Eßbauer für die Bereitstellung und Klaus Freimüller für die geduldige Einführung am Mikroskop des Instituts für Mikrobiologie der Bundeswehr München.

Genauso vielen Dank an Herr Prof. Dr. Gerd Sutter und Herr Dr. Robert Fux vom Lehrstuhl für Virologie der Tierärztlichen Fakultät der Universität München, für die Möglichkeit wunderschöne Bilder meiner Immunfluoreszenz-Experimente aufzunehmen.

Ich danke meiner Familie und meinen Freunden, insbesondere Ellen, für die Unterstützung, die sie mir nicht nur während dieser Arbeit, sondern in meinem ganzen Leben sind.

Ohne den wichtigsten Menschen in meinem Leben wäre diese Arbeit niemals möglich gewesen - und damit ist nicht nur die technisch und statistische Ausarbeitung dieser Doktorarbeit gemeint. Vielen Dank an dich, Lukas!